Functional Analysis of the Apoptosis-Inducing Factor (AIF)

Inaugural-Dissertation

zur
Erlangung des Doktorgrades
Dr. rer. nat.
des Fachbereichs
Biologie und Geographie
an der
Universität Duisburg-Essen

vorgelegt von

Nicola Vahsen

geboren in Mülheim an der Ruhr

Datum der mündlichen Prüfung: 05.April 2006

Gutachter:
Guido Kroemer, Prof.Dr.med.Dr.rer.nat. (Institut Gustave Roussy,Villejuif,Frankreich)
Prof.Dr.Dr. Brigitte Pützer, Prof.Dr.med.Dr.rer.nat. (Universtät Rostock)
Prof.Dr. Helmut Esche, Prof.Dr.rer.nat. (Universität Duisburg-Essen)

Abbreviations

µg	Microgramme
µl	Microlitre
ADP	Adenosine biphosphate
AIF	Apoptosis-inducing factor
AIFL	AIF-like protein
ANT	Adenine nucleotide transporter
Apaf-1	Apoptosis protease activating factor 1
APS	Ammonium persulphate
ATP	Adenosine triphosphate
Bcl-2	B-cell leukemia/lymphoma 2
BH	Bcl-2 homology
BN	Blue native
BSA	Bovine serum albumin
BSO	Buthionine sulfoximine
C	Celsius
C.elegans	*Caenorhabditis elegans*
CAD	Caspase-activated DNAse
cDNA	Complementary DNA
CHAPS	3-[(3-Cholamidopropyl)-dimethylammonio)]-1-propane sulfonic acid
CIA30	Complex I assembly factor 30
Cox1/ Cox2	Cytochrome c oxidase subunit 1/2
CPEO	Chronic external ophtamoplegia
CPS6	Ced-3 protease suppressor 6
CTL	Cytotoxic T lymphocytes
CY	Cyclophosmamide
CypA	Cyclophilin A
Cyt *c*	Cytochrome *c*
cytB	Cytochrome B
Da	Dalton
DAPI	4',-6-diamino-2-phenylindole-dihydrochloride
DCF-DA	2'7'-dichlorodihydrofluorescein diacetate
DCPIP	Dichlorophenol-indophenol
DIABLO	Direct IAP-binding protein with low PI
DISC	Death inducing signalling complex
DMSO	Dimethyl sulfoxide
DNA	Deoxyribonucleic acid
dNTP	Deoxyribonucleotide triphosphate
dsDNA	Double-stranded DNA
dsRNA	Double-stranded RNA
DTT	Dithiothreitol
EDTA	Ethylene diamine tetraacetic acid
EGTA	Ethylene-glycol-bis(2-aminoethylether)-N-N-N-N'-tetraacetic acid
EM	Electron microscopy
EndoG	Endonuclease G
ER	Endoplasmic reticulum
ES cells	Embryonic stem cells

Abbreviations continued

F	Farad
FACS	Fluorescence-activated cell sorter
FAD	Flavine-adenine dinucleotide
FADD	Fas-associated death domain protein
FCS	Fetal calf serum
FITC	Fluorescein isothiocyanate
g	Gramme
GAPDH	Glyceraldehyde-3-phosphate deshydrogenase
GFP	Green fluorescent protein
GPT	Glutamate-pyruvate-transaminase
GSH	Glutathione
H_2DCFDA	Dichlorodihydrofluorescein diacetate
HIV	Human immunodeficiency virus
HnRNPA1	Heterogenous nuclear ribonucleoprotein A1
Hsp	Heat shock protein
HtrA2	High temperature required protein A2
IAP	Inhibtior of apoptosis protein
ICAD	Inhibitor of caspase-activated DNAse
Ig	Immunoglobulin
IP	Immunoprecipitation
KO	Knock-out
l	Litre
LDH	Lactate-dehydrogenase
LIF	Leukemia inducing factor
M	Molar
mA	milli-Amper
MELAS	Mitochondrial encephalopathy lactic acidosis syndrome
ml	Millilitre
mM	Millimolar
MnTBAP	Mn(III)tetrakis(4-benzoic acid)porphyrin chloride
MOMP	Mitochondrial outer membrane permeabilization
mRNA	Messenger RNA
NAD	Nicotinamide adenine dinucleotide
NADP	Nicotinamide adenine dinucleotide phosphate
NAO	Nonyl acridine orange
ND1/ ND6	NADH dehydrogenase subunit 1/6
NDUFA9	NADH-ubiquinone oxydoreductase 1 alpha subcomplex 9
NDUFB6	NADH-ubiquinone oxydoreductase 1 beta subcomplex 6
NDUFS7	NADH-ubiquinone oxydoreductase FeS protein 7
nm	nannometre
NSCLC	Non-small-cell-lung carcinoma
OD	Optical density
OXPHOS	Oxidative phosphorylation
PAGE	Polyacrylamide gel electrophoresis
PAR	Poly(ADP ribose)

Abbreviations continued

PARP	Poly(ADP ribose) polymerase
PBS	Phosphate-buffered saline
PFA	Paraformaldehyde
PTP	Permeability transition pore
RISC	RNA-induced silencing complex
RNA	Ribonucleic acid
ROS	Reactive oxygen species
S.cerevisiae	*Saccharomyces cerevisiae*
SDS	Sodium dodecyl sulfate
siRNA	small interfering RNA
Smac	Second mitochondria-derived activator of caspases
SOD	Superoxide dismutase
SSB protein	single-strand DNA binding protein
ssDNA	single-stranded DNA
ssRNA	single-stranded RNA
STS	Staurosporine
TAE	Tris-acetate EDTA
tBid	Truncated Bid
TEM	Transmission electron microscopy
TNF	Tumor necrosis factor
TOM40	Translocase of outer membrane 40
TRADD	TNF-receptor-associated death domain protein
tRNA	Transfer RNA
U	Units
UV	ultra violet
V	Volt
VDAC	Voltage-dependent anion channel
w/v	M
WAH-1	Worm AIF homologue 1
Z-VAD.fmk	Benzyloxycarbonyl-Val-Ala-Asp (OMe) fluoromethylketone

Contents

Contents continued

Contents continued

1. Introduction

Cells are very complex and it has taken evolution more than two billion years to develop a eukaryotic cell like the ones that form the human body today. Every cellular process, ranging from replication, differentiation, and energy production to intercellular signalling and cell death, is precisely regulated and executed by proteins. To provide enough "workmen", thousands of proteins are being expressed in a single cell. Since a lot of different functions are required, the cells have developed an extremely efficient system in which many of these proteins fulfill several tasks.

One of these multifunctional proteins is the apoptosis-inducing factor (AIF, Figure 1-1), a mitochondrial flavoprotein that translocates to the nucleus upon apoptosis induction where it participates in apoptosis-associated chromatinolysis. To study and explore AIF's functions, its cellular environment as well as the signalling pathways this protein is involved in, need to be understood.

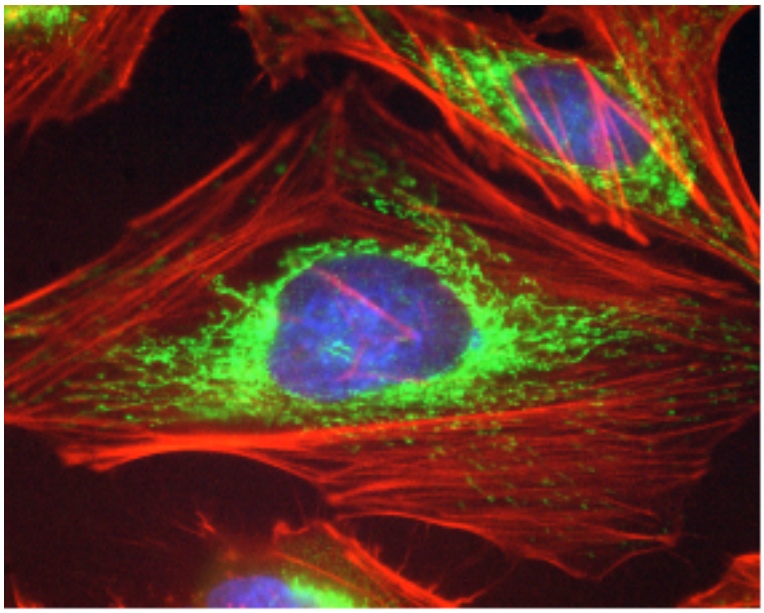

Figure 1-1. AIF in mitochondria of vital cells. *HeLa cells were stained with antibodies specific for AIF (green) and actin (red), as well as with Hoechst 33342 (blue) to visualise the DNA.*

1.1. Mitochondria

One important step in the development of the eukaryotic cell was the acquisition of mitochondria. More than a billion years ago, aerobic bacteria invaded eukaryotic cells that lacked the ability to use oxygen metabolically (Gray et al., 1999). A symbiotic relationship formed that allowed the host cell to produce energy by respiration, a much more efficient way than anaerobic glycolysis. The symbiosis became permanent and the eubacteria evolved into mitochondria (Dyall et al., 2004).

1.1.1. Structure

Depending on the cell type, there are between a few hundred and many thousand mitochondria per cell. Tissues requiring a lot of energy, like muscle tissue, possess a large number of mitochondria.

The organelle contains four different compartments: the outer mitochondrial membrane, the inner mitochondrial membrane, the intermembrane space, and the matrix, which is the central space inside the inner membrane (Figure 1-2). The surface area of the inner membrane is increased by numerous infoldings, called cristae, which protrude into the matrix. Based on tomography studies, these cristae have recently been considered as a separate compartment that are connected by tubular regions (Mannella et al., 2001).

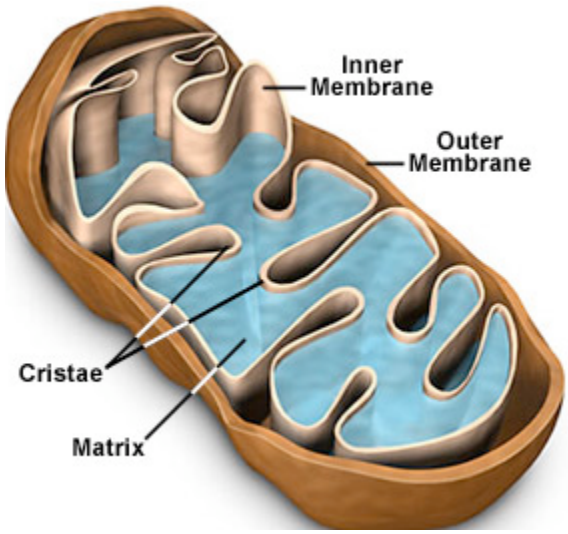

Figure 1-2. **Structure of mitochondria.** *Schematic representation of the profile of mitochondria and its compartments. Between the inner and outer mitochondrial membrane is the intermembrane space.*

Mitochondria possess their own DNA, even though most of the bacterial genes were transferred to the nucleus (Dyall et al., 2004). Today's eukaryotes contain multiple copies of mitochondrial circular DNA encoding proteins essential for organellar function as well as some of the ribosomal and transfer RNA's required for the translation of mitochondrial DNA encoded proteins. However, the large majority of the more than 900 proteins that have been identified to be localised to mitochondria is expressed by nuclear genes and imported from the cytoplasm via the import machinery situated in the mitochondrial membranes. While the mitochondrial DNA is located in the matrix, many of the biochemical reactions take place in the membranes and the intermembrane space.

1.1.2. Multifunctional organelle

Mitochondria perform multiple tasks in living as well as in dying cells. They play a pivotal role in energy production harbouring the respiratory chain, the cell's principal source of ATP. The

latter is the most important molecule for capturing and transferring free energy inside the cell. This process, in which ADP is phosphorylated as a result of the transfer of electrons from NADH or $FADH_2$ to molecular oxygen by a series of electron carriers is called oxidative phosphorylation (OXPHOS) and will be described in detail below. Other reactions that are necessary to fuel the respiratory chain, like the citric acid cycle, also take place in the mitochondria.

During the process of OXPHOS, potentially dangerous byproducts are generated as electrons "leak" out of the respiratory chain and react with oxygen to form superoxide anion (Kudin et al., 2004). Superoxide anions, as well as other highly reactive molecules, like hydrogen peroxide or hydroxyl radicals, are called reactive oxygen species (ROS). They can attack and destroy proteins, lipids, polysaccharides, and DNA, and therefore need to be neutralized in order not to harm the cell or the organism. Certain enzymes localised in mitochondria are there to protect the cell from these ROS. Prominent examples are the superoxide dismutase 2 (SOD2), catalase, and glutathione peroxidase (Radi et al., 1991; Warner et al., 1996).

Moreover, mitochondria play an important role in the metabolism of amino acids, fatty acids, and steroids, as well as in maintaining the intracellular homeostasis of many important metabolites and ions, such as calcium and hydrogen.

Over the last two decades, an additional function of mitochondria has been discovered and intensively studied: its role in apoptosis, a genetically programmed cell suicide that is induced when the cell is no longer needed in the organism or not functioning correctly. During apoptosis, the outer mitochondrial membrane is permeabilised. Some mitochondrial proteins are released and help, directly or indirectly, to degrade cellular components and thus to kill the cell (Green and Kroemer, 2004; Kroemer and Reed, 2000). Mitochondria are therefore important regulators of programmed cell death since they seclude potentially toxic proteins in vital cells and only release them when apoptosis is induced.

1.1.3. The respiratory chain

The respiratory chain is the cell's principal source of ATP. This energy carrier is generated by the OXPHOS system via the concerted action of five protein complexes (I, II, III, IV, and V) and two mobile electron carriers, ubiquinone and cytochrome *c* (Cyt *c*, Figure 1-3). Potential energy of electrons derived from food metabolites such as malate or succinate is used to pump protons from the matrix into the intermembrane space across the inner mitochondrial membrane. This results in the formation of a proton concentration gradient and an electric potential ($\Delta\Psi_m$) across the inner mitochondrial membrane. The ATP synthase (F_0F_1-ATPase or respiratory chain complex V) utilizes this energy potential to convert ADP into ATP concurrent with the proton flow back into the matrix (Figure 1-3).

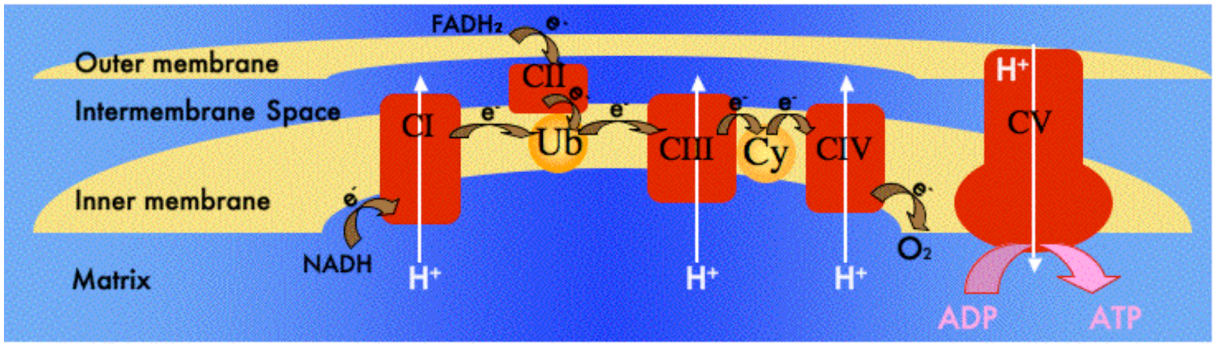

Figure 1-3. **The respiratory chain.** *Schematic representation of the electron transport in mitochondria. The respiratory chain complexes I-V (CI-CV) as well as the electron shuttles ubiquinone (Ub) and cytochrome c (Cy) are localised in the inner mitchondrial membrane. Electrons (e^-) derived from NADH or $FADH_2$ enter the transport chain at complex I or complex II, respectively. They are passed on to complex III via ubiquinone and further on to complex IV via cytochrome c before they reach the final electron acceptor, molecular oxygen, yielding water. Complex I, III, and IV pump protons (H^+) from the matrix into the intermembrane space, thus creating a proton gradient. The energy derived from the flow of protons back into the matrix is used by the ATP synthase (complex V) to phosphorylate ADP to ATP.*

1.1.3.1. The electron transport

The multiprotein complexes I-V are all localised in the inner mitochondrial membrane. Electrons enter the respiratory chain via complex I and II. The NADH dehydrogenase (complex I) oxidizes NADH and transfers the electrons to ubiquinone (coenzyme Q). The latter can also be reduced by complex II, which derives the electrons from $FADH_2$, which in turn is reduced by succinate in intermediary metabolism. Complex II is therefore called succinate-dehydrogenase. In the respiratory chain, the electrons are then transferred from ubiquinol, the reduced form of ubiquinone, to cytochrome *c* by complex III (ubiquinone-cytochrome *c* oxidoreductase). In a final step, the electrons are shuttled to molecular oxygen, thereby producing water, by the cytochrome *c* oxidase (complex IV).

Complex I, III, and IV utilize the energy liberated during the redox-reactions to pump H^+ protons from the matrix into the intermembrane space across the inner mitochondrial membrane. The ATP synthase works like a tiny rotary motor. The flow of protons back into the matrix through the membrane-spanning complex enables it to phosphorylate molecules of ADP generating ATP (Elston et al., 1998). The constant delivery of ADP substrates into the mitochondrial matrix and the transport of ATP out of the mitochondria is the function of the ADP/ATP transporter (ANT) (Shertzer and Racker, 1976). Thus, chemically bound energy in form of ATP can reach every part of the cell to fuel all kinds of reactions and processes.

1.1.3.2. Structure of the mammalian complex I

With the exception of complex II, the respiratory chain complexes are transmembrane protein complexes, embedded in the inner mitochondrial membrane and projecting into the matrix. They are concentrated at the cristae, the infoldings of the inner mitochondrial membrane.

Each one of the respiratory chain complexes is made up of numerous proteins. Few of these subunits are encoded by the mitochondrial DNA, while the vast majority is encoded by nuclear DNA and imported into the organelle (Table 1). Complexes I-IV contain each at least two prosthetic groups, such as flavins, irons-sulfur clusters, or hemes, that serve as oxidation-reduction centres.

	Complex I	Complex II	Complex III	Complex IV	Complex V
Size	~ 980 kDa	~ 140 kDa	~ 250 kDa	~ 200 kDa	~ 600 kDa
Total subunits	~ 46	4	11	13	~ 16
Mitochondrial DNA encoded subunits	7	0	1	3	2

Table 1. **Composition of the respiratory chain complexes.**

NADH dehydrogenase is the largest and most complex enzyme of the respiratory chain. The bovine complex I has been adopted as a model for the human enzyme. Electron microscopy has revealed the bovine complex I as an L-shaped structure (Guenebaut et al., 1997)(Figure 1-4). The vertical arm that projects into the matrix contains the NADH binding site. The horizontal arm is hydrophobic and is buried into the membrane. The NADH dehydrogenase binds to NADH and transfers its high-potential electrons to the non-covalently bound prosthetic group flavin mononucleotide. The electrons are then passed on to a series of iron-sulfur clusters, the second type of prosthetic group in complex I, after which they are shuttled to coenzyme Q. The flow of two electrons through complex I leads to pumping of four H^+ protons from the matrix into the intermembrane space (Brown and Brand, 1988).

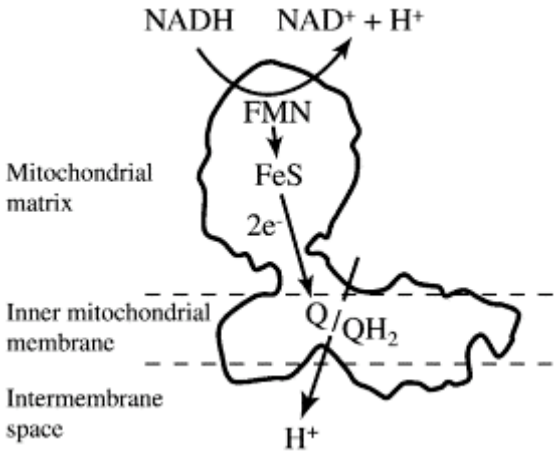

Figure 1-4. **Structure of complex I (adapted from Hirst et al. 2003).** *Complex I is a transmembrane L-shaped multi-protein complex consisting of an arm protruding into the mitochondrial matrix and a hydrophobic arm buried into the inner mitochondrial mebrane. The NADH binding site as well as the majority of the electron-shuttling iron-sulphur clusters are located in the matrix, whereas the ubiquinone-binding site lies within the membrane.*

Developments in proteomics have recently allowed the identification of several additional subunits bringing the total number of bovine structural proteins to 46, seven of which are encoded by the mitochondrial DNA and 39 by the nuclear DNA. Their combined molecular mass is 980kDa (Hirst et al., 2003). Although some of the subunits have been associated with a specific function, the exact mechanism of how electron transfer and proton pumping are coupled inside this complex remains to be elucidated. The subunits encoded by the mitochondrial DNA and seven of the nuclear encoded subunits have been defined as the "core subunits" since they contain all the redox cofactors of the enzymatic complex as well as its substrate binding sites and seem to be sufficient for energy transduction (Walker, 1992). The other 32 "accessory" subunits are less well characterised. It has been proposed that they function as a protective scaffold for escaping electrons (Vogel et al., 2004) or that they are responsible for the assembly and the stability of the complex (Hirst et al., 2003).

1.1.3.3. Assembly of complex I

Very little is known about the biogenesis of the respiratory chain complexes. The assembly has been studied in different species, for example in the fungus *Neurospora crassa* and in human cells, and various assembly models have been proposed (Antonicka et al., 2003; Tuschen et al., 1990). There seem to be subcomplexes that are formed first before they assemble into the whole complex. The composition of these subcomplexes as well as the order of events during the formation vary in the different models, pointing out the complexity of the system. Several subunits of the human complex I have been found to be essential for the correct assembly of the enzyme complex including mitochondrial DNA-encoded core subunits (Bai and Attardi, 1998; Hofhaus and Attardi, 1993) as well as accessory subunits (Huang et al., 2004; Scacco et al., 2003).

Increasing evidence suggests that other mitochondrial proteins, that are not themselves part of the complexes, are indispensable for its correct biogenesis. These proteins are not part of the final structure, but have been shown to cycle between the bound and unbound state. So-called assembly or maintenance factors have been identified for complex IV in human cells (Papadopoulou et al., 1999; Williams et al., 2004) as well as for complex I in *Neurospora crassa* (Kuffner et al., 1998).

1.1.3.4. Mitochondrial diseases

About 10 to 15 per 100,000 persons suffer from respiratory chain deficiencies (DiMauro and Schon, 2003). Diseases like Friedreich's ataxia, mitochondrial encephalopathy lactic acidosis and stroke-like episodes (MELAS), chronic external ophtalmoplegia (CPEO), and Leigh syndrome, are caused by mutations in nuclear or mitochondrial DNA. The phenotypic manifestations of mitochondriopathies are extremely diverse and can theoretically give rise to any symptom, in any organ or tissue (Munnich and Rustin, 2001). The most affected tissues

are usually those requiring a high energy production like brain, heart, kidney and skeletal muscle (Dahl and Thorburn, 2001). Thus, patients may suffer from seizures, ataxia, and blindness. They exhibit weakness and exercise intolerance and can develop cardiomyopathies and lactic acidosis, which is often fatal in infants. Respiratory chain deficiencies mostly start at birth or early childhood and many of the clinical symptoms are progressive and worsen over time. These multi-system disorders often have a fatal outcome.

Recently, neurodegenerative disorders like Huntington disease, Parkinson and Alzheimer's disease also have been associated with mitochondrial dysfunction (Orth and Schapira, 2001; Reichmann and Janetzky, 2000).

Over 100 mutations of mitochondrial DNA have been associated with human disease. They can affect protein-encoding genes, therefore modifying the structure of the respiratory chain complexes, which normally leads to dysfunction (Schapira, 2002). Disease-causing mutations can also be found in mitochondrially-encoded transfer or ribosomal RNAs, which cause a defect in the expression of all mitochondrially-encoded proteins. This can result in the downregulation of the activity of one or several respiratory chain complexes (Schapira, 2002).

More recently, mitochondriopathies have been associated with mutations in nuclear encoded subunits of the electron transport chain (Dahl and Thorburn, 2001), particularly those of complex I. Moreover, mutations in genes coding for mitochondrial proteins other than subunits of the complexes can also influence the functioning of the respiratory chain. These proteins may be responsible for the mitochondrial import of proteins, the correct assembly of the multiprotein complexes, or for the detoxification of ROS (Hirst et al., 2003; Vogel et al., 2004). Among the oxidative phosphorylation diseases, complex I deficiencies are probably the most common enzyme effect (Triepels et al., 2001).

Due to a wide range of mutations that can cause mitochondriopathies as well as different phenotypes in patients with the same mutation, treatment is limited and not very effective.

1.2. Apoptosis

In multicellular organisms, cells that are in excess or potentially harmful need to be eliminated. These cells undergo programmed cell death, or apoptosis, a genetically programmed cell suicide distinct from the pathological necrotic cell death, which occurs, for example, in response to tissue damage. Necrotic cells swell and burst, releasing their intracellular contents (Majno and Joris, 1995), which can damage surrounding cells and frequently cause inflammation. In contrast, apoptotic cells degrade all potentially toxic or immunogenic cellular components, shrink, and release membrane-bound apoptotic bodies, which are phagocytosed by other cells.

Apoptosis is essential for embryogenesis and aging, organ metamorphosis, and tissue homeostasis. During mammalian embryogenesis, the vast majority of cells, for example neurons unable to form synaptic connections with their targets or immature lymphocytes that lack appropriate receptor specificities, are extinguished by apoptosis. The hollowing-out of solid structures to form tubes, as in bones, is an example of apoptosis in organ metamorphosis (Vaux and Korsmeyer, 1999). In the case of infection, programmed cell death plays a crucial role in the removal of both the infected cells and the majority of the specific immune cells after the infection has ceased (Opferman and Korsmeyer, 2003). Dysregulation of apoptosis can therefore result in disease as is discussed below.

The morphological features of apoptotic cells, first observed by Kerr *et al.* in 1972, include the condensation of cytoplasm and nuclei, which leads to cell shrinkage (Kerr et al., 1972). Other hallmarks are the cleavage of chromatin, plasma membrane blebbing, and exposure of cell surface molecules such as phosphatidyl serines. The latter serve as "eat me"-signals and provoke the engulfment of the apoptotic cells by adjacent healthy cells (Fadok et al., 2000). Apoptosis therefore results in the complete elimination of the cell and its debris.

1.2.1. Signalling pathways leading to apoptosis

Apoptosis can be induced by extracellular stimuli (extrinsic pathway) and intracellular stimuli (intrinsic pathway, Figure 1-5). Both induce a signalling cascade that results in the apoptotic morphological phenotype described above.

Extracellular stimuli are instructive signals from neighbouring cells or soluble ligands. They are transmitted into the cell's interior by "death receptors", a specialized subset of the tumor necrosis factor receptor (TNF-R) superfamily, such as CD95-Fas (Krammer, 2000). Upon activation, the receptors aggregate and adapter proteins, like FADD, TRADD and RAIDD, form a death-inducing signalling complex (DISC) at the intracellular domain of the receptors, the death-domain (Kischkel et al., 1995). The DISC represents the caspase-activating complex of the extrinsic apoptotic pathway (Figure 1-5). Caspases are cysteine proteases that play a key role in the execution of the apoptotic programme and that are responsible for many morphological changes in apoptotic cells (Hengartner, 2000). They are highly conserved throughout evolution and are found in many species including mammals, fruit flies and nematodes. There are over a dozen distinct caspases in mammalian cells of which at least seven contribute to cell death. Apoptotic caspases are generally divided into two classes: the initiator caspases (caspases 2, 8, 9, 10) and the effector caspases (caspases 3, 6, 7). All caspases are expressed as catalytically inactive zymogens that must undergo proteolytic activation during apoptosis (Riedl and Shi, 2004). Initiator caspases are auto-activated, but require a multi-component complex, like DISC, to induce proximity (Muzio et al., 1998). Once activated, initiator caspases are responsible for the cleavage of more

caspases, both initiator and effector caspases, therefore declenching a caspase cascade. The effector caspases are activated by initiator caspases and cleave specific substrates which eventually leads to the death of the cell. The over 100 targets of effector caspases include nuclear lamins, cytoskeletal proteins, and an inhibitor of a DNAse (Nicholson, 1999), the latter provoking the degradation of DNA. Caspases also cleave anti-apoptotic proteins of the Bcl-2 family that act on mitochondria as described below. Thus, caspases are often called the central executioners of apoptosis. However, growing evidence suggests that programmed cell death can also take place when caspases are inhibited (Perfettini and Kroemer, 2003). Certain apoptosis-inducing players of the intrinsic pathway can act in a caspase-independent fashion.

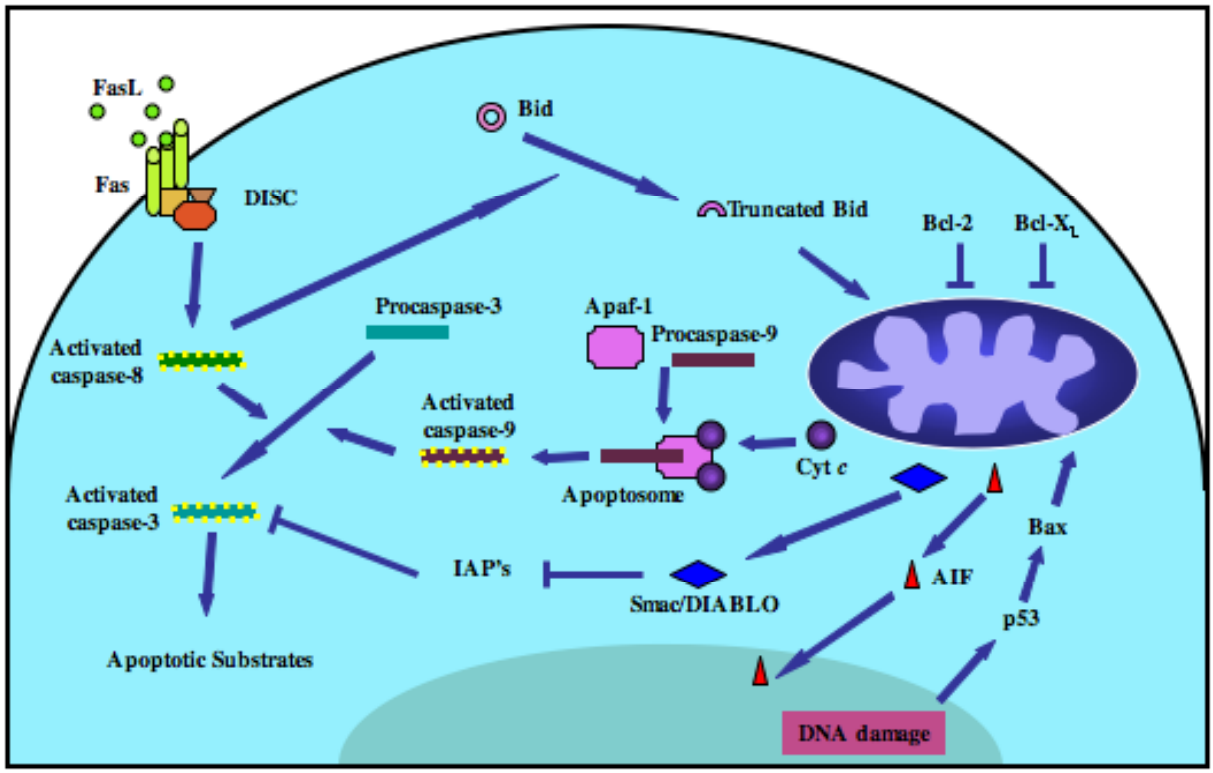

Figure 1-5. **Apoptotic pathways.** *Extracellular apoptotic stimuli, like FasL binding to Fas, trigger receptor clustering and the formation of the death inducing signalling complex (DISC), that includes different proteins like TRADD and FADD, at the intracellular domain of the receptors. DISC then induces activation of the initiator caspase-8, which in turn activates the effector caspase-3. Activated downstream caspases cleave different targets, thus contributing to the phenotype of an apoptotic cell. Intracellular apoptotic stimuli, like DNA damage, act on mitochondria via members of the Bcl-2 protein family that can provoke (eg Bax) or inhibit (eg Bcl-2) mitochondrial outer membrane permeabilisation (MOMP). After MOMP induction, proteins normally confined to the mitochondrial intermembrane space are released into the cytosol, where they exert their pro-apoptotic activities. Cytochrome c forms together with Apaf-1 and ATP the apoptosome which activates the pro-caspase-9, which then cleaves other caspases. AIF translocates to the nucleus where it participates in chromatinolysis. Smac/DIABLO blocks members of the IAP (inhibitor of apoptosis protein) family, which usually inhibit caspase activity. Note that not all mitochondrial proteins are shown that are known to be involved in the apoptotic process. The extrinsic and intrinsic pathway converge on mitochondria, one prominent example being Bid that gets cleaved by activated caspase-3. The truncated form of Bid (tBid) can then induce MOMP and thus liberate mitochondrial proteins.*

The intrinsic apoptotic pathway is triggered by intracellular cues like DNA damage, glucocorticoids, perturbations in redox balance, ceramide generation, or loss of growth factor signals. These diverse response pathways converge on mitochondria as described in the next paragraphs. Other organelles, like lysosomes or the endoplasmic reticulum can also be involved in apoptotic pathways (Jaattela et al., 2004; Rao et al., 2004).

1.2.2. Mitochondria and apoptosis

As mentioned earlier, a mitochondrion is not only the cell's powerhouse but also its arsenal. They sequester potentially cytotoxic proteins, which are released during apoptosis. It has been suggested that prokaryotes, which preceeded the mitochondria in evolution, released redox proteins to kill the ancestors of the eukaryotes (Punj and Chakrabarty, 2003). Thus, the liberation of cytotoxic proteins might be an ancient mechanism. In vital cells, most of them are localised in the mitochondrial intermembrane space, therefore, the initial step in the mitochondrial apoptotic pathway is the permeabilisation of the outer mitochondrial membrane.

1.2.2.1. Mitochondrial outer membrane permeabilisation (MOMP)

Several models have been proposed on how the mitochondrial membrane gets permeabilised involving different sets of proteins or mechanical events. The mechanism might depend on the apoptotic stimulus. However, it is suspected that there is a significant overlap between the different pathways (Green, 2005).

There is little doubt that members of the Bcl-2 family can induce MOMP either by inserting into the mitochondrial membrane and forming channels or by interacting with other proteins to induce the formation of pores (Sharpe et al., 2004). The protein family comprises more than a dozen proteins, which share one to four Bcl-2 homology (BH) domains. The family members fall into at least three groups that can interact and modify each other's activity: multidomain death antagonists (e.g. Bcl-2, Bcl-X_L) and death agonists (e.g. Bax, Bak) can protect or disrupt the integrity of mitochondrial membranes, respectively. The third group comprises pro-apoptotic BH3-only proteins (e.g. Bid, Bad, Noxa, Puma) that serve as ligands to activate pro-apoptotic Bcl-2 family members or inactivate anti-apoptotic Bcl-2 family members. Alterations in expression, subcellular localisation, phosphorylation status, and proteolytic processing of Bcl-2 family members can determine whether the cell death programme will be activated by MOMP induction.

A prominent example of a pro-apoptotic Bcl-2 protein is Bax, which, upon apoptosis induction, inserts into the outer mitochondrial membrane where it oligomerizes to form a channel (Wolter et al., 1997). The anti-apoptotic protein Bcl-2 is able to inhibit this MOMP induction by sequestering Bax in a monomeric state (Mikhailov et al., 2001). Bcl-2 is often upregulated in cancer cells, which hence cannot induce apoptosis via this intrinsic pathway.

The BH3-only protein Bid provides a link between the extrinsic and the intrinsic apoptotic pathway. Bid gets cleaved by caspase-8 which is activated in the caspase cascade induced by death receptor signalling (Li et al., 1998). The truncated form of Bid (tBid) inserts into the mitochondrial membrane where it acts in a similar pro-apoptotic fashion to Bax.

Besides the Bcl-2 family, there are other mitochondrial proteins that can induce mitochondrial membrane permeabilisation. A proposed model describes that the voltage-dependent anion channel (VDAC) in the outer mitochondrial membrane forms a permeability transition pore (PTP) by interaction with the adenine nucleotide transporter (ANT) in the inner mitochondrial membrane and other accessory proteins (Zamzami and Kroemer, 2001). The opening of the PTP allows the equilibration of ions between the matrix and the cytoplasm, which implies a dissipation of the inner mitochondrial membrane potential. Due to osmotic pressure, water enters and induces swelling of the matrix, which can be sufficient to break the outer mitochondrial membrane and thus produce MOMP.

Interactions between members of the Bcl-2 family and ANT or VDAC have been described pointing out the complexity of the MOMP process (Brenner et al., 2000; Marzo et al., 1998; Shimizu et al., 1999).

There are many controversial reports discussing the implication and importance of the different factors contributing to MOMP. It seems obvious that there are various mechanisms to release the mitochondrial intermembrane space proteins. These mechanisms might depend on cell type and apoptotic stimulus and probably overlap.

1.2.2.2. How do intracellular signals provoke MOMP?

Since there are many intracellular stimuli that can provoke mitochondrial membrane permeabilisation, the pathways leading to its induction are very diverse. DNA damage, for example, leads to the activation of the transcription factor p53 that can provoke apoptosis by both upregulation of expression of pro-apoptotic genes and direct interaction with pro-apoptotic mediators in the cytosol. Target genes of p53 are, among many others, the pro-apoptotic Bcl-2 family members Bax, Puma, and Noxa, and p53 itself (Vousden and Lu, 2002). Recently, it has been shown that cytosolic p53 directly activates Bax to permeabilise mitochondria (Chipuk et al., 2004).

Another link between intracellular stimuli and MOMP induction is a change in cytosolic pH, that can influence the localisation of Bax (Khaled et al., 1999). Changes in ion concentrations can also provoke apoptosis. Calcium, for example, that controls the Ca^{2+}-responsive phosphatase calcineurin. One of the targets of calcineurin is the BH3-only protein Bad that can exert its pro-apoptotic function once it is dephosphorylated (Wang et al., 1999).

1.2.2.3. Apoptotic factors released from mitochondria

There are many proteins released from the mitochondrial intermembrane space once the outer membrane is permeabilised, only a few of them, probably the most intensively studied, will be discussed here, namely Cyt *c*, endonuclease G (EndoG), Smac/DIABLO, and HtrA2/Omi. AIF is also one of these factors, but will be described in detail below.

Cyt *c* serves as an electron shuttle of the respiratory chain in vital cells and becomes lethal once it is released from the mitochondria during apoptosis. It is a very prominent example of a protein with a dual function. Once in the cytosol, Cyt *c* interacts with the apoptotic protease-activating factor-1 (Apaf-1) to form a multiprotein complex called apoptosome, which consists of Cyt *c*, Apaf-1, ATP, as well as caspase-9. The apoptosome induces caspase activation (Li et al., 1997). Bound by Cyt *c*, Apaf-1 easily associates with ATP and is able to recruit and activate the pro-caspase-9, which in turn recruits and activates caspase-3. Thus, the release of Cyt *c* provokes the cleavage of an effector caspase, which will then proteolyse downstream targets.

EndoG has been identified in the supernatant fraction of tBid-treated mouse liver mitochondria. Upon apoptosis and MOMP induction, EndoG translocates to the nucleus where it is involved in DNA degradation (Li et al., 2001). It is an evolutionary conserved protein, with orthologues known in bacteria and nematodes. The downregulation of the worm orthologue CPS-6 in *C.elegans* results in the impairment of DNA degradation and a delay in cell death (Parrish et al., 2001) indicating its important role in DNA degradation *in vivo*. In mammals two controversial reports have been published describing the effect of the genetic disruption of the EndoG gene: while it was first reported that the knock-out of the EndoG gene resulted in embryonic lethality (Zhang et al., 2003a), a second study showed that EndoG-null mice showed no abnormalities in development or programmed cell death (Irvine et al., 2005).

The human protein Smac and its murine orthologue DIABLO have also been found in supernatants of permeabilised mitochondria. Once released, they bind to different members of the inhibitor of apoptosis protein (IAP) family (Du et al., 2000; Verhagen et al., 2000). IAP's bind to caspases and counteract both their activation and their activity (Salvesen and Duckett, 2002). Smac/DIABLO displaces the IAP’s from caspases and therefore accelerates the apoptotic degradation process.

HtrA2/Omi is a ubiquitously expressed serine protease in the mitochondrial intermembrane space. Once in the cytosol, it exhibits a similar mode of action as Smac/DIABLO by inhibiting IAP's (Hegde et al., 2002). In addition, HtrA2/Omi can also induce apoptosis by its protease activity, acting independently of caspases (Saelens et al., 2004).

Mitochondrial apoptosis is regulated and controlled on several levels. If a small amount of Cyt *c* leaks out of the mitochondria, for example, it might not be sufficient to induce

apoptosis, because IAP's still block the caspase cascade. If there is a great damage to mitochondria or a high number of permeabilised mitochondria leading to the release of other factors like Smac/DIABLO and HtrA2/Omi, the IAP's get blocked liberating caspases and thus provoking cell death.

1.2.3. Nuclear events during apoptosis

One of the most defining hallmarks in apoptotic cells is DNA degradation. Nuclear changes during programmed cell death involve "pyknosis" (condensation of nuclei with clumped, condensed chromatin) and "karyorrhexis" (nuclear fragmentation)(Zamzami and Kroemer, 1999) and can be divided into two phases: stage I is characterised by rippled nuclear contours and partial chromatin condensation mostly around the nuclear membrane. In the later stage II, nuclear condensation is more advanced and the chromatin is tightly packed. At the end of stage II, nuclear bodies are formed.

The DNA is most likely degraded by the coordinated action of several enzymes in a multi-step process. During nuclear apoptosis stage I, DNA is cleaved into large-scale (50-300 kilobase) fragments. Subsequently, DNA is digested into oligonucleosomal sized (~180 base pairs) fragments, an event, which coincides with nuclear apoptosis stage II (Lecoeur, 2002).

Several enzymes have been identified as important factors in the apoptotic DNA degradation process. AIF is a protein that can induce chromatin condensation and large-scale DNA fragmentation. Its effect in apoptotic nuclei will be discussed in detail below.

One of the enzymes that can generate oligonucleosomal sized DNA fragments during apoptosis is the caspase-activated DNAse (CAD) (Liu et al., 1997). In vital cells, CAD is inactivated by the association to the inhibitor of CAD (ICAD) (Enari et al., 1998). After apoptosis induction, ICAD is cleaved by caspase-3 and CAD is liberated (Sakahira et al., 1998). The activity of CAD therefore depends on caspase activation. Oligonucleosomal DNA degradation can still be detected in CAD-deficient cells, which is probably due to the activity of EndoG. Once liberated from mitochondria during apoptosis, EndoG can induce caspase-independent DNA fragmentation (Li et al., 2001). It has been suggested that EndoG exhibits its DNA degrading activity in concert with both exonucleases and DNAse I in apoptotic cells (Widlak et al., 2001). Other factors like L-DNAse II (Torriglia et al., 2001), cathepsin B (Vancompernolle et al., 1998), or Acinus (Zamzami and Kroemer, 1999) have also been shown to be involved in apoptotic nuclear and DNA degradation.

Growing evidence points to cooperation between several enzymes in apoptotic chromatinolysis. AIF has been shown to interact with cyclophilin A in mammals and with EndoG in *C.elegans* (see below). In nematodes, the EndoG orthologue CPS-6 has also been found to cooperate with CRN-1 (Parrish et al., 2003) leading to the proposition of a

"degradosome" consisting of several proteins to induce DNA degradation (Parrish and Xue, 2003).

Oligonucleosomal fragmentation of DNA can also take place after the engulfment of the apoptotic cell by phagocytes. The lysosomal DNAse II cleaves DNA in the endocytic pathway and hence assures the complete removal of DNA (McIlroy et al., 2000).

1.2.4. Caspase-independent apoptosis

As mentioned before, members of the scientific community do not all share the same opinion on the importance of caspases in apoptosis. There is no doubt that caspases are very efficient players in the apoptotic process. However, it was shown in a growing number of cell death scenarios that apoptosis can be induced by signalling pathways that do not involve or require caspases (Cerisano et al., 2004; Deas et al., 1998; Liu et al., 2004; Lorenzo and Susin, 2004).

Several pro-apoptotic proteins can act independently of caspases. The permeabilisation of the outer mitochondrial membrane does not necessarily rely on caspase activation, Bax and Bak can be activated by p53 or BH3-only proteins like Puma, Noxa, and dephosphorylated Bad (Kroemer and Martin, 2005). Downstream effectors of MOMP like EndoG and HtrA2/Omi can execute DNA degradation as well as proteolysis, respectively, in a caspase-independent fashion (Saelens et al., 2004). Interestingly, Cyt *c* can also translocate to the nucleus and initiate chromatin condensation in the absence of caspase activation (Nur et al., 2004). AIF is another example of a caspase-independent pro-apoptotic protein and will be described below.

It is therefore not surprising that cells also undergo apoptosis in the presence of caspase inhibitors. However, *in vivo*, it is most likely that caspase-dependent and caspase-independent pathways occur in parallel and, most importantly, activate each other. The importance and order of activation of involved molecules probably depends on cell type and apoptotic stimulus (Cande et al., 2004a).

1.2.5. Apoptosis and disease

Dysregulation of apoptosis plays a crucial role in many diseases.

Resistance to apoptosis is, next to limitless replicative potential, a fundamental requirement for the development of cancer. Cells that are cancerogen should eliminate themselves by programmed cell death, but if mutations in tumor suppressor genes stop the cell from undergoing apoptosis, one very important control mechanism is abrogated often resulting in tumor formation (Hanahan and Weinberg, 2000). Failure of apoptosis can also provoke autoimmune diseases.

Increased cell death occurs in neurodegenerative disorders, such as Alzheimer's disease (Vila and Przedborski, 2003), and plays a major role in the pathology of stroke (Martin-Villalba et al., 2001) and heart attack (Scott, 2004).
Many pathogens abuse the apoptotic pathway of the human host to their advantage. The human immunodeficiency virus (HIV), for example, escapes the immune system by inducing apoptosis in immune effector cells, such as T cells (Gougeon, 2003).
By manipulating apoptosis through drugs, it may offer new possibilities for the prevention and treatment of these illnesses.

1.3. The apoptosis-inducing factor AIF

The apoptosis-inducing factor (AIF) was first discovered and cloned in Dr.Guido Kroemer's laboratory in 1999 as one of the proteins in the supernatant of permeabilised mitochondria (Susin et al., 1999). His group further showed that recombinant AIF causes chromatin condensation as well as large-scale DNA fragmentation in isolated nuclei. In healthy cells, AIF is confined to the mitochondrial intermembrane space. Upon apoptosis induction, AIF translocates from the mitochondria to the nucleus where it takes part in apoptosis-associated chromatinolysis (Susin et al., 1999). Since then, numerous papers have been published on AIF's function in apoptosis pointing to an important role in several cell death scenarios like ischemia-reperfusion (Zhu et al., 2003), a condition relevant to brain damage and myocard infarction, or cavitation of embryoid bodies, the very first wave of cell death during mouse morphogenesis (Joza et al., 2001). AIF is a phylogenetically old protein with its orthologues found in distinct species including *M.musculus*, *C.elegans*, and *S.cerevisiae* (Cande et al., 2002). Results on the implication of caspases in AIF-induced death have been controversial and it seems that the cell type and the apoptosis-inducing stimulus determine whether AIF acts in a caspase-dependent or independent manner (Cande et al., 2004a). Recently, a vital function of AIF has been proposed, namely a radical scavenger function inside the mitochondria (Klein et al., 2002).

1.3.1. AIF expression, structure, and localisation

The mammalian AIF gene is localised on the X chromosome. In human cells it is found within the region Xq25-26, which is syntetic to the murine X chromosome region A6, where the murine AIF gene is located (Daugas et al., 2000a). AIF seems to be ubiquitously expressed in all tissues throughout embryonic development as well as adulthood. There have been reports on downregulation of AIF expression with age in parts of the brain not including the cerebellum (Zhu et al., 2003) and, controversially, an increase of the expression level in cerebellum maturation with its peak in adulthood (Cao et al., 2003). These different observations may be explained by tissue specific expression levels. However, the

incompetence of AIF-deficient murine embryonic stem cells to develop into mice leaves little doubt on the importance of AIF's role in early morphogenesis (Joza et al., 2001).

There are only few reports on transcriptional regulation of AIF expression. In rat brains after focal ischemia (Zhao et al., 2004) and in human coronary artery endothelial cells after treatment with the pro-atherosclerotic oxidized low-density lipoprotein (Zhang et al., 2003b), enhanced AIF expression led to excessive apoptosis. In the vast majority of studies, including others on ischemia in rat brains, AIF's expression level was unaffected. This is to be expected since its pro-apoptotic activity is also controlled by other means, such as the confinement to mitochondria and the interaction with the endogenous inhibitor HSP70 as described below (Ravagnan et al., 2001).

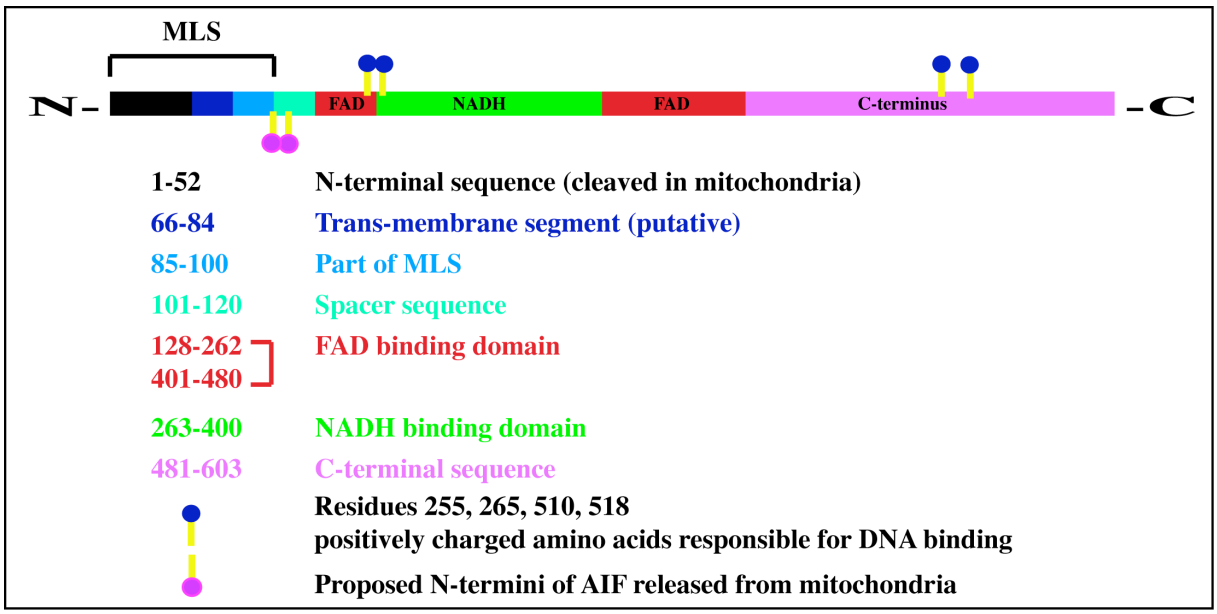

Figure 1-6. **Linear structure of human AIF.**

The human AIF precursor consists of 612 amino acids (613 in mouse, Figure 1-6) which bare a highly significant homology with oxidoreductases from eukaryotic and prokaryotic kingdoms. Based on sequence alignments and phylogram calculations, the C-terminal domain (amino acids 128-612) possesses significant homology with NADH ferredoxin reductase from both eubacteria and archaebacteria (Lorenzo et al., 1999) (Susin et al., 1999). Among eukaryotes, several plant ascorbate oxidoreductases closely resemble AIF (Lorenzo et al., 1999). In accord with its structure, the mature protein AIF is a flavoprotein that binds FAD and exhibits an oxidoreductase activity (Susin et al., 1999) (Miramar et al., 2001) (see 1.3.8 Vital functions of AIF). This mature form of the protein resides in the intermembrane space of mitochondria of healthy cells (Figure 1-7). It is generated by cleaving off part of the 101 amino acid mitochondrial localisation sequence at the N-terminus of the ~ 67kDa precursor protein after import into the organelle (Susin et al., 1999). The molecular size of the processed mitochondrial AIF of ~ 57kDa was recently questioned by

Dr. Mihara's group estimating mitochondrial AIF to be a ~ 62kDa protein (Otera et al., 2005). His group also showed that, in HeLa cells, an N-terminal sequence of only 52 amino acids was cleaved off in the matrix by the mitochondrial processing peptidase MPP. A cluster of hydrophobic amino acids (residues 66-84) might constitute a transmembrane segment anchored in the inner membrane and exposing the C-terminal portion of AIF to the intermembrane space (Otera et al., 2005). The conclusion that AIF is a type-I inner membrane protein is consistent with a previous report that found AIF to be associated with the mitochondrial inner membrane (Arnoult et al., 2002).

The overall crystal structures of both human and murine AIF have been elucidated. Both proteins, which share an identity of 92%, possess three domains apart from the mitochondrial localisation sequence at the N-terminus, namely an FAD binding domain (amino acids (aa)122-262 and 400-477 in mouse AIF; aa 128-262 and 401-480 in human AIF), an NADH binding domain (aa 263-399 in mouse AIF; aa 263-400 in human AIF) and a C-terminal domain (aa 478-610 in mouse AIF; 481-603 in human AIF) (Ye et al., 2002) (Mate et al., 2002) (Figure 1-6). AIF possesses a glutathione reductase-like fold, with an insertion in the C-terminal domain (aa 509-559) not found in glutathione reductase (Mate et al., 2002). This region contains a PEST sequence characteristic for proteins with rapid turnover, which could explain the disappearance of AIF in the cytosol of activated T lymphocytes (Dumont et al., 2000). The sites for the noncovalent binding of FAD and relatively weak binding for NADH have been precisely mapped, and the mutants E313A and K176A have been shown to reduce FAD binding (Mate et al., 2002). Intriguingly, the C-terminal region of AIF also contains an RNA binding motif (aa 549-567), which is typical of some ribosomal proteins and suggests a possible interaction between AIF and RNA (Lorenzo and Susin, 2004). As opposed to RNA, AIF's interaction with DNA has recently been demonstrated. Strong positive charges on the surface of AIF were shown to bind to DNA in a sequence-independent manner (Ye et al., 2002). Although the crystal structure of murine AIF did not reveal any obvious DNA-binding structural motifs, it has been speculated, based on the dimensions of a groove formed by dimeric murine AIF, that this groove could serve to accommodate a double-stranded DNA molecule (Lorenzo and Susin, 2004). The capacity to bind DNA serves AIF to propagate apoptosis once it has translocated to the nucleus after cell death induction.

1.3.2. Isoforms

The AIF gene consists of 17 exons. There are two known isoforms for human and murine AIF, which differ only in the alternative usage of exon IIa or exon IIb for isoform 1 and isoform 2, respectively. The affected sequence is part of the mitochondrial localisation sequence, but studies with GFP-fusion proteins using AIF isoform 1 or 2 revealed mitochondrial localisation

in both cases (Loeffler et al., 2001). It remains to be determined whether isoform 2, which is less abundant in cells, has another, maybe tissue specific, function, different from that of isoform 1.

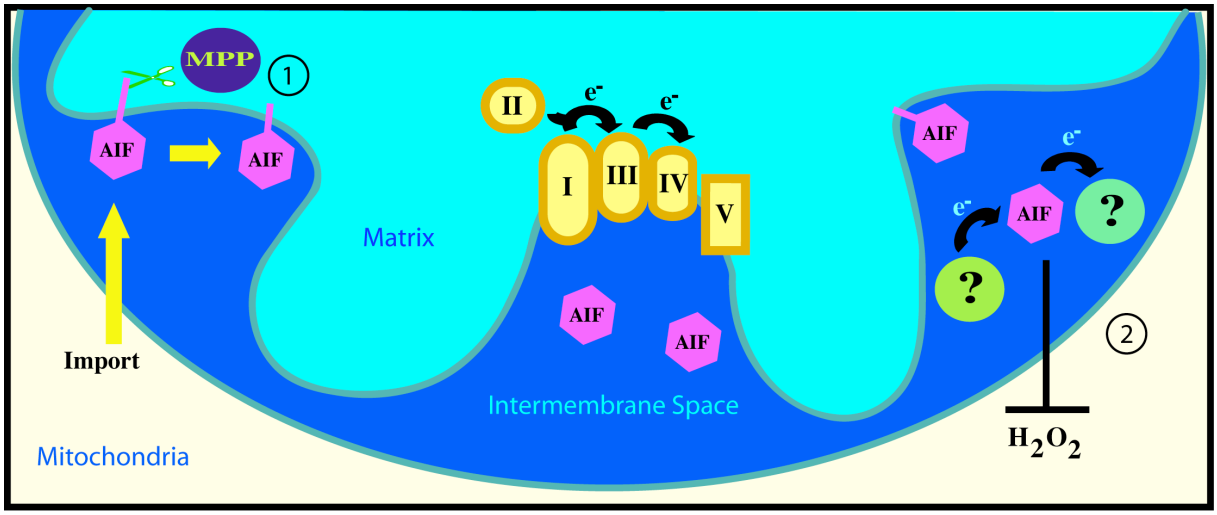

Figure 1-7. **Mitochondrial processing and functions of AIF.** *After AIF is imported into mitochondria, its N-terminal sequence is cleaved off by the mitochondrial processing peptidase MMP (1). AIF is an oxidoreductase, whose electron donor and acceptor in cells are not known. AIF might be involved in radical scaveging (3). Due to controversial reports, AIF is shown both attached to the inner membrane and entirely in the intermembrane space.*

1.3.3. Non mammalian orthologues and mammalian homologues

Although most of the facts known about AIF are based on experiments in the mammalian system (murine and human cells), studies of orthologues have given important insights into the evolution of AIF's functions in apoptosis and inside the mitochondria.

AIF is a phylogenetically old flavoprotein with orthologues in most, if not all eukaryotic species including insects, nematodes, fungi, and plants (Cande et al., 2002). This, the significant identity between the human and murine AIF (92%), as well as interesting results with orthologues from the nematode *C.elegans*, the slime mold *D.discoideum*, and the fungus *S.cerevisiae*, point to well conserved functions of AIF throughout the eukaryotic kingdom.

In *C.elegans*, the identification of the worm orthologue of AIF (WAH-1) and its involvement in apoptosis was an important discovery in order to prove the implication of mitochondria in worm cell apoptosis. Until then it was believed that mitochondria play a minor role, since caspases are not activated via a Cyt c-dependent pathway in those cells, but rather directly by homologues of BH3-only proteins. WAH-1 exhibits 37% identity and 54% similarity to the AIF protein (Wang et al., 2002). Wang *et al*. showed that the worm orthologues of AIF and EndoG are released from the mitochondria during apoptosis and cooperate during chromatinolysis. This cooperation is discussed in more detail in section "How does AIF exert its effect on DNA?".

The slime mold, although a single-cellular organism, manifests, while undergoing cell death, apoptotic features like phosphatidylserine exposure on the outside of the plasma membrane, loss of mitochondrial membrane potential, and DNA fragmentation (Arnoult et al., 2001). It was thus not surprising to discover a pro-apoptotic AIF orthologue, which also translocates from the mitochondria to the nucleus. Functional similarity to human AIF is striking, as the *D.discoideum* homologue could trigger the breakdown of mammalian nuclei in a cell-free system (Arnoult et al., 2001).

Another unicellular organism *S.cerevisiae* undergoes apoptosis-like cell death as a consequence of oxidative stress or chronological aging. Although apoptosis in yeast was thought to be entirely dependent on the caspase homologue YCA1, the AIF orthologue Aif1p was recently discovered in *S.cerevisiae* and shown to be pro-apoptotic (Wissing et al., 2004).

Two homologues were found inside the human genome, PRG3/AMID and the AIF-like protein AIFL. PRG3/AMID (p53-inducible gene 3/ AIF-homologous mitochondrion associated inducer of death) is located in the cytoplasm or confined to the mitochondria according to two conflicting reports (Wu et al., 2002) (Ohiro et al., 2002). The gene has p53-responsive elements and is thus upregulated by p53 during apoptosis. It clearly exhibits pro-apoptotic activity, which is caspase-independent, but, unlike AIF's cytotoxicity, not inhibited by Bcl-2. The latter would point to an ectopic (non-mitochondrial) localisation of the protein.
AIF-like protein (AIFL) shares 35% homology with AIF, is also localised to the mitochondria, and is involved in caspase-dependent cell death (Xie et al., 2005).

1.3.4. The apoptotic function

There are over 200 articles published on AIF, most of them focus on the apoptotic activity of this protein. In many cell types, overexpression of AIF can induce cell death, while inhibition of its expression or activity can delay or abrogate apoptosis. During the process of apoptosis, mitochondrial membrane permeabilisation regulated by members of the Bcl-2 protein family enables AIF, along with other potentially cytotoxic proteins normally confined to the mitochondria like Cyt c, EndoG, Omi/HtrA2, and Smac/DIABLO, to exert its pro-apoptotic function (Figure 1-8).

1.3.4.1. Cell-free systems

Studies in cell-free systems gave important insights on how AIF actually induces cell death. Recombinant AIF missing its mitochondrial localisation sequence (MLS) AIFΔ1-100, thus mimicking the released form of the protein, rapidly induces peripheral chromatin condensation and large-scale (50 kbp) DNA fragmentation in isolated nuclei, yet fails to cause oligonucleosomal DNA fragmentation (Susin et al., 1999) (Susin et al., 2000). However, the protein has no degrading effect on naked DNA, suggesting that AIF relies on a

co-factor to exert its effect in the nucleus (Susin et al., 1999). Moreover, mitochondria exposed to recombinant AIF, in the presence of cytosolic extracts, undergo membrane permeabilisation and release proteins like Cyt c and pro-caspase-9 (Susin et al., 1999).

1.3.4.2. In vivo

Similar effects are seen in cells, when recombinant AIF is microinjected into the cytoplasm (Susin et al., 1999) or when AIF∆1-100 is overexpressed (Loeffler et al., 2001). Signs of apoptosis appear within three hours in the case of microinjection and within 24 hours after transfection with AIF-expressing plasmids. AIF causes nuclear chromatin condensation and affects mitochondria leading to a loss of the transmembrane potential and the release of Cyt c (Loeffler et al., 2001; Susin et al., 1999). Overexpressed full-length AIF is located in the mitochondria and thus does not induce apoptosis (Loeffler et al., 2001).

These functions of AIF play an important role in the life of a cell, as was proven by studies on endogenous AIF, which has been shown to be involved in numerous cell death scenarios including different cell types and various pro-apoptotic stimuli. AIF translocation to the nucleus was first shown in fibroblasts after ATP depletion or after treatment with the serine-threonine kinase inhibitor staurosporine (STS) (Susin et al., 1999). In addition, the topoisomerase II inhibitor etoposide, the DNA damaging drugs cisplatin and adriamycin, and the second messenger ceramide also induced the mitochondrio-nuclear translocation of AIF (Daugas et al., 2000b). Overexpression of the membrane permeabilising protein Bax in HeLa cells (Arnoult et al., 2002) or apoptosis induction by oxidative stress in human cervical cancer cells (Kang et al., 2004) similarly resulted in AIF release and cell death. In human immune cells, AIF translocation was observed after stimulation with granulysin (Pardo et al., 2001) or radiation (Murahashi et al., 2003). Unfortunately, not all tested cell death models involving AIF can be mentioned here. Nevertheless, because of very convincing data, the role of AIF in neuronal cell death needs to be stressed. Numerous research groups have shown the implication of AIF in neuronal apoptosis after induction by p53 (Cregan et al., 2002) or hypoxia ischemia (Cao et al., 2003; Zhang et al., 2002; Zhao et al., 2004; Zhu et al., 2003). AIF was found to translocate to the nucleus and to induce large-scale DNA fragmentation in neuronal cell lines (Cregan et al., 2004) as well as in neonatal (Zhu et al., 2003) and adult rat brains (Zhang et al., 2002). Ischemia also efficiently induced mitochondrio-nuclear translocation of AIF in rat hearts (Kim et al., 2003) pointing to a role of AIF as a death inducer especially sensitive to hypoxia.

1.3.4.3. Downregulation of AIF

The data discussed above might suggest that the redistribution of AIF is a general feature of the apoptotic process. However, there have been reports on apoptotic processes where AIF does not translocate to the nucleus and therefore cannot act pro-apoptotically (Roue et al.,

2003). To find out whether AIF could be useful as a therapeutic target, it needs to be determined whether AIF is not only part of the apoptotic process, but also essential in the killing of a cell. Inhibiting apoptosis by blocking AIF's translocation or function has proven the importance of AIF as a pro-apoptotic player. The most dramatic case is the knockout of the AIF gene by genetic recombination in mouse embryonic stem cells. These AIF-deficient cells ($AIF^{-/y}$) exhibit a complete block in cavitation, a wave of controlled programmed cell death in embryonic development essential for gastrulation. Thus, the AIF-knockout cells do not develop into mice, apparently because they cannot undergo the cavitation-associated apoptosis (Joza et al., 2001). Embryonic stem cells deficient in other apoptotic regulators like Apaf-1, caspase-9 or caspase-3 do not show any defects in cavitation pointing to an essential role for AIF in this particular cell death (Joza et al., 2001). Interestingly, $AIF^{-/y}$ ES cells are sensitive to apoptosis induced by STS, etoposide, or UV radiation, yet they are resistant to cell death induction by serum withdrawal and menadione, the latter only in the presence of the caspase inhibitor z-VAD.fmk (Joza et al., 2001). Therefore, AIF seems to play an essential role only in response to some pro-apoptotic stimuli as well as in embryonic morphogenesis.

Suppression of AIF by small interfering RNA (siRNA) has recently been used to study AIF's importance in cell death. AIF downregulation in cervical cancer cells effectively protected against oxidative stress induced apoptosis (Kang et al., 2004). Similar protective effects of AIF siRNA were found in UVA-treated Raji cells (Yuan et al., 2004). Injection of an AIF-specific antibody also prevents chromatin condensation and cell death in STS-treated Rat-1 (Susin et al., 1999) and in U1810 cells, a non-small-cell-lung-carcinoma cell line (Gallego et al., 2004).

Overexpression of anti-apoptotic Bcl-2 blocks AIF translocation and thus its effect on nuclear DNA in different cell types including fibroblasts (Susin et al., 1999), neurons (Cregan et al., 2002; Zhao et al., 2004), and lymphocytes (Pardo et al., 2001). Even though it does prove that the release of AIF is regulated via mitochondrial membrane permeabilisation, it cannot prove AIF's implication in apoptosis. Bcl-2 overexpression also efficiently blocks the release of other pro-apoptotic factors from the mitochondria, namely Cyt c, EndoG, Omi/HtrA2, and Smac/DIABLO. Thus, if apoptosis is inhibited by Bcl-2, one cannot conclude that it is due to the inhibition of AIF's translocation.

Downregulation of WAH-1 by RNA interference in *C.elegans* proves that this gene is essential for apoptosis occurring during the development of the worm (Wang et al., 2002). The lack of AIF delays the removal of apoptotic bodies and allows extra cells to exist. Moreover, the apoptotic defect found in *ced 3* and *ced 4* mutants (the orthologues of caspase-9 and Apaf-1, respectively) can be exacerbated by the loss of AIF (Wang et al.,

2002). Cells with a defect in the gene for the orthologue of EndoG, CPS6, were not affected by the downregulation of AIF pointing to a cooperation of these genes in apoptosis.
The knockout of the yeast AIF homologue *aif1* renders more cells resistant to oxidative stress induced apoptosis. Conversely, AIF1p overexpression induces excessive killing after stimulation with hydrogen peroxide suggesting that the protein, which shows 41% similarity to AIF, is responsible for apoptotic effects in yeast. AIFp1 is localised to mitochondria, translocates to the nucleus during cell death, and recombinant protein exhibits a weak nuclease activity on plasmid DNA (Wissing et al., 2004).

1.3.5. AIF translocation

The mitochondrial localisation of AIF and the translocation to the nucleus seem to be a very conserved way of regulating AIF's activity since it was found in many organisms throughout the eukaryotic kingdom including mammals, worms, and fungi.

1.3.5.1. How is AIF released?

There are different models of the liberation process of AIF. One factor they all have in common is mitochondrial membrane permeabilisation. The fact that Bcl-2 can prevent AIF release from mitochondria, and is known to inhibit the pro-apoptotic effects of Bax and Bak, strongly suggests a role of the latter in the liberation process of AIF (Susin et al., 1999; Zhao et al., 2004). This conclusion is further supported by the finding that overexpression of Bax induces AIF's release from mitochondria (Arnoult et al., 2002).
Intriguingly, recombinant Bax or the truncated form of Bid cannot liberate AIF from isolated mitochondria, yet they liberate Cyt c. Dr. Ameisen's group explains this phenomenon by AIF's association to the inner mitochondrial membrane, which has been recently confirmed (Otera et al., 2005; Uren et al., 2005). If that was the case, AIF is likely to require a two-step process to be liberated from the mitochondria, similar to Cyt c, which is anchored to cardiolipin (Ott et al., 2002). In addition to the permeabilisation of the outer mitochondrial membrane, a protease in the intermembrane space, which remains to be determined, has to cleave AIF from the inner membrane giving rise to the ~ 57kDa pro-apoptotic form of AIF (Otera et al., 2005). Indeed, most recently, two different groups found that AIF needs to be cleaved by cysteine proteases in order to be released from mitochondria. This can either happen in a Ca^{2+}-dependent manner involving the calcium-activated protease calpain or in a Ca^{2+}-independent manner (Polster et al., 2005), in which case the cathepsins B, L, and S process AIF (Yuste et al., 2005a). All of them generate a truncated form of AIF, which starts at the amino acid 103 of the N-terminus.
It needs to be mentioned that AIF itself has a permeabilising effect on mitochondria liberating more AIF as was shown by microinjection of recombinant AIF into AIF-GFP transfected Rat-1 cells. AIF in the cytosol could release AIF-GFP, as well as Cyt c-GFP proteins, normally

confined to mitochondria, suggesting AIF's engagement in a positive feedback amplification loop (Loeffler et al., 2001). How AIF exerts its effect on mitochondria remains a conundrum, although it seems clear that AIF recruits another cytosolic factor, since the recombinant protein can only permeabilise mitochondria in a cell-free system in the presence of cytosolic extracts (Susin et al., 1999).

An interesting interaction has been found between AIF and the nuclear DNA-repair and protein-modifying enzyme Poly(ADP-ribose) polymerase 1 (PARP-1) (Yu et al., 2002). In response to DNA damage, PARP-1 is activated and transfers 50-200 residues of poly(ADP-ribose) (PAR) to acceptor proteins such as DNA polymerases, histones, topoisomerases, transcription factors, and itself using NAD^+ as a substrate. That way PARP-1 regulates DNA repair, transcription, and replication, as well as other protein activities in order for the cell to survive (Hong et al., 2004). Overactivation of PARP-1, for example through excessive DNA damage induced by radical oxygen species (ROS), can lead to cell death. Since PARP-1 is cleaved by caspases, this pathway only occurs in caspase-independent scenarios. Further, PARP-1 mediated apoptosis seems to be dependent on AIF translocation to the nucleus. Fibroblasts exposed to H_2O_2 or DNA-alkylating agent to trigger PARP-1 mediated cell death were protected against death by microinjection of AIF antibodies into the cytosol. Moreover, PARP-$1^{-/-}$ fibroblasts failed to exhibit the AIF mitochondrio-nuclear translocation seen in their wild-type counterparts (Yu et al., 2002). These results strongly suggest a role of AIF as a downstream effector in PARP-1 induced cell death. Several models have been proposed on how the nuclear factor PARP-1 can stimulate AIF in the mitochondria. Which one of them is correct remains to be determined, although a combination of these models also seems possible. PARP-1 might initiate a specific signal by the ADP-ribosylation of a key regulatory protein that can translocate to the cytosol and/or the mitochondria. Recently, PARP-1 was discovered in the mitochondria and inhibition of this protein prevented AIF release of mitochondria (Du et al., 2003). Whether the interaction between these two molecules is direct or indirect is not clear and localisation of PARP-1 to the mitochondria remains controversial (Ye et al., 2002). Another model suggests that the NAD^+ and ATP depletion caused by intense NAD^+ utilization during PARP-1 overactivation induces the mitochondrial membrane permeabilisation and AIF release (Alano et al., 2004). Finally, PAR could play a role as a signalling molecule in cell death and translocate from the nucleus to the mitochondria (Hong et al., 2004). The PAR polymer is able to bind to many different proteins and might activate or inhibit cell death regulatory proteins. One could speculate that it might be PAR that activates the protease required to cleave AIF off the mitochondrial inner membrane.

1.3.5.2. Are caspases required?

Over the last years there have been controversial views on caspase involvement in AIF induced apoptosis. There is no doubt that caspases can trigger mitochondrial membrane permeabilisation, via members of the Bcl-2 protein family, and thus the release of Cyt c, EndoG, AIF and other pro-apoptotic factors. However, several groups have shown that AIF mitochondrio-nuclear translocation can occur in the presence of caspase inhibitors. This is the case, for example, during apoptosis in HIV-infected primary T cells (Ferri et al., 2000) and after ischemia in neonatal rat brains (Zhu et al., 2003) as well as in rat hearts (Kim et al., 2003). When AIF is microinjected into Rat-1 cells, the pan-caspase inhibitor z-VAD.fmk cannot abrogate the deadly effect of the recombinant protein, either (Susin et al., 1999). In contrast, Arnoult and colleagues have found that, in a cell-free system, recombinant Bax or the truncated form of Bid can induce the release of Cyt c, yet fail to liberate AIF and EndoG pointing to the requirement of additional factors (Arnoult et al., 2003). However, this could be explained by the involvement of calpain and cathepsins in the AIF liberation process (Yuste et al., 2005a). In HeLa cells, Bax overexpression, staurosporine or actinomycin D did not induce AIF translocation into the nucleus in the presence of caspase inhibitors (Arnoult et al., 2002). The AIF homologue WAH-1 in *C.elegans* has been described to act in a mostly caspase-dependent manner, too. In animals lacking the functional caspase homologue Ced3, a greatly attenuated number of cells exhibit WAH-1 release from mitochondria (Wang et al., 2002).

These controversial results demonstrate the complexity of the apoptotic process. They can, nevertheless, be explained by a cell-type specific involvement of caspases in AIF-induced apoptosis. That not only the cell type, but also the stimulus can influence AIF's dependency on caspases is nicely demonstrated in AIF-knockout embryonic stem cells. While apoptosis induced by serum withdrawal is completely abrogated in the absence of AIF, cell death in these cells induced by menadione is only inhibited when the caspase inhibitor z-VAD.fmk is present (Joza et al., 2001). Thus, there are obviously two pathways by which AIF can come into action, one requiring caspase activation and the other one not requiring caspase activation. Which one of them is activated first depends on the cell type and the apoptotic stimulus (Cande et al., 2004a). It is important, that these two pathways can interact with and amplify each other. The facts that there are no homologues of "classical" caspases in the slime mold *D.discoideum*, and that AIF translocation still occurs, suggest that the caspase-independent release of AIF evolved earlier (Arnoult et al., 2001). Moreover, the implication of lysosomes (Bidere et al., 2003; Jaattela et al., 2004) or ER-dependent Ca^{2+} release (Mattson et al., 2000) in AIF's liberation of the mitochondria indicates that there might be other factors involved in AIF release that substitute for caspases in certain cell death scenarios.

Apoptosis induced by PARP-1 overactivation and AIF release cannot occur when caspases are activated since PARP-1 is one of the primary targets of effector caspases and therefore cleaved when caspases are active. Accordingly, AIF translocation stimulated by oxidative stress or glutamate receptor stimulation via PARP-1 is caspase-independent (Yu et al., 2002). In neurons, immunodepletion of AIF prevented p53-induced apoptosis in Apaf$^{-/-}$ cells, but had no effect in wild-type cells (Cregan et al., 2002), pointing to an AIF-dependent alternative pathway in those cells that is activated when caspases are inactive.

In conclusion, there are caspase-dependent and independent ways to induce AIF translocation, which are, depending on cell type and death inducing stimulus, activated one at a time or one after the other in a specific order (Cregan et al., 2004).

1.3.5.3. When is AIF released?

Another subject of controversy is the order of the release of mitochondrial pro-apoptotic factors. Different reports discuss whether the release of Cyt c precedes that of AIF, thus activating caspases upstream of AIF, or vice versa. It was first shown after staurosporine treatment that AIF was liberated before Cyt c, in accord with AIF being activated before caspases (Daugas et al., 2000b). However, it remains possible that these immunofluorescence studies were not sufficiently sensitive to detect small amounts of Cyt c released before AIF. But other research group found similar results in different cell lines: in fibroblasts when apoptosis was induced by PARP-1 overactivation, AIF was also seen in the nucleus before Cyt c in the cytoplasm (Yu et al., 2002). Cerebral hypoxia-ischemia in neonatal rat brains caused AIF translocation immediately after the insult, while Cyt c release occurred first after 30 minutes and had its peak later than AIF, pointing to different modes of release (Zhu et al., 2003). In myocardial cell death by ischemia-reperfusion, hardly any Cyt c release was detected, although AIF translocation played a crucial role. Similarly, in staurosporine-treated T cells, AIF mitochondrial liberation occurred independently of Cyt c. In contrast to this convincing amount of data are reports where Cyt c release is detected well before that of AIF suggesting a cell-type and stimulus-specific order similar to that of caspase dependency. In HeLa cells, AIF stays in the mitochondria until Cyt c has activated the caspase cascade via the “apoptosome” consisting of Cyt c, Apaf-1, caspase-9 and ATP. This observation has led to the following model: during apoptotic signalling, the permeabilisation of the outer mitochondrial membrane may initially not be extensive, leading to the release of only smaller molecules like Cyt c, which would then indirectly elicit the feedforward loop, through caspase activation, to induce liberation of other intermembrane space proteins including AIF (57kDa). In accord with this theory is the anchorage of AIF at the inner membrane that needs to be cleaved in order to liberate AIF. The required cysteine proteases

calpain and cathepsins depend on activation that can involve caspases (Foghsgaard et al., 2001; Johnson, 2000) and occur downstream of Cyt c release.

Just like the dependency on caspases, the order of the release of AIF and Cyt c seems to depend on cell type and apoptotic stimulus. These differences may be due to specific processing of AIF and Cyt c, required to release them from the inner membrane. In some experimental system, the processing machinery liberating AIF may be activated before that of Cyt c and *vice versa*. There may even be different pools of AIF, like for Cyt c, that can also be affected differently in certain cell types.

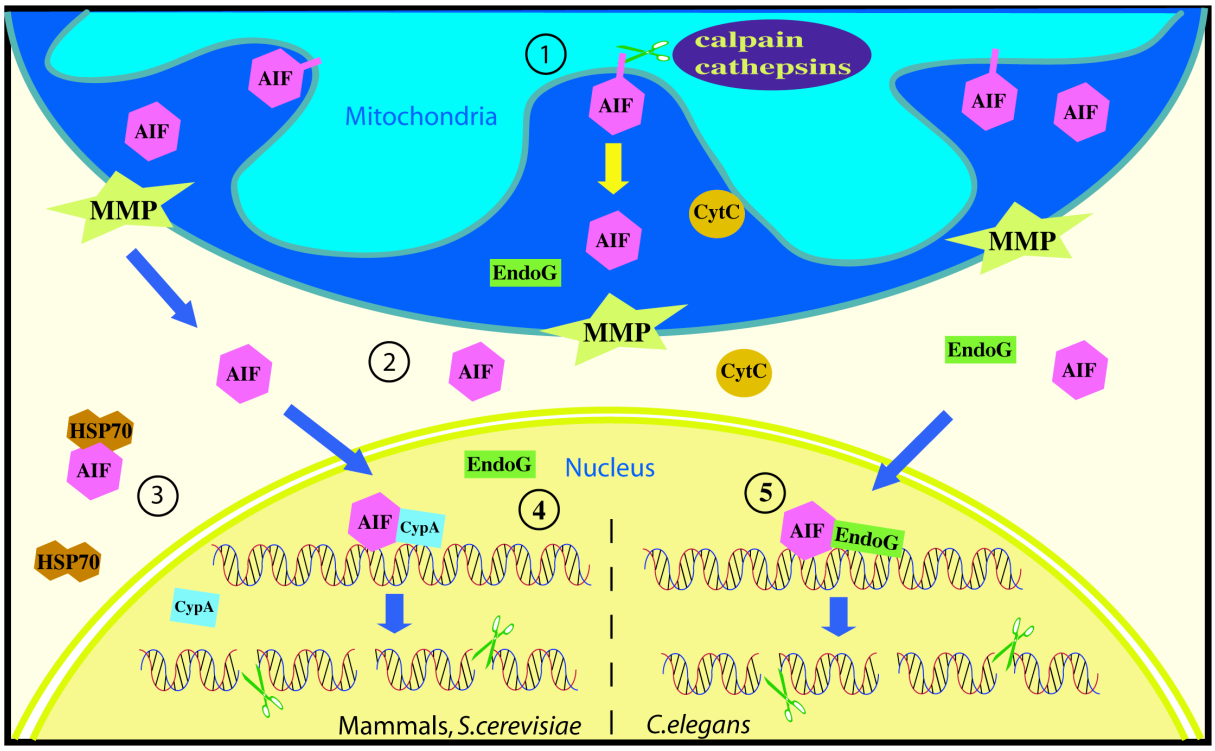

Figure 1-8. **AIF's functions in apoptosis.** *After apoptosis induction, AIF is cleaved off the inner mitochondrial membrane, probably by calpein or cathepsin (1) and mitochondrial membrane permeabilisation (MMP) allows its release into the cytosol together with other pro-apoptotic factors like cytochrome c (Cyt c) and endonuclease G (EndoG, 2). Note, that not all proteins released from mitochondria are shown. If AIF is not sequestered in the cytosol by Hsp70 (3), the protein translocates to the nucleus, where it interacts with cyclophilin A (CypA) in mammals and S.cerevisiae (4) and with EndoG in C.elegans (5) to induce chromatin condensation and large-scale DNA fragmentation.*

1.3.6. Control of AIF activity by HSP70

What happens to AIF once it is released from the mitochondria into the cytosol? There seems to be at least one protein that controls AIF's activity outside the mitochondria before it enters the nucleus. Hsp70 belongs to the family of heat shock proteins and is a prominent cytoprotective factor. Its upregulation can protect against apoptosis in response to cellular stress and confers resistance to cancer cells in chemotherapy (Garrido et al., 2001). Hsp70 had been known to interact with Apaf-1 in order to prevent caspase activation during apoptosis (Saleh et al., 2000). Interaction between AIF and Hsp70 might be an additional

way of controlling cell death. Indeed, the proteins have been shown to interact directly and independently of the domain that binds to Apaf-1 (Ravagnan et al., 2001). Further experiments have mapped the interaction domain of AIF to the amino acid residues 150-228 (Gurbuxani et al., 2003). In cell-free systems, Hsp70 can prevent AIF-induced chromatin condensation of purified nuclei. Cells overexpressing Hsp70 were protected against the apoptogenic effects of microinjected AIF or transfected plasmids expressing AIF targeted directly to the cytosol (Ravagnan et al., 2001). That this interaction might be important in treating diseases was shown in neonatal hypoxic/ischemic brain injury where Hsp70 overexpression significantly reduces cell death by inhibiting AIF nuclear translocation (Matsumori et al., 2005). On the contrary, human colon cancer cells were more sensitive to curcumin-induced apoptosis when Hsp70 expression was downregulated by antisense cDNA, although this might only be in part due to the reduced interaction with AIF since the release of Cyt c and Smac/DIABLO was also affected (Rashmi et al., 2004).
However, it seems that Hsp70 sequesters released AIF in the cytosol and thus inhibits the pro-apoptotic nuclear changes induced by AIF once in the nucleus (Gurbuxani et al., 2003) (Figure 1-8). Hsp70 is, next to mitochondrial membrane permeabilisation, another control mechanism of potentially cytotoxic proteins.

1.3.7. How does AIF exert its effect on DNA?

Once translocated from the mitochondria to the nucleus, AIF induces peripheral chromatin condensation and large-scale (50kbp) DNA fragmentation (Susin et al., 1999). This has been observed in many different cell types in response to numerous apoptotic stimuli. However, other factors like CAD, lysosomal DNAse II, and EndoG seem to be responsible for the oligonucleosomal DNA fragmentation seen during apoptosis (Widlak and Garrard, 2005). In cell-free systems, AIF also induces chromatin condensation and high molecular weight DNA fragmentation in isolated nuclei (Susin et al., 1999). Indeed, AIF was found to bind DNA in a sequence-independent manner, although it does not degrade naked DNA (Ye et al., 2002). This interaction is mediated by a strong positive electrostatic potential at the surface of AIF. Replacement mutations of a few positively charged arginine residues that were substituted by neutral alanine residues abolish the interaction (Ye et al., 2002). Moreover, while retaining nuclear translocation, these AIF-DNA-binding mutants fail to induce apoptosis identifying the interaction with DNA as the essential apoptotic function (Ye et al., 2002).
The fact that AIF did not degrade naked DNA or DNA of pre-heated nuclei (Susin et al., 1999) indicated the direct or indirect interaction with another nuclear factor to induce apoptosis-associated chromatinolysis. Until now, two co-factors were identified: Cyclophilin A in mammalian cells and EndoG in *C.elegans* (Figure 1-8).

In the nematode, the AIF homologue WAH-1 and the EndoG homologue CPS6 interact with each other and synergize to mediate DNA degradation. The recombinant proteins together induce degradation of naked plasmid DNA, while WAH-1 or CPS6 alone do not or hardly show any DNAse activity, respectively. In cells, they act in a single mitochondria-initiated apoptotic pathway that is caspase-dependent (Wang et al., 2002).
In mammalian cells however, no such interaction has been found and it has been proposed that these factors act independently of one another in nuclear chromatin breakdown (Li et al., 2001; Susin et al., 1999).

In mammalian cells, AIF has been shown to interact directly with cyclophilin A (CypA) (Cande et al., 2004b). Cyclophilins were fist identified as intracellular receptors for the immunosuppressive drug cyclosporine A, but some members of the large protein family including CypA have also been shown to have a calcium/magnesium-dependent nuclease activity (Montague et al., 1994). Recombinant AIF and CypA proteins form an active DNAse *in vitro* and degrade plasmid DNA and DNA loss in purified nuclei. Moreover, AIF is a more potent apoptosis inducer in CypA-expressing cells than in CypA knockout cells (Cande et al., 2004b). These cooperative effects of AIF and CypA have been confirmed in S.*cerevisiae*, where overexpression of the homologue Aifp1, in combination with oxidative stress, kills less cells of a cpr1 (the yeast homologue of CypA) knockout strain compared to the wild-type strain (Wissing et al., 2004).

1.3.8. The vital functions

The overall structure of AIF including several protein domains and especially its homology to oxidoreductases pointed to another role of the protein. *In vitro*, AIF has been shown to have a redox activity accepting electrons from NADH to form superoxide anion (Miramar et al., 2001). Nevertheless, it was not until 2002 that the group of Dr. Ackerman published the first convincing report of a non-apoptotic role of AIF *in vivo*.

1.3.8.1. Radical scavenger function

Harlequin (Hq) mutant mice, who display progressive degeneration of cerebellar and retinal neurons with aging, exhibit a strong suppression (80%) of AIF expression in all tissues due to a retroviral insertion in the first intron of the Aif gene (Klein et al., 2002). They further developed ataxia at the age of three months. Cultured cerebellar granule cells of these mice were much more susceptible to apoptosis induced by hydrogen peroxide than their wild-type counterparts. Conversely, retroviral transduction of wild-type AIF rescued the Hq granule cells, suggesting that AIF served as a radial scavenger (Klein et al., 2002). Indeed, further studies with these mice showed higher genomic instability due to oxidative damage in all

brain regions (Stringer et al., 2004). How AIF protects these cells from oxidative stress has not been elucidated.

1.3.8.2. AIF and cytoplasmic stress granules

Another non-apoptotic role for AIF was discovered by the observation that cytoplasmic stress granules accumulated in AIF-deficient cells more than in AIF-positive controls in response to oxidative stress (Cande et al., 2004c). Cytoplasmic stress granules are foci of stalled translation initiation complexes that are generated in response to environmental stress. Moreover, cells lacking AIF depleted the endogenous pool of reduced glutathione much more rapidly than AIF-expressing cells after an oxidative insult. Since exogenous glutathione can inhibit cytoplasmic stress granule formation elicited by arsenate, AIF might be responsible for maintaining the glutathione levels in stress conditions using its oxidoreductase domain (Cande et al., 2004c).

1.3.9. AIF is a bifunctional protein

It is very important to point out that the oxidoreductase function of AIF and the pro-apoptotic function can be dissociated and are completely independent from each other. Recombinant ApoAIFΔ1-100 lacking FAD has no NADH oxidase activity, yet exhibits a similar potential to induce apoptosis to that of holoAIFΔ1-100 when microinjected into cells (Miramar et al., 2001). Conversely, blockade of the apoptogenic function of AIFΔ1-100 with a thiol reagent does not affect its NADH oxidase activity (Miramar et al., 2001). Accordingly, re-expression of AIF proteins with mutations in the redox-active domains in AIF-deficient cells cannot inhibit the accumulation of cytoplasmic stress granules like wild-type AIF can (Cande et al., 2004c). In conclusion, AIF has vital and apoptotic functions that seem to depend on different domains of the protein.

1.3.10.AIF in disease

There are several diseases and pathological conditions in which AIF is assumed to play a role and could thus serve as a therapeutic target.

1.3.10.1. AIF and cancer

In cancer, AIF is important in inducing apoptosis in response to several stimuli including irradiation and staurosporine. Although AIF has not yet been shown to be downregulated in cancer cells, its cytotoxic potential may be used in order to promote the killing of cancer cells during treatment. This theory is supported by the fact that the PARP-1-AIF-mediated cell death pathway seems to be responsible for the death induced by survivin downregulation in neuroblastomas (Shankar et al., 2001). AIF has further been shown to determine the chemoresistance to staurosporine of non-small-cell-lung carcinomas (NSCLC). If AIF is

immunodepleted, significantly less NSCLC cells undergo apoptosis (Gallego et al., 2004). AIF is one of the key factors in T cell death induced by UVB-radiation (Murahashi et al., 2003). These data suggest that stimulating the apoptotic activity of AIF in cancer cells in combination with anti-cancer drugs or irradiation might enhance the effects of the therapy significantly in numerous kinds of cancer.

AIF's potential to bind to the cytoprotective factor HSP70 has already proved useful in rendering human cancer cells more sensitive to apoptosis induction. A protein called ADD70 is made up of the HSP70-interacting domain of AIF (residues 150-228) and binds to Hsp70 in the cytosol of cells. Cancer cells where HSP70 is sequestered by ADD70 died more rapidly in response to a variety of death stimuli, suggesting a novel strategy to kill cancer cells more efficiently (Schmitt et al., 2003).

1.3.10.2. AIF in acute cell loss

Excessive apoptotic activity of AIF can also be harmful in certain diseases including death induced by hypoxia or by pathogens. The mitochondrio-nuclear translocation in neurons and myocards after ischemia clearly needs to be investigated further in order to provide treatment of neuronal or cardiac injury. Hypoxia/ischemia damages tissues after pathologies like stroke or traumatic insults. It affects not only the affected cells, but also the surrounding tissue, worsening the condition of a patient. That inhibiting AIF translocation to the nucleus might be promising technique to prevent excessive cell death in brain injury was demonstrated in Hsp70 overexpressing mice. These mice exhibited less neuronal cell death after hypoxic/ischemic brain injury, because Hsp70 inhibited AIF's nuclear translocation (Matsumori et al., 2005). Moreover, Hq mice, expressing less AIF, exhibit extended neuroprotection against DNA damage and glutamate-excitotoxicity confirming the role of AIF in accute cell loss (Cheung et al., 2005).

1.3.10.3. AIF in infectious diseases

AIF is released from the mitochondria during apoptosis induced by the envelope glycoprotein complex Env of HIV (Castedo et al., 2003) as well as during infection with HIV (Ferri et al., 2000). Inhibiting the AIF pathway might reduce the extensive cell death during HIV infection. Moreover, the bacterial toxin pneumolysin from Pneumococcus induces translocation of AIF and thus apoptosis in brain cells during meningitis. Since apoptotic neurons in the hippocampus contribute to the over 30% death rate in Pneumococcal infections, AIF might also prove to be a useful target to prevent cell death (Braun et al., 2002).

2. Materials and Methods

2.1. Materials

2.1.1. Instruments

Product	Manufacturer
ABI PRISM 7000 Detection System	Applied Biosystems
Agitator (for bacterial cultures)	G25, New Brunswick Scientific Co.
Blotting system	Mini Trans-blot, Bio-Rad
Centrifuge (for cells)	C4i Jouan
Centrifuge (for Maxi-Preps)	HiCen21, Herolab
Centrifuge (for Molecular Biology)	Sigma 3K15, Bioblock Scientific
Clark electrode	Hansatech Instruments Ltd
Confocal microscope	LSM 510 Zeiss
Electroporator	Gene Pulser Xcell, BioRad
Eletron microscope	CEM-902, Zeiss
FACS Vantage	Becton Dickinson
Fluorescence microscope	DMIRE2, Leica
Generator	PS 1006, Apelex
Hood	HeraSafe, Heraeus
Incubator (bacteria)	SR2000, Thermosi
Incubator (for cells)	HeraCell, Heraeus
Luminometer	EG&G Berthold
Microplate reader	MRX II, Dynex Technologies
Nucleic acid electrophoresis system	Embi Tec
pH-meter	Hanna Instruments
Potter	Heidolph
Protein electrophoresis system	Mini-PROTEAN 3, Bio-Rad
Spectrophotometer (dual wavelength)	DW 2000 Aminco/SLM, SLM Instruments
Thermoblock	Bioblock Scientific
Ultracentrifuge	Beckman
Waterbath	Polystat 33, Bioblock Scientific

2.1.2. Small Material

Product	Manufacturer
15ml and 50ml polystyrene tubes	Becton Dickinson
Autoradiography film	Amersham
Cell culture 6- and 12-well vessels	Becton Dickinson
Cell culture flasks	Becton Dickinson
Cryotubes	Nunc

Small Material continued	Manufacturer
Electroporation cuvettes	Bio-Rad
FACS tubes	Falcon, Becton Dickinson
Needles	Terumo
Petri dishes (plastic)	Corning
PipetAid	PolyLabo
PipetMan	Gilson
Pipette tips	Corning
Pipettes	Becton Dickinson
Plastic tubes (1 and 2ml)	Eppendorf

2.1.3. Kits

Kit	Manufacturer
Bioluminiscence Assay kit HSII	Roche
Plasmid Maxi-Prep kit	Qiagen
Protein assay kit	Bio-Rad
RNeasy Mini kit	Qiagen

2.1.4. Chemicals

Reagent	Manufacturer
β-Mercaptoethanol	Sigma
Acrylamid/Bisacrylamid	Bio-Rad
ADP	Sigma
Agarose	Amersham
Aminohexanoic acid	Sigma
APS	Bio-Rad
ATP	Sigma
BSO	Sigma
CHAPS	Sigma
Coomassie Brilliant Blue G-250	Bio-Rad
DAPI	Molecular Probes
DCF-DA	Molecular Probes
DCPIP	Sigma
Deoxy-glucose	Sigma
Digitonin	Sigma
Dihydrorhodamine	Molecular Probes
Dodecylmaltoside	Sigma
DTT	MBI Fermentas
EDTA	Sigma
EGTA	Sigma
Ethanol	RPE

Chemicals continued	Manufacturer
Ethidium bromide	Sigma
Fructose	Sigma
Galactose	Sigma
Glucose	Sigma
Glycerol	QBioGene
GSH ethyl ester	Sigma
Hydrogen Peroxide	Sigma
Imidazole	Sigma
Isopropanol	RPE
KCl	Sigma
KCN	Sigma
L-Glutamine	Sigma
Malate	Sigma
Mannitol	Sigma
Menadione	Sigma
$MgCl_2$	Sigma
MnTBAP	Calbiochem
NaCl	Sigma
NAD	Sigma
NADH	Sigma
NADP	Sigma
NADPH	Sigma
NaF	Sigma
NAO	Molecular Probes
NaOH	Sigma
Na-phosphate	Sigma
Paraformaldehyde	Fisher
Penicillin	Gibco
Percoll	ICN Biomedicals
Picric Acid	Sigma
PMS	Sigma
Propidium Iodide	Sigma
Pyronin Y	Sigma
Pyruvate	Sigma
Saccharose	Sigma
SDS	Bio-Rad
Sodium pyruvate	PAA
Streptomycin	Calbiochem
STS	Sigma
Succinate	Sigma
SYBR gold	Molecular Probes
TEMED	Bio-Rad

Chemicals continued	Manufacturer
TES	Sigma
To-Pro-3	Molecular Probes
Tris	Sigma
Trypan blue	Roche
Tween	Sigma

2.1.5. Buffers

Buffer	Manufacturer
One Phor All buffer	Amersham Biosciences
Running buffer (SDS-PAGE)	Bio-Rad
TAE buffer	Promega
Transfer buffer (western blot)	Bio-Rad

2.1.6. Enzymes

Enzyme	Manufacturer
DNAse I	Roche Diagnostics
LDH	Sigma
LIF	Sigma
MuLV reverse transcriptase	Applied Biosystems
Restriction nucleases	Promega
RNAse A	Sigma
Trypsin	Sigma

2.1.7. Antibodies

Primary Antibody	Species	Manufacturer
Actin	mouse monoclonal	Chemicon
AIF	Rabbit	Chemicon
AIF	mouse monoclonal	SantaCruz
complex I 17kDa subunit	mouse monoclonal	Molecular Probes
complex I 20kDa subunit	mouse monoclonal	Molecular Probes
complex I 30kDa subunit	mouse monoclonal	Molecular Probes
complex I 39kDa subunit	mouse monoclonal	Molecular Probes
complex III core 1 subunit	mouse monoclonal	Molecular Probes
complex III core 2 subunit	mouse monoclonal	Molecular Probes
complex III FeS subunit	mouse monoclonal	Molecular Probes
complex IV subunit IV	mouse monoclonal	Molecular Probes
Cyt *c*	mouse monoclonal	Pharmingen
EndoG	Rabbit	ProSci
GAPDH	mouse monoclonal	Chemicon

Primary Antibodies continued	Species	Manufacturer
Grim 19	mouse monoclonal	Abcam Limited
HnRNPA1	mouse monoclonal	Santa Cruz
HSP60	Mouse	Sigma
HSP60	Rabbit	MBL
TOM40	Rabbit	Santa Cruz
VDAC	mouse monoclonal	Calbiochem

Secondary Antibody	Conjugate	Manufacturer
Goat anit-rabbit	HRP	Southern Biotechnologies
Goat anti-mouse	Alexa 568	Molecular Probes
Goat anti-mouse	Alexa 488	Molecular Probes
Goat anti-mouse	HRP	Southern Biotechnologies
Goat anti-rabbit	Alexa 568	Molecular Probes
Goat anti-rabbit	Alexa 488	Molecular Probes

2.1.8. Diverse

Product	Manufacturer
Bacteria (heat shock competent)	Strategene
BSA	Sigma
Cell culture medium	PAA
DNA ladder (low molecular weight)	Invitrogen
dNTP's	Roche
ECL Reagent	Pierce
FCS	Gibco
FITC-labeled beads	Becton Dickinson
LB-Agar	Gibco
Lipofectamine	Invitrogen
Milk powder	Regilait
Mini complete (protease inhibitors)	Roche
Oligofectamine	Invitrogen
Opti-MEM	Gibco
pH indicator paper test strips	Indigo
Protein A sepharose	Amersham Biosciences
Random Hexamers	Applied Biosystems
RNA (PolyA, PolyG, PolyC, PolyA/U, PolyC/G)	Sigma
SOC medium	Invitrogen
Z-VAD.fmk	Bachem, Torrance, CA

2.2. Methods

2.2.1. Molecular Biology

2.2.1.1. Transformation

To amplify plasmid DNA, it was transformed into competent bacteria by heat shock. Sudden heat induces permeabilisation of the bacterial membrane allowing the DNA to enter.

50µl aliquots of bacteria, which were kept at -80°C, were thawn on ice for 20 minutes. 50-200ng of DNA plasmids containing a gene for antibiotic resistance were added and incubated on ice for 30 minutes agitating every 5 minutes. Tubes containing bacteria and DNA were then transferred into a thermoblock at 42°C for 50 seconds. Immediately after the heat shock, ultra pure SOC medium was added and bacteria were grown at 37°C for 1 hour. 10-100µl of the mixture were then plated on LB-agar plates supplemented with ampicilline (100µg/ml) and incubated overnight at 37°C. Clones were picked the next day or kept at 4°C.

2.2.1.2. Maxi-Prep

Bacteria containing the plasmid DNA of choice were amplified and lysed in order to extract and purify the plasmid DNA.

After transformation, a bacterial colony was picked and grown in a 250ml overnight culture containing LB medium supplemented with ampicilline (200µg/ml) at 37°C agitating. The following day, bacteria were pelleted at 6000g for 15 minutes. The Maxi-Prep kit (QIAGEN) was then performed following the manufacturer's instructions. Briefly, bacteria were resuspended and treated with lysis buffer for no longer than 5 minutes. The lytic reaction was stopped by adding neutralization buffer. Bacterial cell walls, proteins, and the genomic DNA attached to the bacterial membrane were separated from the plasmid DNA by allowing the latter to pass through a cartridge. The solution containing the plasmid DNA was run over an affinity column where the DNA was first washed and then eluted. Subsequently, DNA was precipitated with isopropanol and washed with 70% ethanol at 4°C. Pelleted plasmid DNA was dried and resuspended in water, the experiment yielding 500-1500µg of plasmid.

2.2.1.3. Bacteria storage and thawing

To keep bacteria containing the plasmid of choice for a longer period of time, they were stored at –80°C. 750µl of the overnight culture were mixed with 750µl of sterile glycerol and immediately frozen at -80°C. To thaw bacteria, some cells were scratched from the frozen bacteria-glycerol mixture with a tooth pick and grown in a 3ml culture for 4-6 hours. Bacteria were then ready to be grown in overnight cultures, for example.

2.2.1.4. DNA restriction

In order to verify the sequence of an amplified plasmid, DNA was subjected to restriction by enzymes which cut specific DNA sequences, therefore yielding DNA segments of predictable size.

1µg of DNA was incubated with 20 units of the restriction enzyme of choice in reaction buffer (provided with the enzyme). The final volume of the reaction mix was 100µl. The incubation time at 37°C was 1-2 hours depending on the enzyme. The size of the generated DNA segments was determined by DNA gel electrophoresis.

2.2.1.5. DNA agarose gel electrophoresis

DNA agarose gel electrophoresis is used to separate DNA molecules according to their size. DNA is visualised with intercalating agents (ethidium bromide or SYBR® gold) which fluoresce when excited by UV light.

DNA samples were mixed with loading buffer and loaded onto a gel containing 1% agarose and 0.5µg/ml ethidium bromide in TAE buffer. Gels were run in a horizontal gel chamber containing TAE buffer at 50-100V for 20-40 minutes. If ethidium bromide was not used, the gel was stained with SYBR Gold (1:10000 in TAE buffer) after electrophoresis for 40 minutes. DNA molecules were observed under UV light and sizes were compared to the standard low molecular weight DNA ladder from invitrogen.

2.2.1.6. Determination of DNA/RNA concentration

The characteristic of nucleic acids to absorb UV light at a wavelength of 260nm at a quantity proportional to their concentration is utilized to determine the optical density (OD) of a DNA or RNA sample.

Samples were diluted in water at a ratio of 1:150 - 1:500 and transferred into quartz cuvettes. The optical density was measured in a spectrophotometre at 260nm and compared to pure water as a reference. An OD of 1 corresponds to a concentration of 50 µg of double-stranded DNA or 40 µg of RNA per ml. To determine the purity of DNA, the OD at 280 nm was measured. An OD_{260}/OD_{280} ratio of 1.6-2.0 reflects high purity of DNA, although a ratio of 1.4 is sufficient for transfection experiments.

2.2.1.7. RNA purfication

RNA was extracted from HeLa or murine embryonic stem cells using the RNeasy Mini kit (Qiagen) following the manufacturer's instructions. Cells were trypsinized, washed once in PBS and lysed in the provided buffer. The sample was homogenized by passing the lysate 5 times through a 20-gauge needle. After RNA precipitation with 70% ethanol, the sample was applied to a column, which binds the RNA. The column was washed and the purified RNA was eluted with water.

2.2.1.8. Quantitative RT-PCR

To quantify the level of expression of specific genes in HeLa or ES cells, mRNA's of a cellular RNA extract were transcribed into cDNA's by the enzyme reverse transcriptase. The sequences of the genes of interest were then amplified by PCR using specific primers and the rate of amplification indicating the level of gene expression was measured by corresponding Taqman-MGB probes in the ABI PRISM® 7000 Sequence Detection System.

1µg of total RNA's were denatured at 70°C for 3 minutes and put on ice. RNA was then transcribed to DNA by the murine leukemia virus (MuLV) reverse transcriptase at 42°C for 1 hour in the following buffer: Tp buffer II (1X), 5mM MgCl2, 100µM dNTP's, Random Hexamer (1X).

The primers and the corresponding Taqman-MGB probes for the mouse and human genes NDUFS7, NDUFA9, NDUFS3, NDUFB6, and the human gene AIF were purchased from Applied Biosystems as assays-on-demand products (www.Aplliedbiosystems.com). For the mouse mitochondrial DNA-encoded genes, the following primers and Taqman-probes were purchased from MWG-Biotech AG :

Gene	Primer and Probes
ND1	Forward 5'-CTCAACCTAGCAGAAACAAACC-3' Reverse 5'-GGCCGGCTGCGTATTCTAC-3' Probe 5'-CCCCCTTCGACCTGACAGAAGGAGA-3'
ND6	Forward 5'-TTGGGAGATTGGTTGATGTAT-3' Reverse 5'-TGCCGCTACCCCAATCC-3' Probe 5'-ATGATGTTGGAGTTATGTTGGAAGGA-3'
Cox1	Forward 5'-TCAGTATCGTATGCTTCAACAAATTTAGA-3' Reverse 5'-TGGTTCCTCGAATGTGTGATATG-3' Probe 5'-TGACTTCATGGCTGCCCTCC-3'
Cox2	Forward 5'-GAGCAGTCCCCTCCCTAGGA-3' Reverse 5'-GTCGGTTTGATGTTACTGTTGCTT-3' Probe 5'-ATGCCATCCCAGGCCGACTAAAT-3'
Cytochrome B	Forward 5'-AAAGCCACCTTGACCCGATT-3' Reverse 5'-GATTCGTAGGGCCGCGATA-3' Probe 5'-CGCTTTCCACTTCATCTTACCATT-3'
ATPase 6	Forward 5'-TCGTTGTAGCCATCATTATATTTCCT-3' Reverse 5'-GAAAGAATGGAGACGGTTGTTGA-3' Probe 5'-CAATCCTATTCCCATCCTCAAAACGCCT-3'
16S RNA	Forward 5'-TGCCTGCCCAGTGACTAAAGT-3' Reverse 5'-AACAAGTGATTATGCTACCTTTGCA-3' Probe 5'-TAACGGCCGCGGTATCCTGA-3'
tRNA Leucine 1	Forward 5'-GGTGGCAGACGGAGGAAA-3' Reverse 5'-TATTAGGGAGAGGATTTGAACCT-3' Probe 5'-TCGGTAAGACTTAAAACCTTGTTCCC-3'

2.2.1.9. siRNA design

To suppress the expression of a specific gene, siRNA's duplexes containing a 21nt sequence recognizing exclusively the gene of interest are designed and transfected into eukaryotic cells. In the cells, the siRNA duplex forms an endonuclease-containing RNA-induced silencing complex (RISC) that cleaves the target RNA which is complementary to the siRNA sequence.

To define the sequence for the siRNA duplex, the software provided by oligoengine was used. Once several sequences were determined, they were subjected to a blast search to exclude the possibility that the same sequence was found in another gene. The following siRNA's were utilized:

Name of siRNA	Forward sequence
"Control" (specific for emerin)	5'-CCGUGCUCCUGGGGCUGGGdTdT-3'
"Control" (specific for murine, not human AIF)	5'-AUGCAGAACUCCAAGCACGdTdT-3'
"AIF"-1	5'-GAUCCUCCCCGAAUACCUCdTdT-3'
"AIF"-2	5'-CUUGUUCCAGCGAUGGCAUdTdT-3'

2.2.2. Cell Biology

2.2.2.1. Cell culture

HeLa cells are derived from a human cervix carcinoma. AIF knock-out murine embryonic stem cells were generated in Dr.Joseph Penninger's laboratory (Joza et al., 2001).

HeLa and ES cells were cultured in Dulbecco's modified Eagle's medium supplemented with 10% fetal calf serum (FCS), 1 mM sodium pyruvate, 2 mM L-glutamine, 100 U/ml penicillin, and 100 µg/ml streptomycin. ES culture medium further contained 1µg/l leukemia inhibitory factor (LIF) and 50 µg β-mercaptoethanol. Both cell lines were cultured in a humidified incubator at 37°C and 5% CO_2. They were passaged on a regular 2-3 day basis, detaching the adherent cells by incubating them with the protease trypsin at 37°C for 3-5 minutes. Culture medium was subsequently added, the FCS inhibited the proteolytic effect of trypsin, and cells were reseeded at appropriate concentrations.

When cells were seeded for experiments, they were counted using a counting chamber and visualising the dead cells by Trypan blue. They were centrifuged at 1200 rpm for 5 minutes and resuspended in the appropriate medium at the desired concentration.

2.2.2.2. Cell storage and thawing

Aliquots of cell lines were kept in liquid nitrogen. New aliquots were thawn on a regular basis in order to avoid artefactual characteristics of the cell lines that may occur after too many passages.

To freeze the cells, they were trypsinized and resuspended in 20% DMSO/FCS at 4°C. They were immediately frozen in cryotubes at -80°C and transferred after 24 hours into liquid nitrogen. To thaw cells, they were taken out of the liquid nitrogen and kept at -80°C for at least 12 hours. The frozen cell were then diluted with large volume of culture medium at 37°C. After centrifugation, cells were resuspended in fresh culture medium, which was exchanged the next day.

2.2.2.3. Apoptosis induction

Apoptosis was induced by the oxidative stress-causing agents hydrogen peroxide and menadione. They were added in different concentrations to the culture medium, on the day after a specific number of cells had been plated in wells. If antioxidants, such as GSH, tocopherol or MnTBAP, were utilised in the same experiment, they were added to the cells at least 1 hour before the oxidative stress inducer.

2.2.2.4. Transfection

To introduce nucleic acids into cells, two different methods were used, the liposome-mediated transfection and electroporation. The liposome-mediated transfection uses the ability of non-charged lipid vesicules that form around the nucleic acids molecules to diffuse through cellular membranes, therefore delivering the nucleic acids into the cells' nuclei. During the short electric pulse cells are exposed to when performing the electroporation experiment, cell membranes are briefly permeabilised allowing nucleic acids at high concentrations to enter.

siRNA transfection

HeLa cells were plated in Opti-MEM supplemented with 10% FCS in 12-well plates at a cell density of 4×10^5 cells per well. They were transfected the next day at a confluency of around 40%. Per well, 4 µl of oligofectamine was incubated for 5-7 minutes in 16µl of Opti-MEM, then, 1.2µg of siRNA in 100µl Opti-MEM was added and liposome vesicles were allowed to form around the siRNA for 20-25 minutes. The mixture was added to the wells, cells were washed the next day and incubated for another 2-4 days before analysis.

Electroporation of plasmid DNA

ES cells were washed in PBS and 5×10^6 cells were resuspended in cell culture medium without FCS. 50µg of plasmid was added and the mixture was incubated on ice for 5 minutes

in an electroporation cuvette. The cuvette was then placed into the Gene Pulser Xcell Electroporation System and cells were electroporated at 250V and 500µF. They were immediately incubated on ice for 5 minutes and then replated. Cells were washed the next day to remove the dead cells and analysed after 48 hours.

2.2.3. Biochemistry

2.2.3.1. Flow cytometry

Cells were passed through a fluorescence-activated cell sorter (FACS®) in order to analyse their number, redox state, death, DNA content, or RNA content. Fluorescent markers that specifically stain relevant cellular molecules are detected by the FACS® and thus allow to determine the number of stained cells as well as the intensity of staining in each cell. FACS analysis was also used to detect the fluorescence emitted by the green fluorescent protein (GFP) to determine the number of transfected and thus GFP-expressing cells.

Cell counts

Cells were trypsinized, washed once in PBS, and stained with 5µg/ml 4',-6-diamino-2-phenylindole-dihydrochloride (DAPI) for 5 minutes at 37°C. DAPI stains the DNA, but can only pass through cell membranes of dead cells, which are permeabilised. To assess the number of living cells, the same amount of FITC-labeled beads was added to each sample and cells were counted until 1000 beads had passed through the FACS®. DAPI-positive (dead) cells were excluded from the counts.

Determination of the redox state of cells

Cell were trypsinized, washed once in PBS, and stained with different fluorochromes at 37°C to assess the redox state of the cells: dihydrorhodamine (50ng/ml, 30 minutes incubation) for ROS detection, 10-N-Nonyl acridine orange (NAO; 500nM, 20 minutes incubation) to determine the level of nonoxidized cardiolipin, monochlorobiman (50µM, 30 minutes incubation) to determine the level of GSH, and 2'7'-dichlorodihydrofluorescein diacetate (H_2DCFDA; 5µM, 60 minutes incubation) to measure peroxides.

Determination of RNA content

The fluorescent probe pyronin Y specifically stains RNA and does not bind to DNA. Thus, the cellular content of RNA can be correlated to the fluorescence intensity following pyronin Y staining. After apoptosis induction, cells were trypsinized, washed in PBS, and incubated with pyronin Y (1µg/ml) for 20 minutes at 37°C.

Cell cycle

Propidium iodide stains the DNA of dead cells. The intensity of the fluorescence of each cell can be correlated with the cell's DNA content, which in turn correlates with the cell cycle phase. Cells in a non-replicating state (G1 or G0 phase) contain 46 chromosomes and thus a certain amount of DNA. During the S phase, the DNA is being replicated and the DNA content is steadily increasing until the number of chromosomes has doubled (G2 phase). After the separation of the two daughter cells, the DNA content is that of cell in the G1 phase again.

Cells were trypsinized, washed once in cold (4°C) PBS, and fixed in cold (-20°) 80% ethanol for 12-24 hours. The next day the cells were washed once in cold (4°C) PBS and treated with DNAse free RNAse (20µg/ml in PBS) for 30 minutes at 37°C. Propidium iodide was added at a final concentration of 100 µg/ml and cells were again incubated at 37°C for 30 minutes.

Determination of the transfection rate

To determine whether cells have been successfully transfected with AIF-GPF constructs after electroporation, the GFP-fluorescence is detected by FACS analysis. Cells expressing the fusion protein emit the GFP-characteristic fluorescence.

Cells were trypsinized and resuspended in PBS. They were subsequently analysed in a FACS vantage and the percentage of GFP-positive cells was determined.

2.2.3.2. Isolation of mitochondria from mouse liver

To obtain purified mitochondria, the tissue had to be mechanically disrupted without disturbing mitochondrial integrity. The mitochondria could then be separated from the other organelles by centrifugation on a discontinuous density gradient.

The murine liver was rapidly removed from the dead animal, rinsed in cold homogenization (H) buffer (300mM saccharose; 5mM N-tris(hydroxymethyl)methyl-2-aminoethanesulfonic acid (TES); 200µM EGTA; pH 6.9), and homogenized in a Potter-Thomas (500 revolutions/minute). Every centrifugation step was performed at 4°C and samples were constantly kept on ice. After a first centrifugation at 760g for 10 minutes, the supernatant was kept and the pellet was resuspended in H buffer and again centrifuged at 760g for 10 minutes. The two supernatants were pooled and centrifuged at 8740g for 10 minutes.

To prepare the Percoll gradient, the following solutions were used:

Percoll buffer: 300mM saccharose; 10mM TES; 200µM EGTA; pH 6.9

Solution A: 90ml Percoll buffer and 2.05g saccharose

Solution B: 90ml Percoll buffer and 3.96g saccharose

Solution C: 90ml Percoll buffer and 13.86g saccharose

Percoll stock solution

18% Percoll: 6.55ml solution A and 1.45ml Percoll solution

30% Percoll: 5.6ml solution B and 2.4ml Percoll solution

60% Percoll: 3.2ml solution C and 4.8ml Percoll solution

A discontinuous 60%/30%/18%-Percoll gradient was prepared in a corex tube containing 4ml of each solution. The pellet of the last centrifugation step was resuspended in 1ml of H buffer and added to the gradient. The corex tube was centrifuged at 8740g for 10 minutes and the mitochondria were recovered between the 60% and 30% layer of the Percoll gradient. They were resuspended in H buffer and centrifuged at 6800g for 10 minutes to remove the Percoll.

2.2.3.3. Enrichment of mitochondria from cells and murine organs

For proper analysis of mitochondrial proteins by spectrophotometry or PAGE, it can be essential to prepare mitochondria-containing fractions from cells or murine organs.

Cells or hemispheres of brains of neonatal or adult mice were homogenized in buffer M (20mM Tris pH 7.2, 250mM saccharose, 2mM EGTA, 40mM KCl, BSA 1mg/ml) using a potter and centrifuged at 20,000g for 20 minutes at 4°C. Pellets containing mitochondria were resuspended in 400-500µl lysis buffer (50mM Tris, 10% glycerin, 2% SDS) and treated at 100°C for 10 minutes.

2.2.3.4. Determination of protein concentration

Concentrations of cell lysates or recombinant proteins were determined using the Bio-Rad protein assay, a colorimetric assay based on the method of Bradford. The acidic dye Coomassie Brilliant Blue G-250 shifts its absorbance maximum from 465nm to 595nm when binding to protein occurs. Therefore, this dye was added to solubilised protein and the absorbance was measured with a microplate reader at 595nm.

Reagents were provided in the Bio-Rad kit.

In detail, 5µl of protein solution, 25µl of SDS-containing solution, and 200µl of the acidic dye was mixed in a microplate and incubated for 15 minutes at room temperature. The absorbance was measured in a microplate reader. The protein concentration of the sample was determined by comparison to a standard curve. The standard used was BSA.

2.2.3.5. Immunoprecipitation

To detect interactions between two proteins, one of them is purified from cells in non-dissociating conditions. It is then determined by western blot whether the potential partner was co-purified with the protein pointing to an association of the two.

Cells were trypsinized, washed twice in PBS, and resuspended in IP buffer (20mM Tris pH 8; 150mM NaCl; 2mM EDTA; 50mM NaF; 1mM Metavanadate). Cells were lysed for 30 minutes at 4°C rotating. Cell lysates were centrifuged at 15,000g for 30 minutes at 4°C. The protein concentration of the supernatant was determined and the pellet discarded. 500µg of proteins were incubated with 2µg of the first antibody (AIF E1, Santa Cruz) for 2 hours at 4°C

rotating. 30µl of protein A sepharose was washed 2 times in IP buffer and 3 times in IP buffer + CHAPS (20mM Tris pH 8; 150mM NaCl; 2mM EDTA; 50mM NaF; 1mM Metavanadate; 2% CHAPS; Mini complete, 1 tablet/10ml). The sepharose was then added to the protein sample and incubated for 1 hour at 4°C rotating. After 5 washes in IP buffer, the proteins were resuspended in 30 µl Laemmli buffer to perform an SDS-PAGE followed by western blot.

2.2.3.6. SDS-PAGE

Sodium dodecyl sulfate polyacrylamide gel electrophoresis is used to separate proteins according to their size. Positively charged proteins migrate to the negatively charged electrode in a network of polyacrylamide. Small proteins can pass through quicker than large proteins.

Cells were trypsinized, washed once in PBS and lysed in lysis buffer (50mM Tris-HCl pH 6.8; 10% glycerol; 2%SDS) at 100°C for 10 minutes. The protein concentration was determined and 20-50 µg or protein was loaded on a gel, after the addition of loading buffer (1mM DTT; 1mM Na-acetic acid, pH 5.2; 0.005% bromophenol blue) and another degradation step at 100°C for 10 minutes. Proteins after immunoprecipitation were denatured in Laemmli buffer at 95°C for 5 minutes.

The gel consisted of a stacking gel (125 mM Tris-HCl pH 6.8; 4% Arcylamide/Bis-Acrylamide 29:1; 0.4% SDS, 0.025% APS) and a resolving gel (375 mM Tris-HCl pH 8.8; 12% Arcylamide/Bis-Acrylamide 29:1; 0.2% SDS; 0.025% APS). The polymerisation reaction was catalysed by TEMED. Electrophoresis was carried out in a vertical gel chamber in tris-glycine buffer (running buffer, Bio-Rad) at a maximum voltage of 110V for about 2 hours. The size of proteins was indicated by a prestained marker.

2.2.3.7. Blue native gels and blue native PAGE

Blue native gels serve to separate the respiratory chain complexes according to their size and visualise them by coomassie blue staining. Mitochondria have to be lysed without disrupting the integrity of the mitochondrial protein complexes. The blue native gel can be followed by an SDS-PAGE to separate the subunits of each complex.

Liver tissue, brain tissue, or sedimented ES cells (10-50mg wet weight each) were homogenized with 500µl sucrose buffer (250mM sucrose; 20mM Na-phosphate, pH 7.2 for tissue specimens; and 83mM sucrose; 7mM Na-phosphate, pH 7.2 for ES cells). Aliquots corresponding to 5 mg heart muscle or brain tissue, or 10 mg ES cells were centrifuged (10 minutes at 10,000 x g). Mitochondria containing pellets were resuspended with 20µl buffer (50mM NaCl; 50mM imidazole; 2mM 6-aminohexanoic acid; 1mM EDTA, pH 7.0), and the OXPHOS complexes solubilised by adding 5 µl dodecylmaltoside (10%) to heart and ES cell samples, and 10 µl dodecylmaltoside (10%) to liver samples. The mixtures were centrifuged at 100,000g for 15 minutes, and the supernatant supplemented with Coomassie blue-G250

dye (5% stock in 750mM 6-aminohexanoic acid) to set a detergent/Coomassie-dye ratio of 4 (g/g). This supernatant was loaded onto 5 x 1.5mm sample wells for BN-PAGE using 4-13% acrylamide gradient gels as described (Schägger, 2003). For resolution of the subunits of mitochondrial complexes, lanes from the BN-gel were cut out and prepared for two-dimensional SDS-PAGE as described (Schägger, 2003).

2.2.3.8. Western Blot

To detect proteins with specific antibodies, they were transferred from the polyacrylamide gel to a nitrocellulose membrane. Antigen-specific antibodies are recognized by secondary antibodies that are conjugated to the reducing enzyme horseradish peroxidase, which can convert nonluminescent substrates into luminescent products. The emitted chemiluminescence is detectable by autoradiography film and the amount can be correlated to the quantity of bound antibody and thus to the amount of specific protein in the sample.

The wet protein transfer is carried out in a Trans-blot cell in transfer buffer (Bio-Rad) at a current of 200mA for 2 hours. The presence of the proteins on the nitrocellulose membrane was verified by rouge ponceau colouring, which was subsequently eliminated by several washes with water.

To prevent nonspecific binding of antibody, the membrane was first incubated with blocking solution (PBS; 0.01% Tween; 5% non fat milk) for 20 minutes at room temperature. The membrane was then incubated with the first antibody (or antibodies) raised against AIF, actin, subunits of the respiratory chain, GAPDH, VDAC, HSP60, or hnRNPA1 in blocking solution for 2 hours at room temperature. After 3 washes with PBS/0.01% Tween for 5 minutes, the peroxidase-conjugated secondary antibody raised against rabbit or mouse was administered. After an incubation for 1 hour at room temperature, the membrane was again washed 3 times with PBS/Tween. The membrane was then developed by an enhanced chemiluminescence system.

2.2.3.9. Densitometric analysis

To quantify the protein detected by western blot, the density of the band on the film can be analysed. The film was scanned and the intensity of the bands was measured using the software Totallab (Phoretix).

2.2.3.10. Determination of the pH

The cell culture medium was collected on day 0,1,2, and 3 and the pH was measured by using a pH metre of Hanna Instruments or by using high accuracy pH indicator paper test strips. The pH metre was first calibrated and the electrode was then submerged into the cell culture medium. The pH indicator paper test strips were dipped into the cell culture medium

and the colour of the test strip was compared to the colour chart provided by the manufacturer.

2.2.3.11. Determination of lactate concentration in culture medium

The culture medium was collected and the adherent cells were trypsinized and counted using a counting chamber.

Lactate content in culture medium was determined by measuring the oxidized 2,6-dichlorophenol-indophenol (DCPIP), which is reduced by phenazine methosulfate (PMS) which in turn is reduced by NADH produced by lactate-dehydrogenase (LDH) which oxidizes at the same time lactate to pyruvate. Diluted cultured medium was analysed in the buffer S (10mM KH2PO4, pH7.8, 2mM EDTA , 1mg/ml bovine serum albumin (BSA); 0.06mM DCPIP, 0.5mM PMS, 0.8mM NAD^+, 1.5mM glutamate, 10 U/ml glutamate-pyruvate-transaminase GPT, 25U/ml LDH) and DCPIP oxidation was spectrophotometrically measured at 600nm.

2.2.3.12. Determination of intracellular ATP levels

The intracellular levels of ATP were measured with the Bioluminescence Assay Kit HSII (Roche). The firefly's enzyme luciferase needs chemically bound energy in form of ATP in order to emit its bioluminescence. Therefore, the intensity of bioluminescence can be correlated with the amount of ATP in a sample.

Cells were trypsinized after 36 hours incubation time in culture medium with (5g/l) or without glucose. According to the manufacturer's standard protocol, the cells were washed once in PBS, resuspended in the kit's dilution buffer and incubated for 5 minutes with the provided lysis buffer. The luciferase agent was added in the luminometre which subsequently measured the bioluminescence. A standard curve was established using several dilutions of the ATP standard provided with the kit.

2.2.3.13. Polarography

Polarography is used to measure oxygen consumption in intact or permeabilised cells. Through the addition of inhibitors and substrates specific for different respiratory chain complexes and the subsequent measurement of oxygen consumption, the activity of these complexes can be determined.

Polarographic studies of intact cell respiration and of mitochondrial-substrate oxidation by digitonin (0.004%)-permeabilised cells (30 to 50µg protein) were carried out in a 250µl-chamber equipped with a Clark electrode containing the buffer S (0.3M mannitol; 10mM KCl; 5mM $MgCl_2$, 1mg/ml BSA; 10mM KH_2PO_4, pH7.4.) After permeabilisation, substrates specific for complex I (malate and pyruvate both furnishing NADH), and complex II (succinate in the presence of complex I inhibitor rotenone) as well as respiratory chain inhibitors (malonate, KCN) were added as described (Rustin et al., 1994).

2.2.3.14. Spectrophotometry

To measure the activity of isolated respiratory chain complexes as well as citrate synthase, mitochondria were enriched, respiratory chain complex-specific substrates were added, and the oxidation of substrates that were oxidized directly or indirectly by one of the respiratory chain complexes was spectrophotometrically measured.

Cells were spun down (2500g for 5 minutes) through a digitonin (0.01%) and Percoll (5%) solution as described (Chretien et al., 2003). Rotenone-sensitive NADH quinone reductase (complex I; EC 1.6.5.3), malonate-sensitive succinate quinone DCPIP reductase (complex II ; EC 1.3.99.1), antimycin-sensitive quinol cytochrome c reductase (complex III; EC 1.10.2.2), cyanide-sensitive cytochrome *c* oxidase (complex IV ; EC 1.9.3.1), oligomycin-sensitive ATP hydrolase (complex V; EC 3.6.3.14), and citrate synthase (EC 4.1.3.7) were spectrophotometrically measured using a dual-wavelength spectrophotometer as described (Rustin et al., 1994).

2.2.3.15. Fluorescence and Confocal Microscopy

To determine the expression and localisation of proteins in cells, they are stained with specific antibodies. These antibodies are visualised with secondary anti-IgG antibodies conjugated to fluorescent molecules that can be observed under a fluorescence or confocal microscope.

Cells were grown and stimulated on cover slips. They were then washed 3 times in PBS and fixed with cold PFA buffer (4% paraformaldehyde and 0.19% picric acid in PBS) for 45 minutes at room temperature. After three washes with PBS, the cells were permeabilised with 0.2% SDS in PBS for 15 minutes. The cells were subsequently washed 3 times with PBS. To prevent non-specific binding of the antibodies, the permeabilised cells were incubated with blocking solution containing 10% FCS in PBS for 20 minutes. After 1 wash with PBS, the first antibody was applied at a concentration of 1µg/100µl (diluted in 1mg/ml BSA in PBS) and incubated for 1 hour. Usually, there were two proteins being stained at the same time by two different antibodies. The cells were washed again 3 times with PBS before the second antibody, that recognized the first antibody, was added at a dilution of 1/500 (in BSA/PBS) for 45 minutes. After 1 wash with PBS, the DNA was stained using Hoechst 33342 (at a dilution of 1/10,000 in PBS) for fluorescence microscopy and To-Pro-3 (at a dilution of 1/1000 in PBS) for confocal microscopy for 5 minutes. The cells were washed 3 last times with PBS and the cover slips were then fixed on slides with mounting medium. The stained cells were then observed under a fluorescence microscope or under a confocal microscope, the latter allowing a more accurate localisation of the proteins inside the cell.

2.2.3.16. Transmission electron microscopy

Electron microscopy allows the visualisation of extremely small molecules like DNA and RNA.

Examination of DNA by EM was performed as described (Delain and LeCam, 1995). Double stranded DNA corresponded to 1444-bp DNA fragments, obtained by PCR amplification from region pC7 of pBR322 (position: 2576-4020)n as previously described (Beloin et al., 2003). Single-stranded DNA was FX174 single-strand DNA (Biolabs). Poly A (MW 100,000 - 1,2000,000) was purchased from Sigma. A chimeric double stranded / single stranded DNA construct had been generated in Dr.Le Cam's laboratory (Institut Gustave Roussy, France). DNA templates and AIF protein were incubated 10 minutes at 20°C in binding buffer (20 mM Tris pH 7.5, 50 mM NaCl, with or without 5 mM $MgCl_2$) at different molar ratios of protein and DNA (10, 20, 30, 50). To obtain a good spreading of ssDNA as a control, T4 SSB gp32 was added to the DNA solution at a ratio of one gp32 tetramer per 5nt . Examination of DNA by EM was performed as described (Delain and LeCam, 1995). Briefly, a 5µl aliquot of the DNA or RNA solution at a final concentration of 0.5µg/ml was deposited on an EM grid coated with a very thin carbon film activated by a glow discharge in the presence of pentylamine (Dubochet et al., 1971). Grids were washed with a 2% aqueous uranyl acetate solution and dried. The samples were observed at a magnification of 85 000 with a Zeiss CEM-902 electron microscope in the annular dark-field mode, filtering out inelastic electrons with the spectrometer in order to improve image quality. Quantification was performed using SIS software.

2.2.3.17. RNA degradation assays

To determine whether RNA was degraded by a protein, the two molecules were incubated together at 37°C and RNA was then analysed by agarose gel electrophoresis.

Total RNA (50µg/ml) was extracted (RNeasy Mini kit, Qiagen) from normal HeLa cells and was exposed to recombinant mouse AIF (50µg/ml) protein or to RNAse A (100U/ml) as a control in a One Phor All buffer for 2 hours at 37°C. The samples were then loaded on an agarose gel stained with ethidium bromide. The RNA was then visualised under UV light.

2.2.3.18. Gel retention assays

Gel retention assays are used to determine if a protein binds to a nucleic acid. Protein and RNA or DNA are incubated and then subjected to horizontal agarose gel electrophoresis. If the protein binds to the nucleic acid, the latter will migrate at a slower rate or not at all compared to the control without added protein.

The interaction of recombinant AIF (0,1µg/µl) with 20 ng/µl DNA molecular weight ladders (low DNA mass ladder**,** Invitrogen) or 100ng/µl total RNA extracts from HeLa cells (purified

RNeasy Mini kit, Qiagen Valencia, CA) was carried out by gel retardation on 1% agarose gels. Recombinant AIF and DNA ladders or RNA were incubated with different Magnesium chloride concentrations (Sigma), different RNA's: PolyA, polyG, polyC, polyA/U, polyC/G (Sigma), or with NAD, NADH, NADP or NADPH (Sigma) for 30 minutes at room temperature in GR buffer (10mM Hepes; 50mM KCl; 5mM $MgCl_2$; 1mM DTT). Samples were electrophoresed in a Tris acetate buffer (50 mM) and stained with the nucleic acid dye SYBR® Gold (Molecular Probes).

3. Aim of the Project

AIF had been discovered as an apoptotic protein that is released from mitochondria and translocates to the nucleus where it takes part in DNA degradation.
Yet, a lot of evidence pointed to a second maybe non-apoptotic role of AIF. Firstly, in healthy cells, AIF is localised in mitochondria. Prominent examples like Cyt *c* elucidated that the localisation to mitochondria does not only prevent the exertion of its cytotoxic effects in the cytosol, but also allowed Cyt *c* to fulfill a vital function, namely to serve as an electron shuttle in the respiratory chain. Secondly, AIF's structure revealed an NADH oxidase domain, which does not seem to play a role in its apoptotic function, and yet is well conserved throughout the AIF orthologues found in different species (Lorenzo et al., 1999). Most importantly, recent findings in harlequin mice showed that downregulation of AIF expression resulted in a phenotype including neuronal and retinal degradation as well as ataxia which was not explicable by the downregulation of the apoptotic function (Klein et al., 2002). One aim of the project was therefore to find out if AIF had a hitherto unknown function in the mitochondria of living cells and, if that was the case, to characterise this function.

Many research groups have shown that AIF's activity in the nucleus is essential for its apoptotic function (Daugas et al., 2000b; Susin et al., 1999; Zhang et al., 2002; Zhu et al., 2003). Moreover, if AIF mutants lack their DNA binding capacity, apoptosis cannot be induced by the expression of these mutants in cells, as it is the case for the wild-type form of AIF (Ye et al., 2002). Modifying the AIF-DNA interaction is therefore a potential therapeutic approach to manipulate the apoptotic process. One of the aims of the project was hence to further identify this interaction by determining, whether AIF preferred binding to single or double-stranded DNA and whether co-factors could inhibit or enhance this interaction.
In our laboratory, various proteins retained on an AIF affinity column have recently been identified as RNA binding proteins. Based on these observations, another aim of this project was to look for an interaction between AIF and RNA and to compare it to the AIF-DNA interaction. One working hypothesis that needed to be investigated was that AIF could also degrade RNA during apoptosis.

4. Results

4.1. AIF compromises oxidative phosphorylation

4.1.1. AIF-deficient ES cells produce more lactate

The first observation that led to the discovery of a mitochondrial function of AIF was a pronounced colour change in the culture medium of AIF-deficient ES ($AIF^{-/y}$) cells. When the same number of $AIF^{-/y}$ cells and of their wild-type counterparts ($AIF^{+/y}$) were incubated for three days, the culture medium of the AIF-deficient cells had gradually turned yellow indicating a change in pH, while the culture medium of the wild-type cells was still red (Figure 4-1A). Indeed, when the pH was measured at different times of incubation, it was found that the $AIF^{-/y}$ cells caused an accelerated acidification of the culture medium (Figure 4-1B).

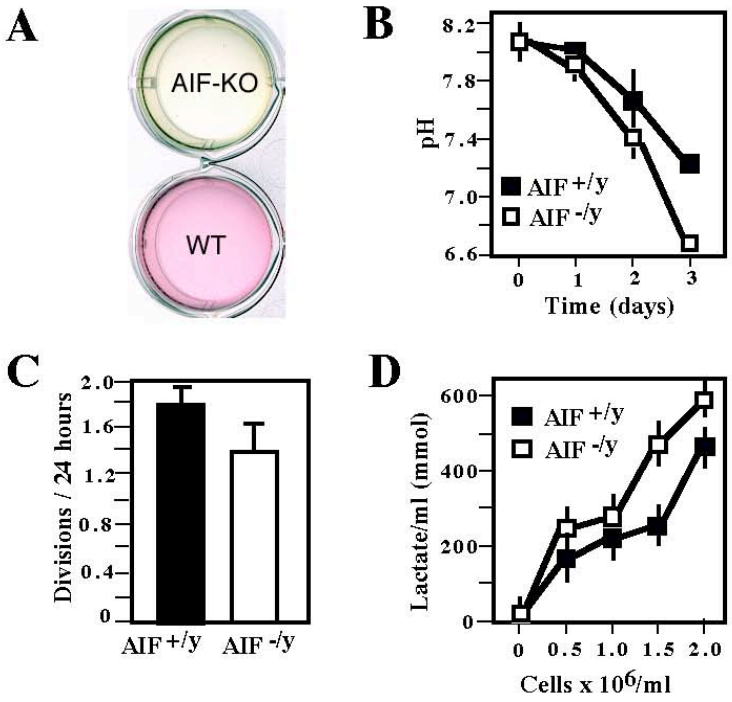

Figure 4-1. **Acidificatin of culture medium due to high lactate production in AIF-deficient cells.** (**A**) *Colour change of culture media of $AIF^{-/y}$ and $AIF^{+/y}$ ES cells. 2.5 × 10^5 cells/ml were seeded and the picture was taken after 72 hours of incubation.* (**B**) *Acidification of media by $AIF^{-/y}$ and $AIF^{+/y}$ cells, as determined in non-confluent cultures (2.5 x 10^5 cells/ml at day 0).* (**C**) *Number of divisions per day of $AIF^{-/y}$ as compared to $AIF^{+/y}$ ES cells. Values are given as X±SD (n=12).* (**D**) *Lactate production by $AIF^{-/y}$ and $AIF^{+/y}$ ES cells, as evaluated at different densities (X±SEM, n=3).*

However, this phenomenon could be due to a higher replication rate, since more cells produce more metabolites that have the potential to provoke a change of the pH of the culture medium. In order to exclude that this observation was due to a faster growing number

of the AIF-deficient cells, the doubling times of the cell lines were assessed and compared. It turned out, that the $AIF^{-/y}$ cells even replicated at a slightly slower rate than the $AIF^{+/y}$ cells (Figure 4-1C) leading to the hypothesis that AIF-deficient cells generate more acidifying metabolites per cell than wild-type cells. The byproduct of the ATP-producing process glycolysis, lactate, is known to be very acidifying. When the lactate content of the culture media was measured over several days and correlated to the number of living cells in the sample, it was found that the $AIF^{-/y}$ cells exhibited an enhanced lactate production (Figure 4-1D).

4.1.2. AIF-deficient ES cells depend on glycolysis

Abnormally high lactate generation in cells can indicate an increased rate of glycolysis. This metabolic pathway takes place in the cytoplasm, does not require oxygen, and produces ATP by converting one molecule of glucose into two molecules of pyruvate. An inhibitor of glycolysis, 2-D-deoxyglucose, was utilized to determine whether AIF-deficient ES cells could survive independently of this process. The control ES cells were not affected by an incubation of 72 hours with deoxyglucose, even at a concentration of 5mM, but the $AIF^{-/y}$ cells already showed an increased mortality at deoxyglucose concentrations of 2 and 4mM (Figure 4-2A). After 72 hours of incubation with 5mM deoxyglucose, the number of dead $AIF^{-/y}$ cells had almost tripled as determined by propidium iodide staining and subsequent cytofluorometric analysis (Figure 4-2A and B).

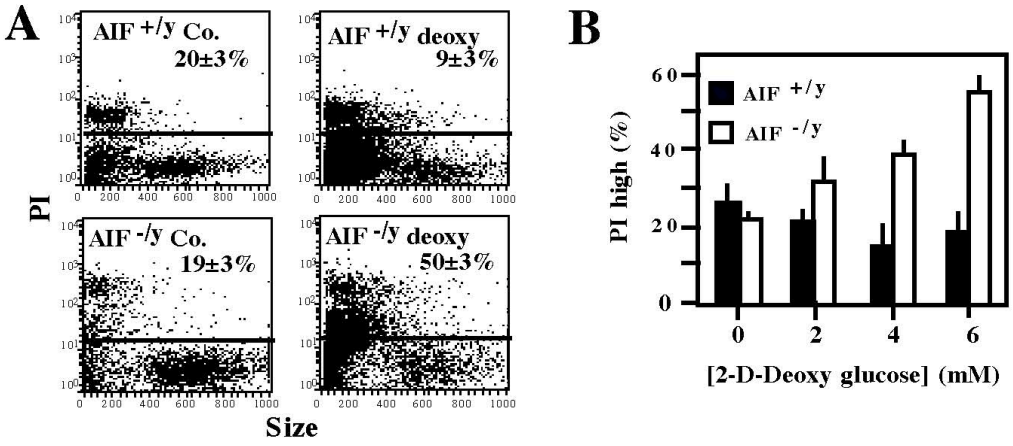

Figure 4-2. **Increased dependence on glycolysis of AIF-deficient cells.** *Increased death of AIF-deficient cells after inhibition of glyclolysis by 2-D-deoxyglucose. Cells ($AIF^{-/y}$ or $AIF^{+/y}$) were cultured for 72 hours in the absence or presence of 6 mM deoxyglucose (**A**) or in the presence of indicated concentrations of deoxyglucose (**B**), followed by staining with propidium iodide (PI) to determine the frequency of dead cells.*

Similar results were observed upon glucose withdrawal. While culturing the cells in medium without glucose had no effect on the replication of $AIF^{+/y}$ cells, it compromised the growth of AIF-deficient cells (Figure 4-3A and B). The latter hardly proliferated and the number of vital cells did therefore not increase the way it did when the culture medium contained glucose at

a concentration of 5g/l. The low rate of replication of AIF$^{-/y}$ cells was also detectable by determining the number of cells per phase of the cell cycle. The concept of the cell cycle analysis is described in materials and methods. The percentage of cells per cell cycle phase was similar in AIF$^{+/y}$ cells after incubation with or without glucose (Figure 4-3C). In contrast, the relative number of AIF$^{-/y}$ cells in the S or in the G2 phase was lower upon glucose withdrawal than in the presence of glucose (Figure 4-3C). Thus, as expected, the low replication rate in the absence of glucose also manifested itself in deficient progression of the cell cycle.

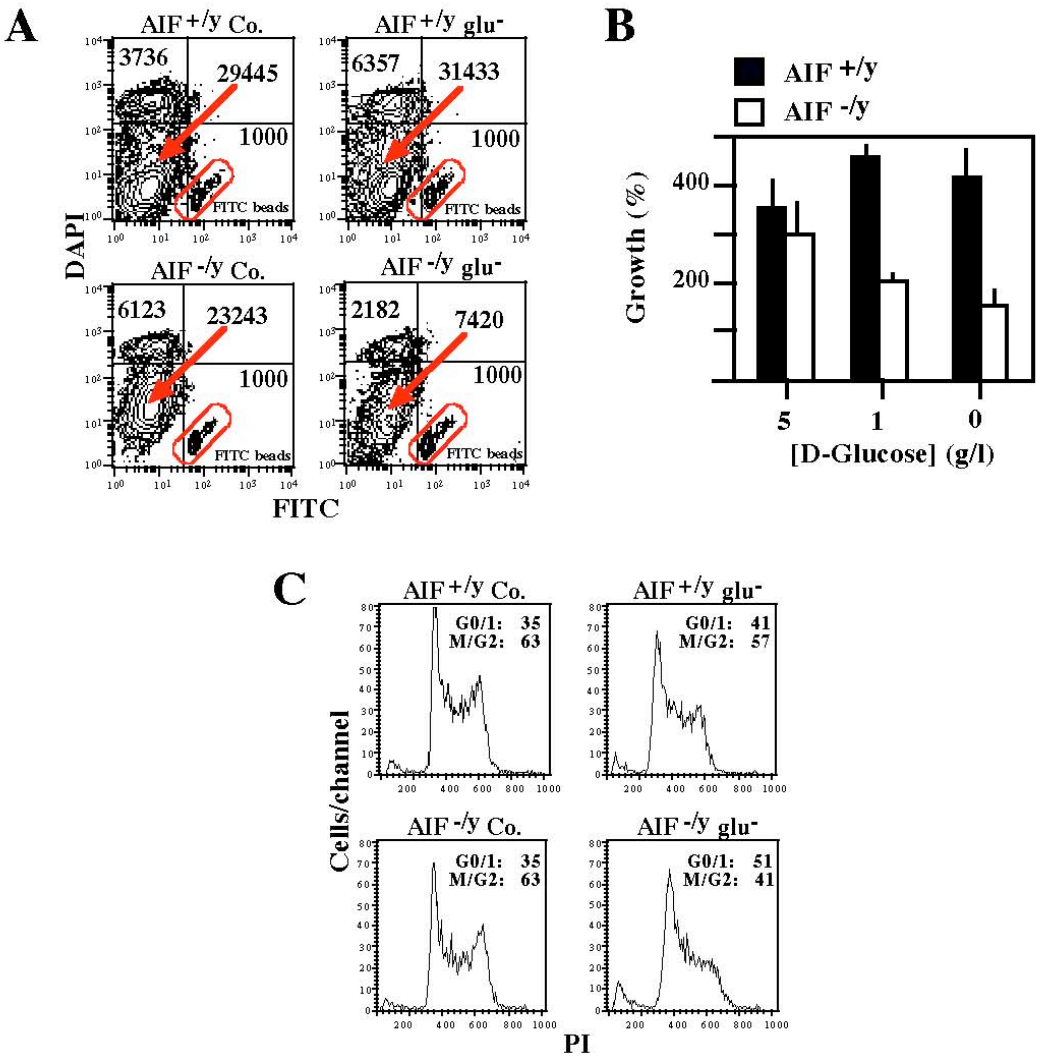

Figure 4-3. **Reduced growth of *AIF$^{-/y}$* cells in the absence of glucose.** (**A**) *AIF$^{-/y}$ and AIF$^{+/y}$ cells were cultured for three days in the presence (5 g/l in Co.) or absence (Glu$^-$) of glucose, and the exact number of viable (DAPI$^-$) cells was determined by adding FITC-labeled beads as an internal standard of the FACS analysis.* (**B**) *The same experiment as in (A) was performed utilizing different concentrations of glucose. Results are means of three independent determinations (X±SD).* (**C**) *Cell cycle profile of AIF$^{-/y}$ and AIF$^{+/y}$ cells cultured for three days in the presence or absence of glucose. Percentages of cells in different cell cycle phases are indicated. Results are representative of three independent determinations.*

When measuring the intracellular ATP levels in AIF$^{-/y}$ ES cells, a strong decline in ATP production could be correlated with the decreased growth rate in glucose-deficient conditions

(Figure 4-4A). This was not the case in AIF$^{+/y}$ cells. However, in the presence of glucose, base line ATP levels were comparable in both cell lines (Figure 4-4A). AIF$^{-/y}$ cells were obviously not able to produce enough energy in the absence of glucose, which could also explain their low rate of replication.

Several attempts were made to rescue the AIF-deficient from their glucose dependency. The only substitute that could restore growth of AIF$^{-/y}$ cells in the absence of glucose, was fructose, a sugar known to readily fuel anaerobic glycolysis (Mazzio and Soliman, 2003) (Figure 4-4B). Other carbohydrates like sucrose or galactose, which poorly enter glycolysis (Mazzio and Soliman, 2003), did not rescue the AIF$^{-/y}$ ES cells. Substrates of the respiratory chain, succinate and pyruvate, also failed to restore growth in cells lacking AIF (Figure 4-4B). Thus, AIF$^{-/y}$ cells strongly depend on ATP production by glycolysis.

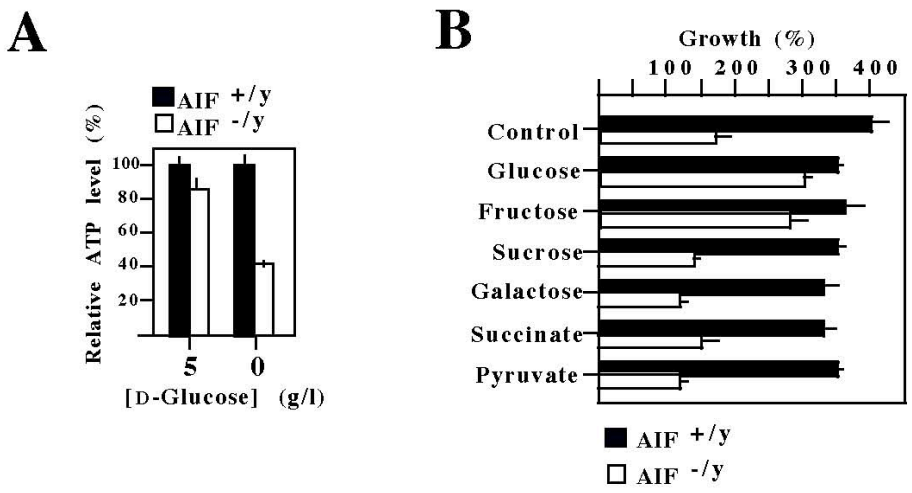

Figure 4-4. **Dependency of *AIF$^{-/y}$* cells on glucose for energy production and growth.** (**A**) *Reduced ATP production in AIF$^{-/y}$ cells upon glucose withdrawal. Cells were cultured for 36 hours in the absence or presence of glucose and intracellular ATP levels were determined among the adherent fraction of cells. ATP content was ratioed to the protein concentration of the samples.* (**B**) *AIF$^{-/y}$ and AIF$^{+/y}$ cells were cultured for three days in the absence (control) or presence of glucose, or in the presence of the indicated sugars or respiratory chain substrates (all at 5 mM), and the exact number of viable (DAPI^{-}) cells was determined by adding FITC-labeled beads as an internal standard of the FACS analysis. Results are means of three independent determinations (X±SD).*

4.1.3. Respiratory chain complex I and III are defective in AIF-deficient ES cells

The high dependency on glycolysis of AIF$^{-/y}$ cells implied that other energy generating processes were not functioning properly. In consequence, these cells had to compensate the lack of ATP by upregulating glycolytic activity, which generated a high amount of lactate and could not function in the absence of glucose. To test this hypothesis, oxidative phosphorylation, the cell's main source of ATP, was assessed in the murine ES cell lines by polarographic measurements of oxygen consumption.

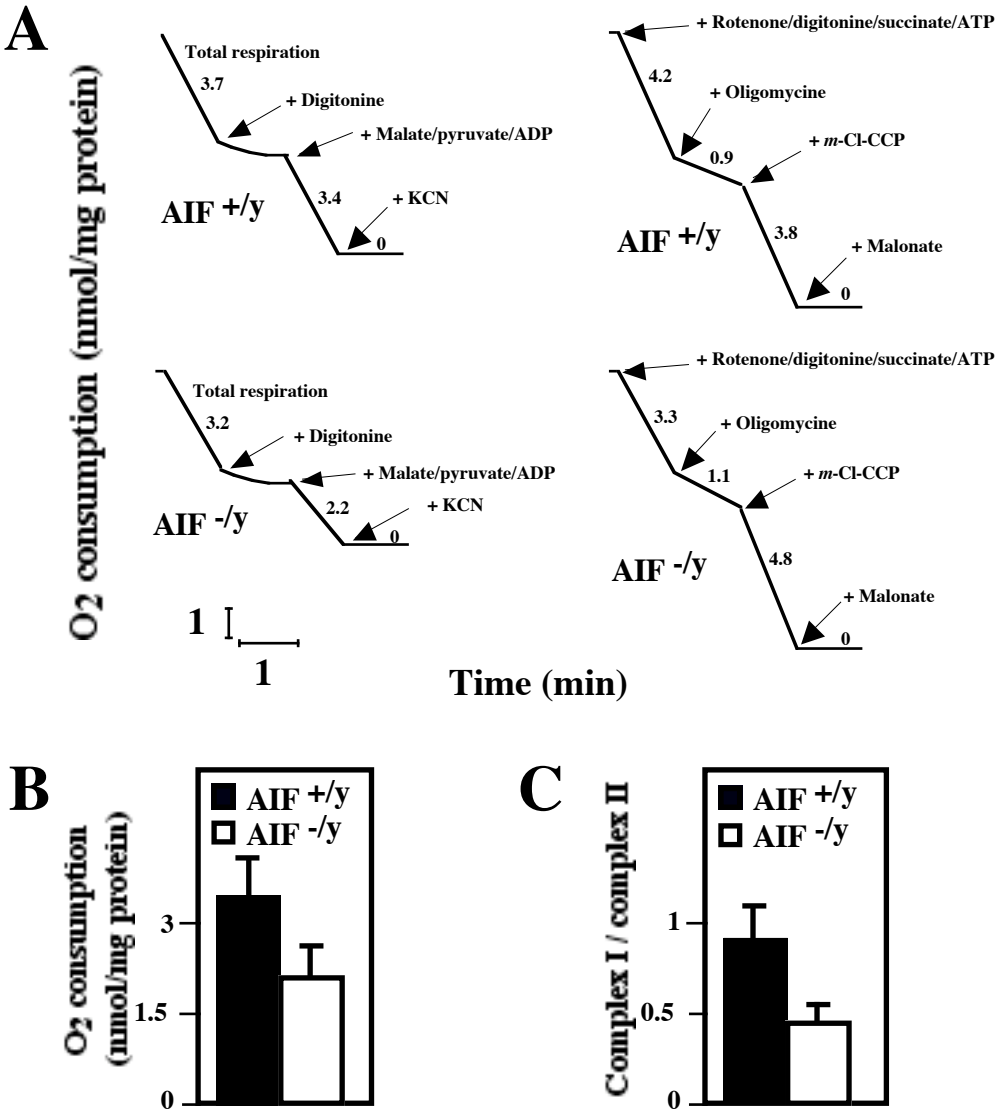

Figure 4-5. **OXPHOS deficiency in *AIF*$^{-/y}$ cells.** (**A**) *AIF*$^{-/y}$ *or AIF*$^{+/y}$ *ES cells were introduced into a polarograph to monitor their oxygen consumption, permeabilised with digitonin, followed by addition of the indicated respiratory substrates and inhibitors. Results are representative of three independent experiments.* (**B**) *Reduced absolute* O_2 *consumption in AIF-deficient cells after addition of malate, pyruvate and ADP.* (**C**) *Reduced pyruvate plus malate oxidation (as compared to succinate oxidation) in AIF-knockout ES cells, as determined by respirometry.*

The total respiration in intact cells was only slightly reduced in AIF$^{-/y}$ cells compared to AIF$^{+/y}$ cells (Figure 4-5A). However, when the complex I-dependent substrate oxidation in digitonin-permeabilised cells was analysed by addition of malate and pyruvate (which both furnish the complex I substrate NADH) as well as ADP (which is converted to ATP in the cell), the AIF-deficient cells showed a marked decrease (~40%) in oxygen consumption (Figure 4-5A and B). The ratio of complex I and complex II -dependent oxygen consumption can serve as an indicator of partial respiratory chain deficiencies (Rustin et al., 1991). Therefore, the activity of complex II was measured by blocking complex I with rotenone and adding the complex II-specific substrate succinate as well as ATP to digitonin-permeabilised cells. Indeed, the complex I/complex II ratio of AIF$^{-/y}$ ES cells was much lower than the one of their wild-type

counterparts (Figure 4-5A and C) strongly suggesting a defect in complex I of the respiratory chain in AIF-deficient cells.

To quantify the enzymatic activity of each complex of the respiratory chain, mitochondria-enriched fractions of the ES cells lines were produced and specific substrate oxidation was measured spectrophotometrically. This analysis confirmed the observation made in the polarography experiments, when a very significant decrease (~80%) in complex I activity in $AIF^{-/y}$ cells compared to $AIF^{+/y}$ cells (Figure 4-6) was detected. Moreover, an about 50% reduction of complex III activity was found in the AIF-deficient cell line as well (Figure 4-6). Thus, cells lacking AIF exhibit a respiratory chain defect affecting mostly complex I, but also complex III.

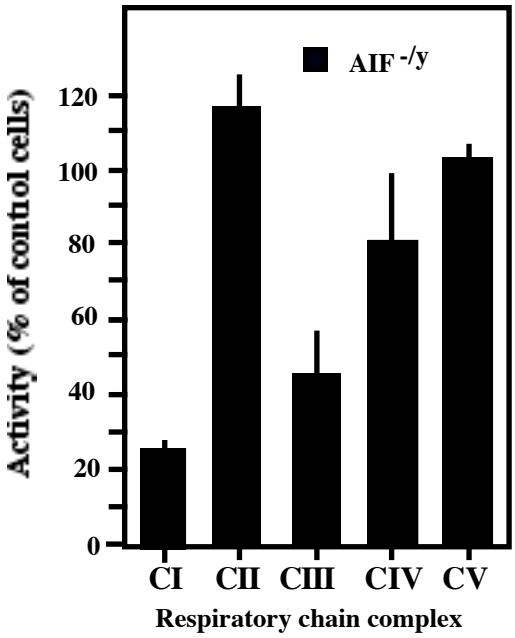

Figure 4-6. Respiratory chain complex activities in *AIF$^{-/y}$* cells. *Measurements of isolated respiratory chain complexes. Mitochondrion-enriched fractions from $AIF^{-/y}$, $AIF^{+/y}$ ES cells were monitored for the activity of each of the respiratory chain complexes. Data (X±SD) were ratioed to the $AIF^{+/y}$ controls, which were considered as 100% value. This experiment has been performed three times, in triplicates, with similar results.*

4.1.4. Development of an RNA interference method to downregulate AIF in human cell lines

To prove that this respiratory chain defect was due to the AIF knock-out in the murine ES cells and not to another non-identified modification of the genome, a second cell line lacking AIF needed to be investigated. A recently developed method serves to downregulate the expression of a specific gene by RNA interference. A small interfering RNA (siRNA) duplex that recognizes a 21-nucleotide sequence unique to the gene of choice is introduced into the cell. In the cytoplasm, they are incorporated into a protein complex, the RNA-induced silence complex (RISC). The antisense strand of the duplex siRNA guides the RISC to the homologous mRNA, where the RISC-associated endoribonuclease cleaves the target

mRNA, resulting in the silencing of the target gene (Martinez et al., 2002). This method was used in the human cervix carcinoma HeLa cell line, which allowed at the same time to determine whether AIF downregulation resulted in an OXPHOS defect and whether this phenomenon was murine-specific or also valid for other species.

Two different 21-nucleotide sequences unique to human AIF were determined as described in Materials and Methods and the corresponding siRNA duplexes were purchased from Proligo. HeLa cells were transfected with one of the AIF siRNA's or with a control siRNA. The control siRNA-1 recognizes the mRNA sequence of emerin, a gene that had been identified as non-essential in tissue culture cells (Harborth et al., 2001). The control siRNA-2 can downregulate the expression of murine AIF, but does not bind to human AIF mRNA. The most effective downregulation of AIF was found to be at 72 hours post-transfection. It was determined by western blot (Figure 4-7A) as well as by immunofluorescence (Figure 4-7B). The AIF-specific siRNA's inhibited AIF expression close to 100% while the control siRNA's did not or only slightly affected AIF abundance in HeLa cells.

The so-called AIF knock-down cells were then utilized to investigate if the AIF deficiency in HeLa cells would also compromise the OXPHOS process.

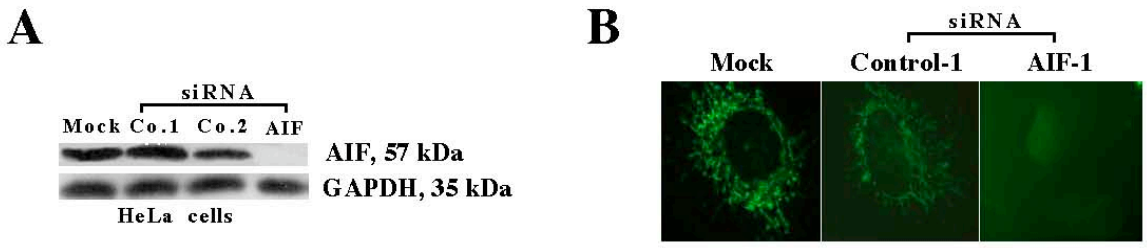

Figure 4-7. **Suppression of AIF expression by siRNA.** (**A**) *HeLa cells were mock-treated or transfected with two different control siRNAs or an AIF-specific siRNA, and the abundance of AIF was determined by immunoblot 72 hours later.* (**B**) *HeLa cells were mock-treated or transfected with a control or an AIF-specific siRNA, fixed, and stained with an AIF-specific antibody 72 hours post-transfection.*

4.1.5. AIF-deficient HeLa cells exhibit a respiratory chain complex I defect

HeLa cells were transfected with AIF-specific or control siRNA's and analysed by polarographic measurements, as described for the ES cells in 4.1.3, 72 hours post-transfection. The downregulation of AIF was verified by western blot in each experiment. Very similar, although not identical, observations to the ones made in AIF-deficient murine ES cells were made in AIF-deficient HeLa cells. The absolute oxygen consumption after addition of pyruvate, malate, and ATP (thus measuring the electron flux through complex I) is reduced by about 30% in AIF knock-down cells compared to control siRNA-transfected cells (Figure 4-8A and B). The complex I/complex II ratio reveals a downregulation of about 50%

in complex I activity of HeLa cells lacking AIF (Figure 4-8A and C) resembling the value for murine ES cells.

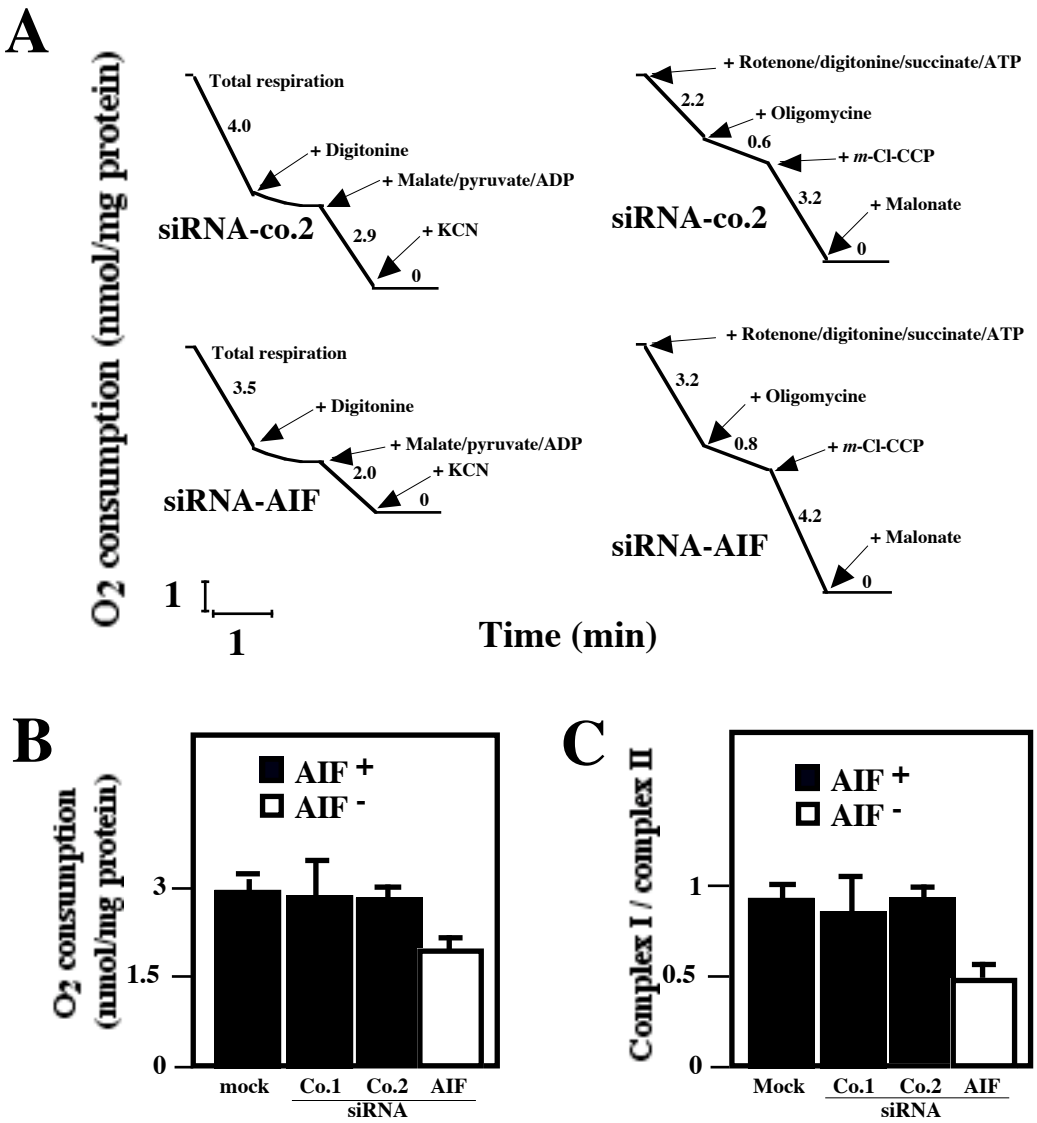

Figure 4-8. **OXPHOS deficiency in AIF-negative HeLa cells.** (**A**) *HeLa cells transfected with a control or AIF-specific siRNA were analysed by polarographic measurements 72 hours post-transfection. Their oxygen consumption was measured before and after permeabilisation with digitonin, followed by addition of the indicated respiratory substrates and inhibitors. Results are representative of three independent experiments.* (**B**) *Reduced absolute O_2 consumption in AIF-negative cells after addition of malate, pyruvate and ADP.* (**C**) *Reduced pyruvate plus malate oxidation (as compared to succinate oxidation) after AIF knockdown in HeLa cells, but not after transfection with control siRNA, as determined by respirometry.*

When the isolated complexes of the respiratory chain were assessed in enriched mitochondria of siRNA treated HeLa cells, the complex I defect in AIF-deficient cells was once more confirmed (Figure 4-9). However, in contrast to the murine ES cells, the AIF knock-down HeLa cells did not exhibit a decrease in complex III activity. Therefore, it can be concluded, that AIF deficiency entails an OXPHOS defect that mostly affects complex I.

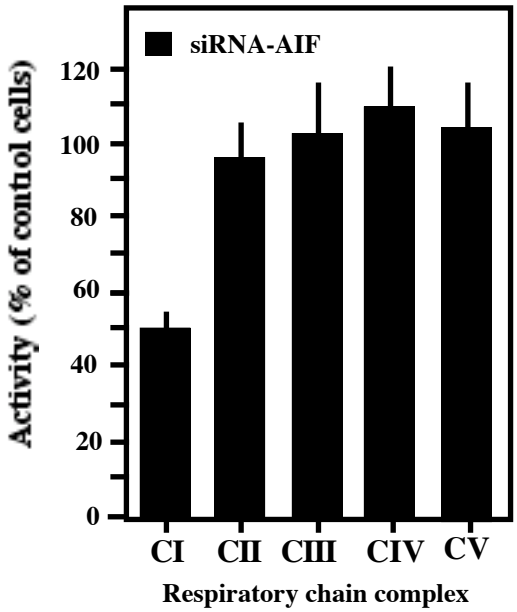

Figure 4-9. **Respiratory chain complex activities in AIF-negative HeLa cells.** *Measurements of isolated respiratory chain complexes. Mitochondrion-enriched fractions from control siRNA and AIF siRNA-treated HeLa cells were monitored for the activity of each of the respiratory chain complexes. Data (X±SD) were ratioed to the AIF-positive controls, which were considered as 100% value. This experiment has been performed three times, in triplicates, with similar results.*

4.1.6. Reduced abundance of complex I and III in AIF-deficient cells

To further characterise this respiratory chain defect, a series of questions had to be addressed. One aim was to find out whether the defect also affected the protein levels or whether the significantly low activity was solely due to functional failure. The expression of different subunits of the NADH dehydrogenase and the ubiquinol-cytochrome *c* reductase in AIF-deficient as well as their control cells was analysed by SDS-PAGE followed by immunoblot. In $AIF^{-/y}$ cells, the complex I subunits 39kDa, 20kDa, 17kDa (also called NDUFA9, NDUFS7, and NDUFB6, respectively), and the recently identified Grim19 were present at extremely low levels compared to $AIF^{+/y}$ cells (Figure 4-10A). The same applied to tested complex III subunits, such as core 1, core 2, and the Rieske iron-sulfur subunit (FeS). While the expression of complex IV subunit IV was only slightly downregulated, other mitochondrial proteins seemed unaffected in their expression (Figure 4-10A). The chaperone HSP60, the building block of the mitochondrial protein import machinery TOM40, and the outer mitochondrial membrane protein VDAC exhibited similar expression levels in both AIF-deficient and AIF-positive murine ES cells. Investigation of the same set of proteins in siRNA treated HeLa cells revealed, in accordance with the activity measurements, a loss of complex I subunits, but not of complex III subunits in AIF knock-down cells (Figure 4-10A). Expression levels of complex IV subunit IV as well as the non-respiratory chain proteins were comparable in AIF and control siRNA cells. To exclude artefacts, these results were also

confirmed in another AIF$^{-/y}$ murine ES cell line and in HeLa cells using different siRNA's to downregulate AIF (Figure 4-10B and 4-10C).

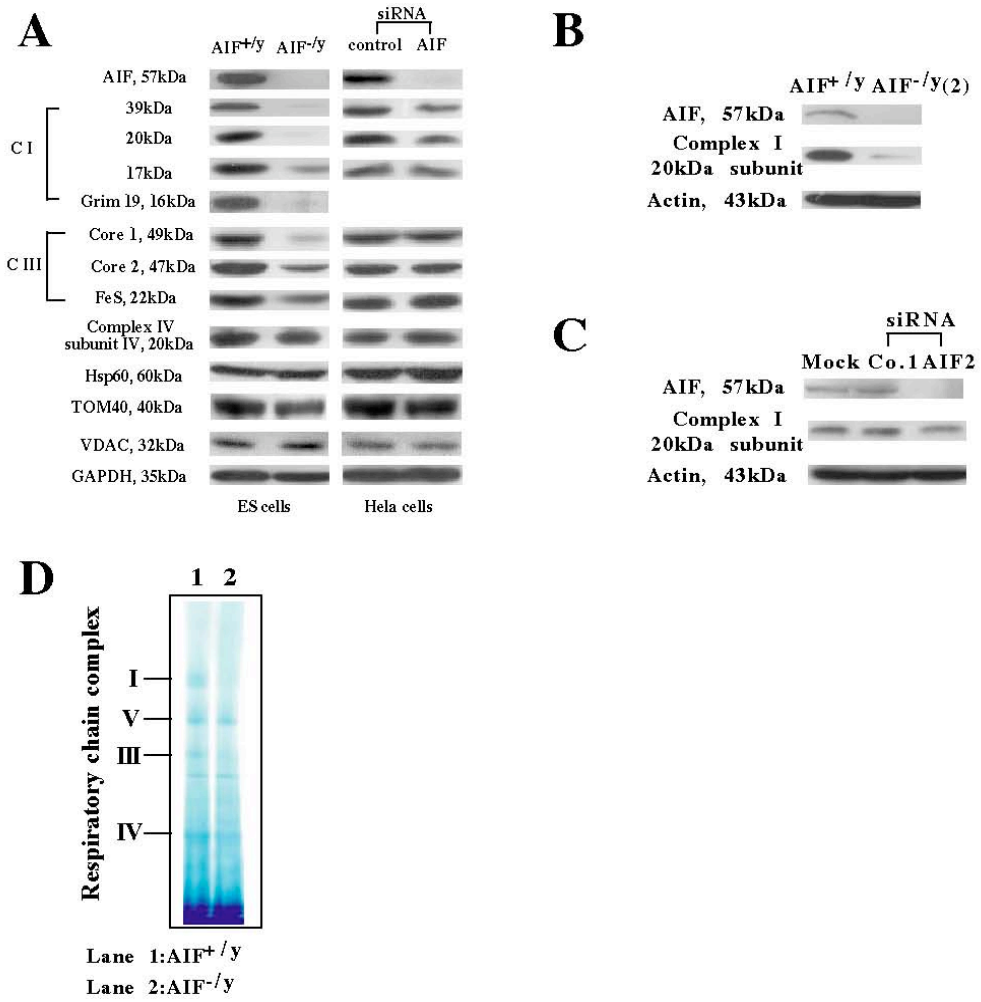

Figure 4-10. **Reduced abundance of respiratory chain complex I and complex III.** (**A**) *SDS-PAGE determination of the subunit composition of complexes I and III as well as other mitochondrial proteins using a number of monoclonal antibodies. Whole cell lysates from AIF$^{-/y}$ or AIF$^{+/y}$ ES and control or AIF siRNA (siRNA-AIF1) HeLa cells were subjected to immunoblot detection of the indicated antigens. This experiment has been reproduced three times.* (**B**) (**C**) *Data were confirmed for another ES knock-out cell line, and additional siRNA's: HeLa cells treated to knock-down AIF with the second AIF siRNA exhibited a complex I deficiency, including the downregulation of the 20 kDa subunit, as determined by immunoblot 72 h later. As a control, an siRNA targeting mouse AIF (which does not reduce the expression of human AIF) was used (B). Analysis of a second, independent AIF knock-out ES cell line for complex I deficiency. The AIF$^{-/y}$ (2) ES cell line, (see supplementary material of Joza et al. 2001) was investigated for a complex I deficiency by immunoblot (C). As a loading control, actin expression was measured.* (**D**) *Blue Native (BN) PAGE of isolated mitochondria from AIF$^{-/y}$ or AIF$^{+/y}$ ES cells. Dodecylmaltoside was used for solubilization and separation of the mitochondrial complexes I, V, III, and IV (I, V, III, IV) by BN-PAGE. Densitometry (normalized to complex V) revealed a relative deficiency in AIF$^{-/y}$ cells in the abundance of complex I (<30% of control AIF$^{+/y}$ value) and in the abundance of complex III (54% of control). No defect was found in complex IV (84%) and V (100%).*

Blue native gel electrophoresis is a method to separate whole respiratory chain complexes according to their size. Due to the usage of mild neutral detergents, the complexes of the respiratory chain are not disintegrated and can therefore be visualised as whole complexes

by coomassie blue staining (Schägger and von Jagow, 1991). Blue native gels of AIF$^{-/y}$ and AIF$^{+/y}$ ES cells revealed that the abundance of the whole complex I and complex III in AIF-deficient cells were remarkably reduced compared to wild-type cells (Figure 4-10C). Considering the results of the immunoblot experiments, this was to be expected. It was interesting, however, that there were no subcomplexes of the respiratory chain complexes detected by blue native gel analysis.

Although manipulation of embryonic stem cells is very delicate, it was attempted to induce re-expression of the complex I and III subunits in AIF$^{-/y}$ cells by retransfection of AIF. Several GFP-constructs were used: one, as a control, coding for GFP only, one encoding the complete murine AIF sequence (full length, FL), and one encoding a mutant of murine AIF in which the mitochondrial localisation sequence had been deleted (Δ1-100). The transfection rate of AIF$^{-/y}$ cells after electroporation was extremely low as determined by GFP-emitted fluorescence measurement by FACS analysis (Figure 4-11A). Nevertheless, a slight increase in the expression levels of complex I and III subunits could be observed in cells transfected with the full length construct, while transfection with the empty vector or the vector coding for the non-mitochondrial AIF did not show any effect (Figure 4-11B). Thus, the mitochondrial localisation of AIF seemed to be essential for its effect on the expression level of the respiratory chain complexes.

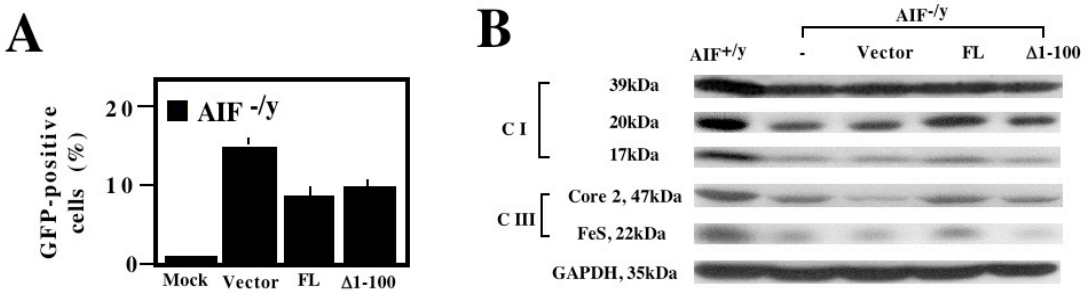

Figure 4-11. Re-expression of AIF in *AIF$^{-/y}$* ES restores complex I subunit expression. *Cells were transfected with full length (FL) AIF, Δ1-100 AIF (which lacks the mitochondrial targeting sequence), or the empty vector. 48 hours later, the transfection rate was determined by FACS analysis of GFP-fluorescence* (**A**) *and the expression of the indicated complex I and III subunits was monitored by immunoblot* (**B**).

4.1.7. The respiratory chain defect in AIF-deficient cells is a post-transcriptional phenomenon

How does AIF exert its effect on the respiratory chain complexes? In order to answer this question, it was assessed whether the reduced expression of the complex I subunits in AIF-deficient cells was due to a defect at the transcriptional level. Since the respiratory chain subunits are encoded by both nuclear and mitochondrial DNA, transcription levels in both organelles had to be tested.

The content of mRNA's of complex I subunits encoded by nuclear DNA was quantified in murine ES cells as well as in HeLa cells by RT-PCR. There were no differences in the transcription of complex I subunits in AIF-deficient cells (Figure 4-12A). As expected, the level of AIF mRNA was reduced in AIF siRNA treated HeLa cells compared to control siRNA treated HeLa cells (Figure 4-12A).

The level of mRNA's of mitochondrially encoded subunits of the respiratory chain as well as the level of the 16S RNA and the tRNA Leu-1 were quantified by RT-PCR. The AIF$^{-/y}$ cells exhibited the same amount of these RNA's as their wild-type counterparts (Figure 4-12B). Thus, a regulation of the activity of the respiratory chain at the level of transcription could be excluded. Moreover, there does not seem to be a gross perturbation of mitochondrial biogenesis nor a depletion of mitochondrial DNA in AIF-deficient cells.

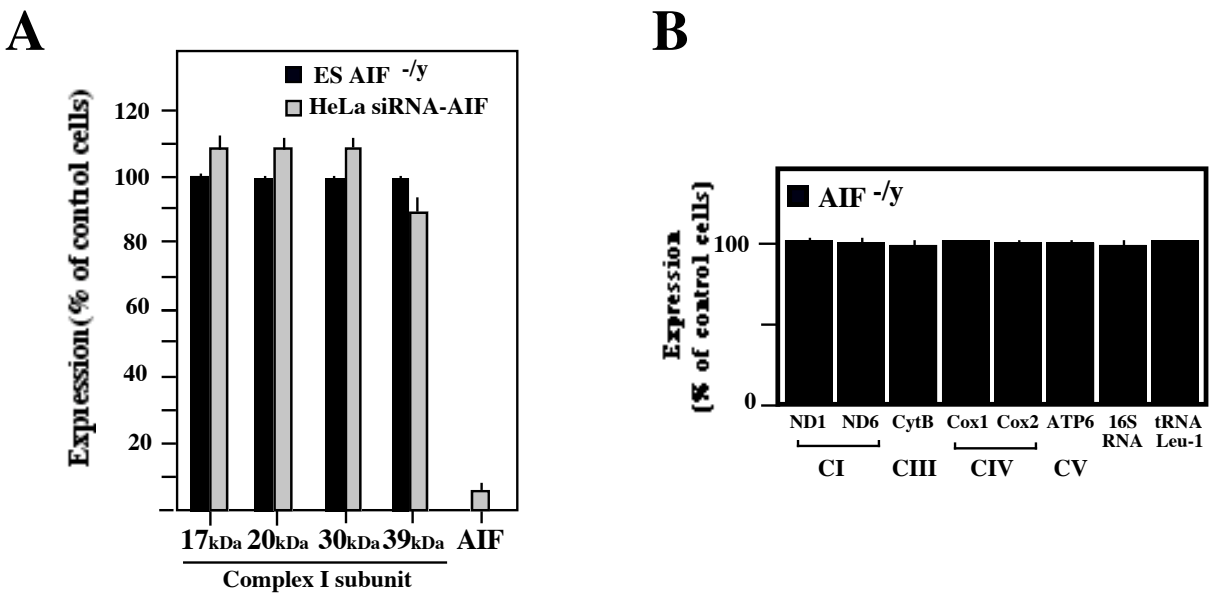

Figure 4-12. **Normal RNA levels in AIF-negative cells.** (**A**) *Expression of nuclear DNA-encoded complex I subunits in AIF-deficient cells, as determined by RT-PCR, normalized to the 18S RNA. The values are given as the percentage of the control cells (AIF$^{+/y}$ ES cells for AIF$^{-/y}$ ES cells and HeLa cells treated with emerin-specific siRNA for HeLa cells treated with AIF-specific siRNA).* (**B**) *Expression of mitochondrial RNA in AIF-negative cells. Total cellular RNA was extracted from AIF$^{+/y}$ and AIF$^{-/y}$ ES cells, and the levels of the indicated RNA species (ND1, NADH dehydrogenase subunit 1 ; ND6 , NADH dehydrogenase subunit 6 ; cytB, cytochrome b ; cox1, cytochrome c oxidase subunit 1; cox2, cytochrome c oxidase subunit 2; ATP6, ATP synthase F0 subunit 6; 16S RNA; tRNA Leu, Leucine 1) encoded by mitochondrial DNA were quantified by RT-PCR. Results ((X±SEM, n=3) were expressed as percentage of control values (100% in AIF$^{+/y}$ ES cells).*

4.1.8. AIF is not part of a respiratory chain complex

Another possibility was that AIF itself was a subunit of a respiratory chain complex and could thus influence its stability and activity. In cooperation with Professor Hermann Schägger of the university of Frankfurt, this hypothesis was tested. Using mitochondrial fractions from mouse brain, the subunits of the respiratory chain were separated in a blue native gel

followed by an SDS-PAGE and silver staining. AIF was subsequently detected by immunoblot. The experiment showed that AIF was not part of one of the complexes (Figure 4-13A). In the immunoblot, AIF appears as a smear rather than a single spot. This is probably due to its water solubility. Hydrophilic proteins do not migrate in an BN-PAGE without the binding of the negatively charged coomassie dye (Schägger and von Jagow, 1991). Binding of different amounts of coomassie molecules to AIF proteins can result in a smear, which is also seen for other water soluble proteins that are not part of a complex, such as Cyt *c*.

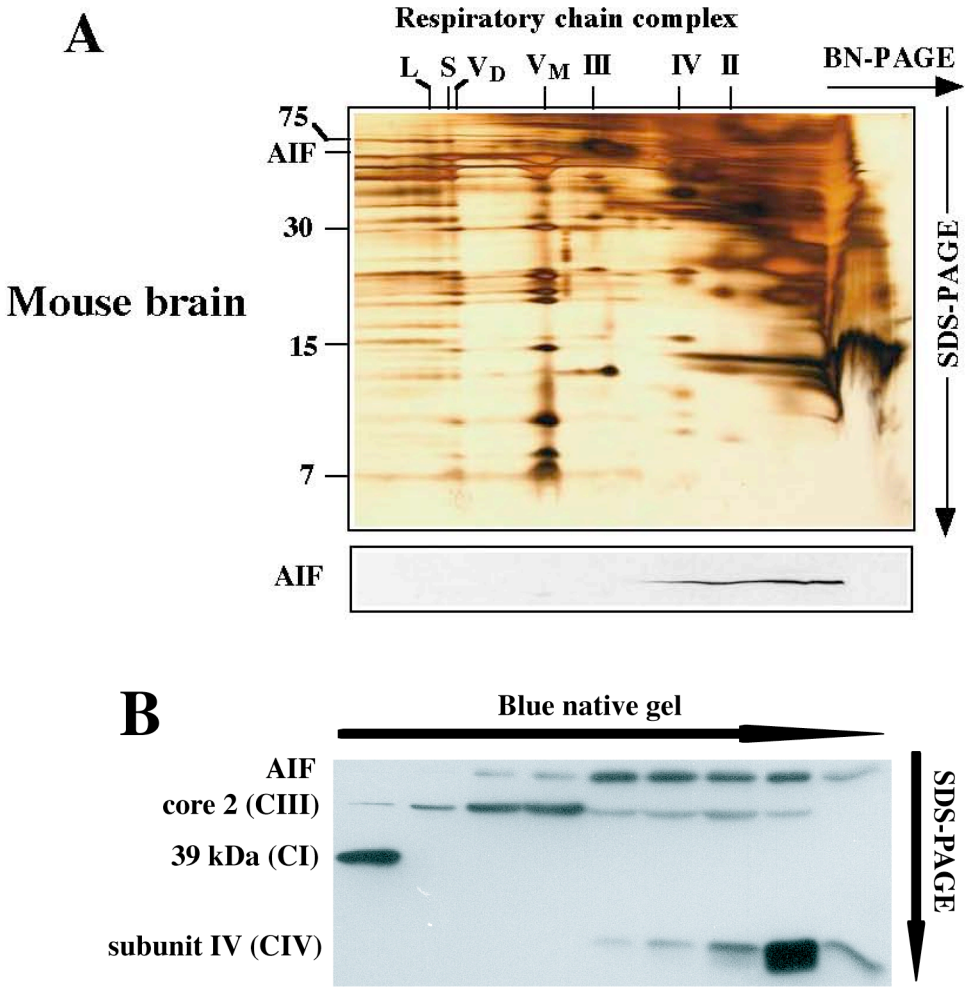

Figure 4-13. **Non-association of AIF with complex I, complex III, or supercomplexes.** (**A**) *Brain mitochondria were solubilized with digitonin and subjected to two-dimensional gel electrophoresis (BN-PAGE from left to right, followed by SDS-PAGE from high to low) to visualise the respiratory chain complexes (roman numbers) including dimeric (V_D) and monomeric (V_M) complex V and the two supercomplexes, the smaller one (S) which contains monomeric complex I and dimeric complex III (total mass ~1.5 MDa) and the larger one (L) which in addition contains monomeric complex IV. The blots were either silver-stained (upper panels) or subjected to immunodetection of AIF (lower panel). Only the ~57 kDa zone of the immunoblot is shown.* (**B**) *The experiment was imitated with mitochondria isolated from mouse liver, but this time, bands were cut out of the BN gel and loaded onto an SDS-PAGE. The presence of subunits of different complexes in these bands were detected by immunoblot utilizing antibodies specific for AIF, complex III core 2 subunit, complex I 39kDa subunits and complex IV subunit IV.*

Please note that this experiment was performed by Hermann Schägger and is only included in this manuscript because of its high relevance.

However, when this experiment was repeated in a similar way in our laboratory, AIF was found to be associated to a complex of a size of about 300kDa (Figure 4-13B).

4.1.9. Assessment of redox state of AIF-deficient cells

Since AIF contains an oxidoreductase domain and since it was recently suggested that AIF had a radical scavenger function (Klein et al., 2002), the redox state of AIF-deficient cells was assessed in order to find an explanation for the dysfunction of the respiratory chain.

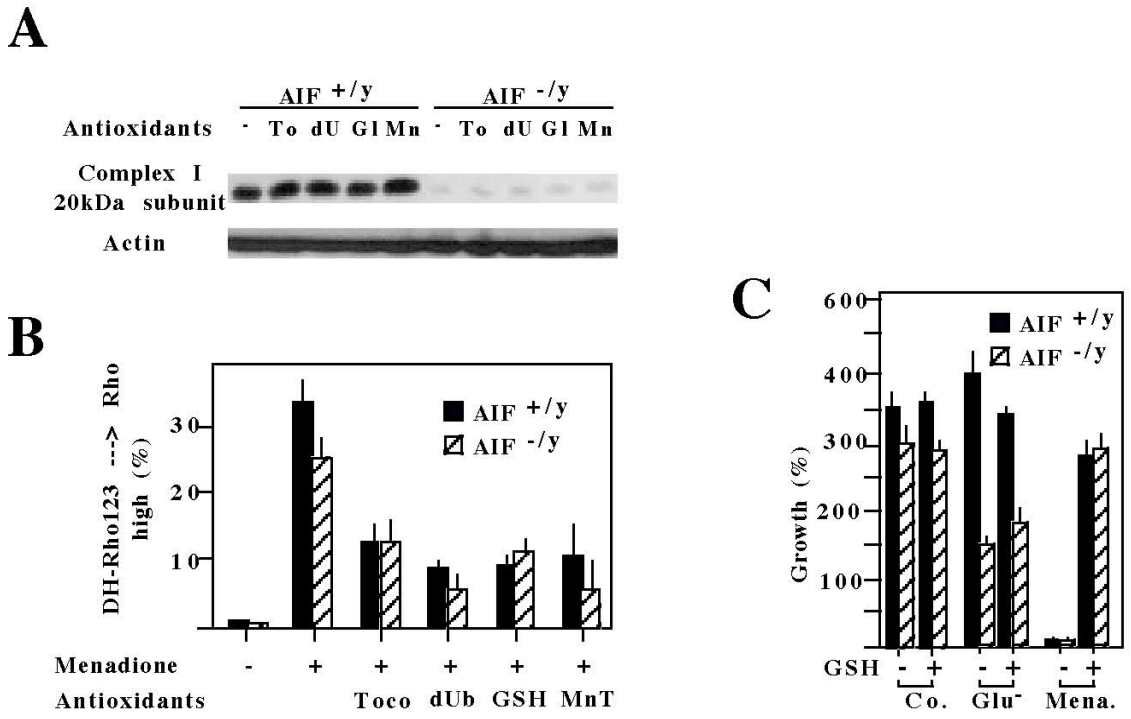

Figure 4-14. **Failure of antioxidants to rescue the respiratory chain defect in *AIF$^{-/y}$* ES cells.** (**A**) *Failure of antioxidants to cause re-expression of the 20 kDa complex I subunit. AIF$^{-/y}$ and AIF$^{+/y}$ cells were cultured for 72 hours in the presence of tocopherol (200μM), decylubiquinone (50mM), GSH ester (10mM) or MnTBAP (50μM), all re-added each 12 hours, followed by immunoblot.* (**B**) *Alternatively, cells were treated for 3 hours with menadione (100μM) and the production of ROS was measured by assessing the oxidation of dihydrorhodamine 123 in the cytofluorometer.* (**C**) *Failure of the antioxidant glutathione to rescue AIF$^{-/y}$ cells from glucose withdrawal-induced cell death. AIF$^{-/y}$ and AIF$^{+/y}$ cells were cultured for 48 hours in medium without glucose and/or 10 mM glutathione ethyl ester, followed by determination of the viability as in Figure 4-3B. As an internal control of the glutathione effect, AIF$^{+/y}$ cells were also cultured in the presence of menadione (100μM). Values are means ±SEM of three independent determinations.*

AIF$^{-/y}$ and AIF$^{+/y}$ ES cells were treated with several antioxidants for three days. Tocopherol is known to be an effective scavenger for reactive oxygen and nitrogen species , decylubiquinone is a ubiquinone derivate and therefore acts directly at the respiratory chain. Glutathione ester is a very strong antioxidant scavenging ROS directly and indirectly through enzymatic reactions, and MnTBAP is an SOD mimetic thus detoxifying superoxide anion. The expression level of the complex I 20kDa subunit was not modified by the antioxidant

treatment, neither in the AIF-sufficient nor in the AIF-deficient cell line (Figure 4-14A). As a control of their antioxidant potential, it was shown that the different agents were able to reduce ROS generation in both $AIF^{-/y}$ and $AIF^{+/y}$ cells after menadione treatment (Figure 4-14B). In accordance with these observations, supplementation with GSH ester could not restore growth of glucose-depleted $AIF^{-/y}$ cells, although it did rescue menadione-treated ES cells (Figure 4-14C). Thus, no oxidative insult was suspected in AIF-deficient cells.

To further verify this assumption, base line levels of several indicators for the redox state of cells were compared in $AIF^{-/y}$ and $AIF^{+/y}$ cells. No significant differences were found. AIF-deficient cells contained slightly reduced levels of ROS, normal (or slightly elevated) levels of nonoxidized cardiolipin and NAD(P)H, normal levels of glutathione, as well as a level of hydrogen peroxide similar to the one seen in AIF-positive cells (Figure 4-15A).

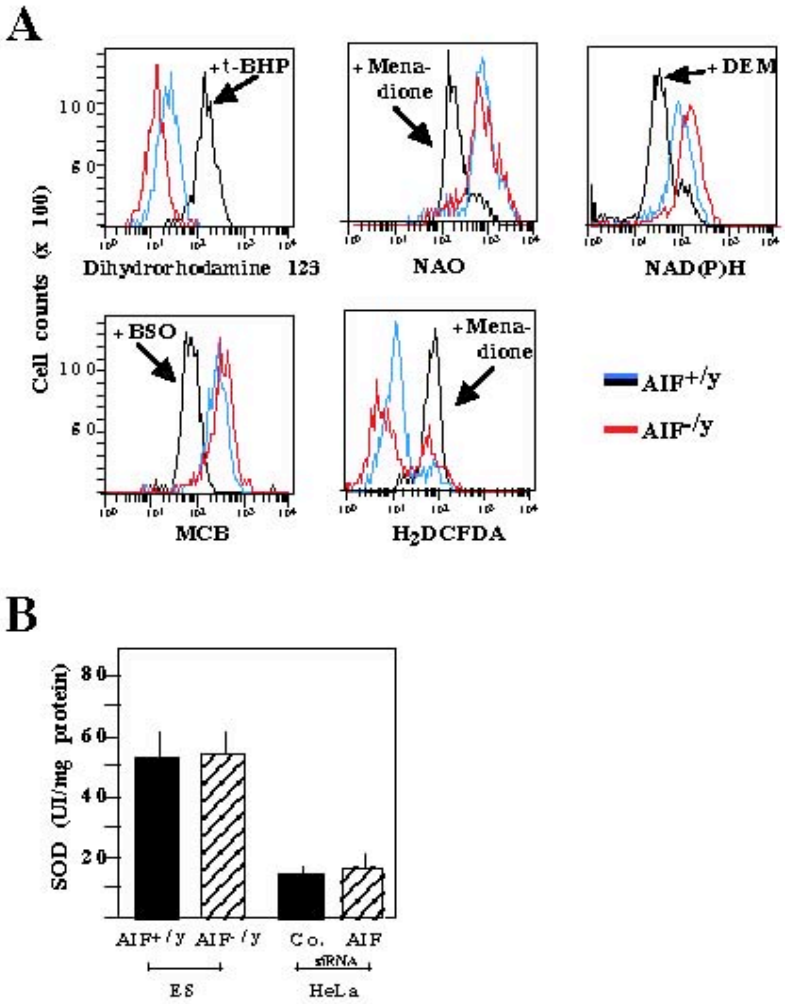

Figure 4-15. **Antioxidant functions of AIF-deficient cells.** (**A**) *Cytofluorometric determination of baseline levels of the production of reactive oxygen species (with dehydrorhodamine 123, control cells were incubated with 8 mM tert-butyl hydroperoxide for 50 minutes), non-oxidized cardiolipin (with nonylacridine orange, control cells were incubated in 1mM menadione for 50 minutes), glutathione (with monochlorobiman, control cells were incubated with BSO for 24 hours), H_2O_2 levels (with DCFDA, control cells were incubated in 1 mM menadione for 50 minutes), and NAD(P)H levels (by determining the autofluorescence excited at 360 nm; control cells were incubated with 50μM diethyl maleate for 30 minutes) while comparing $AIF^{-/y}$ and $AIF^{+/y}$ cells.* (**B**) *Normal SOD levels in AIF-deficient cells. SOD levels were determined biochemically in lysates from $AIF^{-/y}$ and $AIF^{+/y}$ ES cells as well as in control siRNA and AIF siRNA-treated HeLa cells.*

Moreover, the activity of the superoxide dismutase (SOD) was assessed as an inducible marker for increased superoxide production (Geromel et al., 2002). A modification of the SOD activity was not detected, neither in AIF-deficient murine ES cells nor in AIF siRNA treated HeLa cells (Figure 4-15B). In conclusion, under non-stress conditions, the redox status of AIF-deficient cells seemed similar to the one found in AIF-sufficient cells.

However, when murine ES cells were treated with exogenous hydrogen peroxide, $AIF^{-/y}$ cells exhibited a higher mortality than their wild-type counterparts (Figure 4-16). Thus, even though base line redox levels were suggested to be normal, the oxidant defense mechanisms of AIF-deficient cells seemed out of balance.

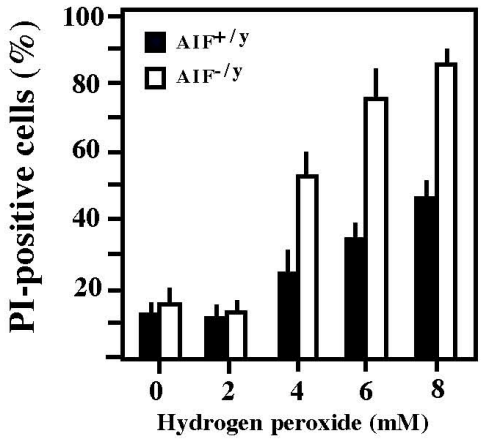

Figure 4-16. **Increased hydrogen peroxide sensitivity of AIF-deficient cells.** *$AIF^{-/y}$ and $AIF^{+/y}$ cells were treated with the indicated concentrations of hydrogen peroxide for 24 hours and stained with propidium iodide (PI) to determine the frequency of dead cells by FACS analysis.*

4.1.10. AIF-deficiency causes a respiratory chain defect in Hq mice

Harlequin mice have recently been described to have a retroviral insertion in the AIF gene that results in 80% downregulation of the AIF expression in all tissues (Klein et al., 2002). These mice exhibit progressive neuronal and retinal degradation. After having assessed the OXPHOS defect in two different AIF-deficient cell line, the harlequin mice served as a model for AIF downregulation *in vivo*. The activity of the respiratory chain complexes was measured in different tissues of 3 months old male harlequin mice (genotype $AIF^{HQ}Y$) and compared to wild-type littermates. $AIF^{HQ}Y$ mice manifested a significant reduction in complex I activity in the brain (~60% of control) and in the retina (~30% of control), but not in the liver or heart (Figure 4-17A). These findings correlated with the phenotypic symptoms of these mice. The activity of other respiratory chain complexes appeared normal in $AIF^{HQ}Y$ mice. Accordingly, the downregulation of the complex I subunit expression at the protein level was also found in the brain and the retina of the harlequin mice, but not in the liver and the heart (Figure 4-17B). These data pointed to a tissue specific role of AIF in OXPHOS.

Brains of harlequin mice at different ages were analysed to determine whether the complex I defect was acquired progressively or not. Brains of neonatal as well as 60 days old harlequin mice showed a similar reduction in complex I subunits when compared to wild-type isogenic controls (Figure 4-17C). The immunoblot bands were quantified by densitometric analysis to detect small differences, but the extent of downregulation of the subunits seemed unchanged in harlequin mice of different age (Figure 4-17C).

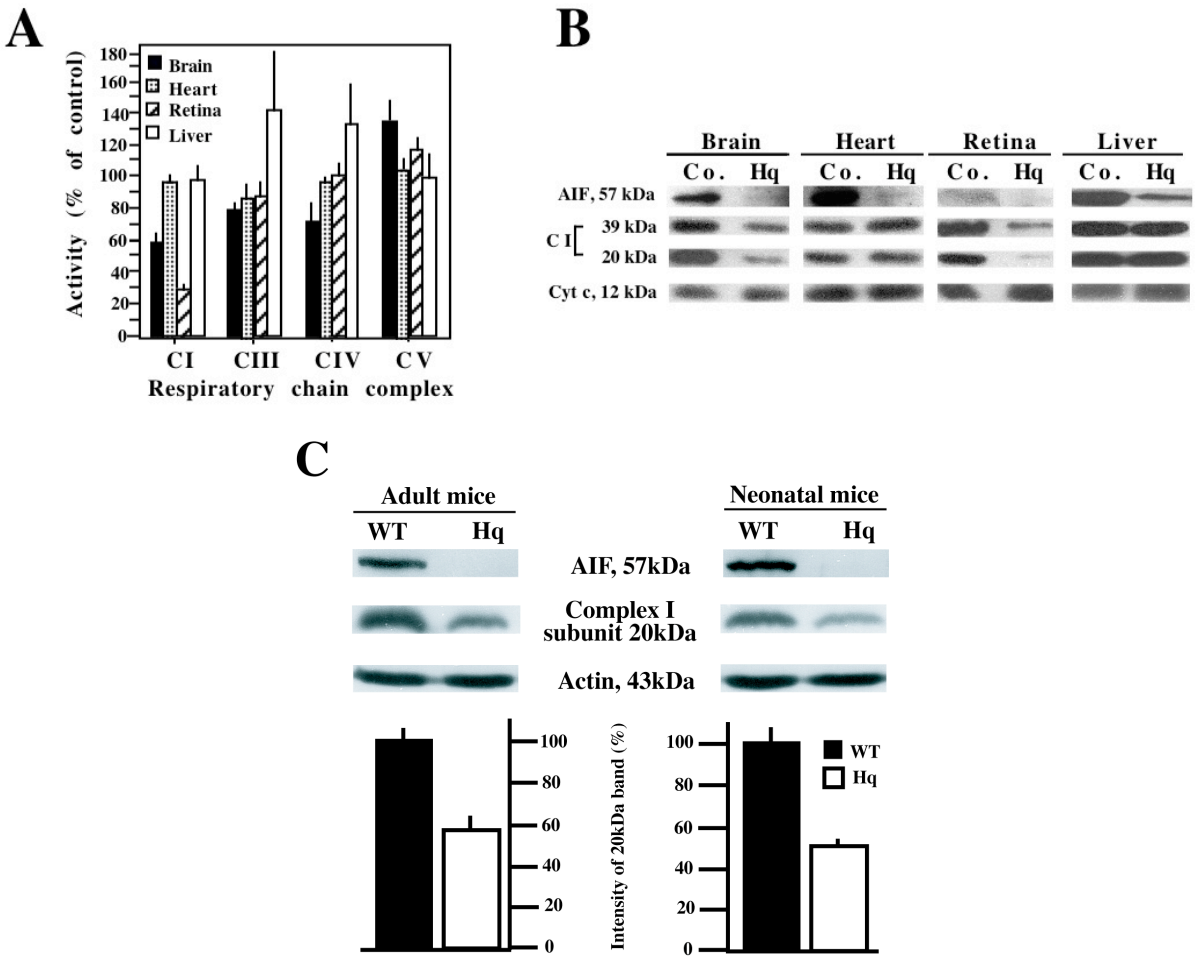

Figure 4-17. **AIF deficiency compromises complex I in harlequin mice.** (**A**) *Respiratory chain complex activities in harlequin mice. Mitochondria from AIF^{Hq} Y (Hq) or AIF^{WT} Y (Co.) tissues were monitored for the activity of each of the respiratory chain complexes. Data (X±SD) were ratioed to the AIF-positive controls, which were considered as 100% value.* (**B**) *Expression of respiratory chain complex subunits in Harlequin tissues. Mitochondria were subjected to the immunoblot detection of AIF and the indicated complex I subunits. Cytochrome c served as a loading control.* (**C**) *Mitochondria of brains of adult (60 days-old) and neonatal harlequin mice and their wild-type counterparts were subjected to immunoblot detection of AIF and the complex I 20kDa subunit. Actin served as a loading control. The intensity of the 20kDa band was measured as the percentage of wild-type controls, normalized on the actin band.*

4.1.11.OXPHOS defect in heart and muscle of AIF-KO mice

The group of Dr.Joseph Penninger at the Institute of Molecular Biotechnology of the Austrian Academy of Sciences in Vienna has generated a mouse that is deficient for AIF in heart and muscles. Organ-specific knock-out of the floxed AIF gene (obtained by crossing male mice

with a floxed AIF gene, AIF^{flox}Y with female mice expressing the Cre recombinase under the control of a creatine kinase promoter, yielding male AIF^{flox}Y/Cre mice) resulted in dilated cardiac hypertrophy, heart failure, skeletal muscle atrophy, and lactic acidosis (Joza et al., 2005). When heart, the fast-twitching gastrocnemius muscle, and the slow-twitching soleus muscle were assessed for defects in the respiratory chain, a significant decrease in complex I activity was found in all tissues lacking AIF (Figure 4-18A). Once again, these defects manifested themselves in reduced protein expression of the complex I subunits (Figure 4-18B). It seemed contradictory, that AIF deficiency provoked a pronounced complex I defect in AIF^{flox}Y/Cre mice, yet caused no phenotype in the heart of harlequin mice. This phenomenon could be explained by the fact that the AIF expression is completely abolished in the AIF^{flox}Y/Cre mice, while in harlequin mice, there is a residual expression of 20% compared to wild-type mice.

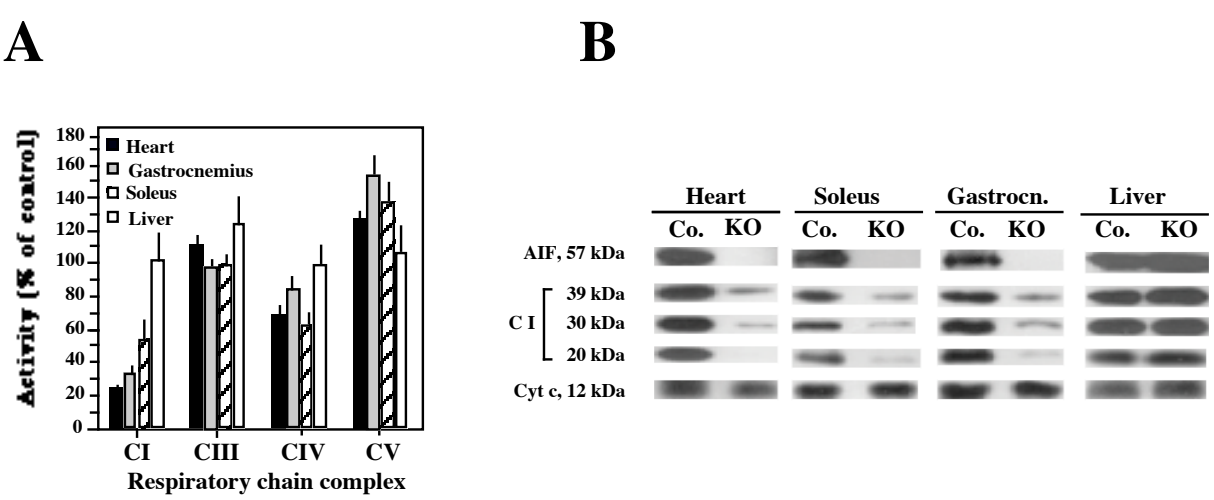

Figure 4-18. AIF deficiency compromises OXPHOS in muscle-specific AIF-knockout mice. (**A**) *Respiratory chain complex activity of different tissues from AIF^{fl}Y; mck-cre^{+} mice as compared to AIF^{WT}Y; mck-cre^{+} controls (defined as 100% value).* (**B**) *Deficient respiratory chain complex I expression in the heart and skeleton muscle from AIF^{fl}Y; mck-cre^{+} mice, as determined by immunoblot.*

4.1.12.Short summary of "AIF and the respiratory chain"

AIF-deficient murine ES cells exhibited a high lactate production and enhanced dependency on glycolytic ATP production. This was due to a severe reduction of the respiratory chain complexes I and III, both in activity as well as at the protein level. A complex I defect was also detected in HeLa cells, in which AIF was knocked down by siRNA. The transcription of nuclear and mitochondrially encoded subunits of the respiratory chain was unaffected and there was no oxidative insult found in AIF-deficient cells. Moreover, AIF did not seem to be a part of a respiratory chain complex. The OXPHOS defect was also observed in certain tissues of harlequin mice and in the heart and muscles of muscle-specific AIF-KO mice.

4.2. Physical interaction of AIF with DNA and RNA

4.2.1. AIF binds to ds and ssDNA in a magnesium-dependent fashion

AIF has been known to bind to DNA *in vitro* and *in vivo* (Cande et al., 2004b; Ye et al., 2002; Zhang et al., 2002). To further characterise this interaction, a series of in vitro experiments was performed utilizing a recombinant human AIF protein. This protein was produced in the laboratory of Hao Wu at the Cornell university in New York and contained a His-tag at the N-terminus as well as at the C-terminus. The 100 amino acids at the N-terminus had been deleted since it is assumed that this sequence is cut off once AIF has been localised to mitochondria (Susin et al., 1999) or, at the latest, when AIF gets released from mitochondria during apoptosis (Otera et al., 2005). Thus, the recombinant AIF used here represents the protein that translocates into the nucleus during apoptosis and interacts with DNA *in vivo*.

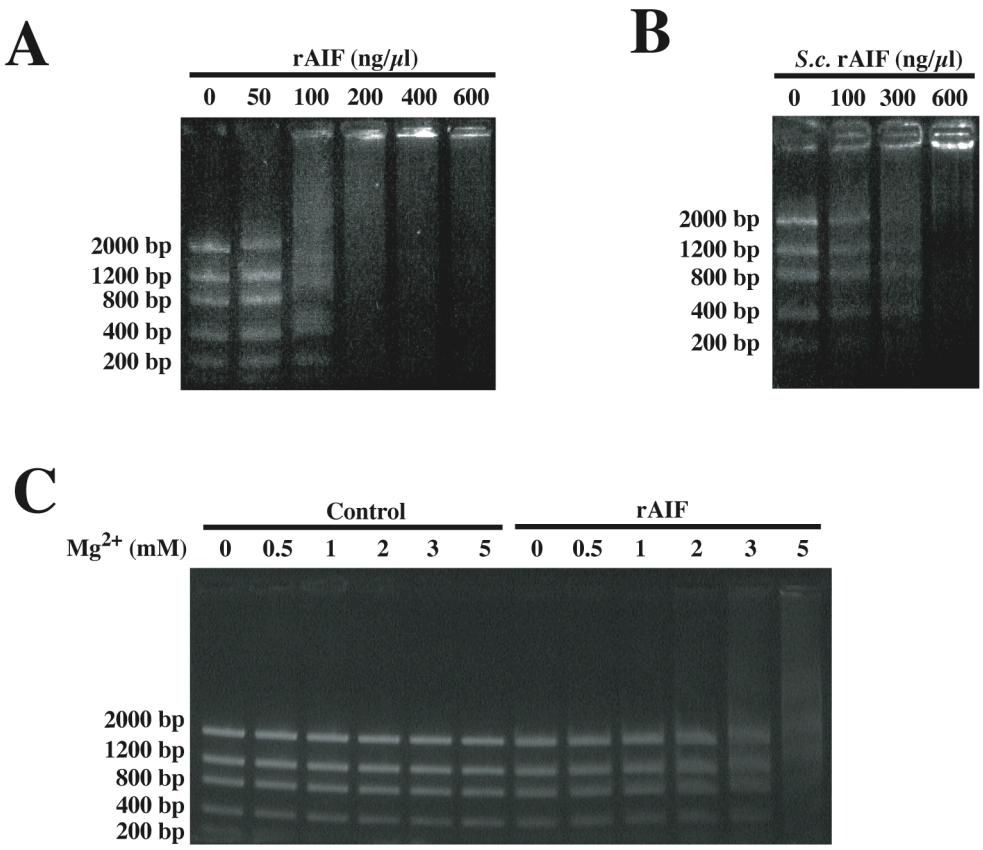

Figure 4-19. **Interaction of AIF with DNA.** (**A**) *DNA binding of recombinant human AIF. A fixed dose of DNA ladder (200ng) was incubated with the indicated doses of AIF, followed by horizontal agarose gel electrophoresis and visualisation of DNA with SybrGold®. This reaction was done in the standard buffer, in the presence of 5 mM Mg^{2+}.* (**B**) *DNA binding of recombinant yeast AIF. The experiment was done as in A, while replacing human AIF by recombinant AIF from S. cerevisiae.* (**C**) *Magnesium dependency of the AIF-DNA interaction. 200ng DNA and 1μg human recombinant AIF were admixed, in buffers containing increasing concentrations of Mg^{2+}, incubated for 30 min, and then subjected to electrophoresis.*

In a gel retention assay, a DNA ladder containing double-stranded DNA (dsDNA) molecules of different length (200, 400, 800, 1200, and 2000 base pairs) was completely retained by recombinant AIF in a concentration-dependent manner indicating the binding of AIF to

purified DNA irrespective of its size (Figure 4-19A). Recently, an orthologue of AIF has been identified in yeast that also translocates to the nucleus during apoptosis where it takes part in DNA degradation (Wissing et al., 2004). Recombinant protein from *Saccharomyces cerevisiae* (kindly provided by Dr.Frank Madeo) generated similar results and also caused the retention of the differently sized DNA molecules in the gel (Figure 4-19B).

The interaction of human AIF and DNA was dependent on the presence of magnesium. At physiological concentrations (5mM), the binding of AIF to DNA was much more efficient than at lower concentrations (Figure 4-19C).

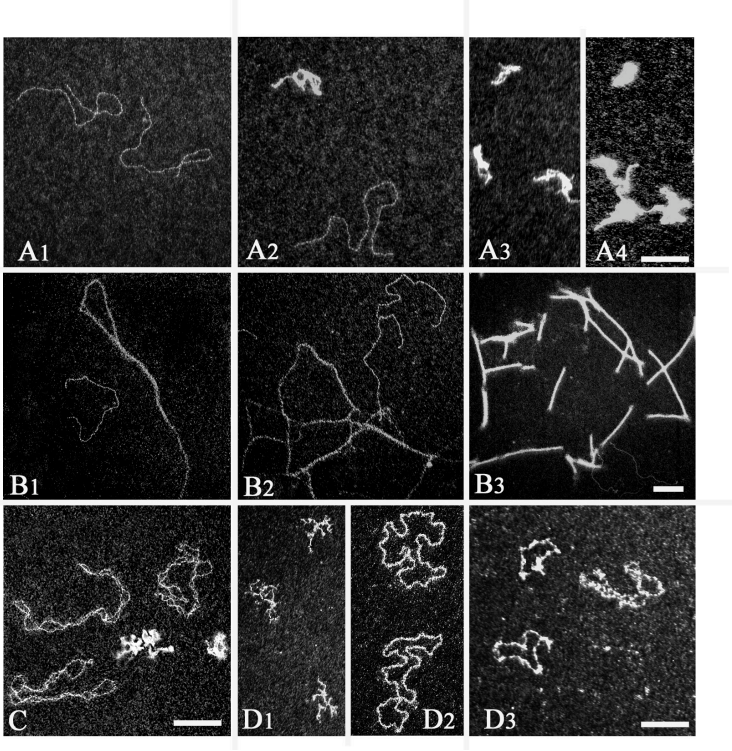

Figure 4-20. **Visualisation of AIF–DNA complexes by positive staining and annular dark-field electron microscopy.** (**A**) *Aspect of DNA-AIF complexes generated in the absence of Mg^{2+}. Linear DNA fragments of 1440 bp were incubated in the absence of AIF (A1) or in the presence of AIF at different protein / DNA fragment molar ratios in binding buffer without magnesium: 10 (A2), 30 (A3), 50 (A4). Note that AIF induces intramolecular condensation. Quantification of the number of condensed molecules and free DNA on series of 200 analyzed molecules gave the following results: 0% of condensed DNA fragments for the control, 4 % , 11 %, 19 %, 31 % and 37 % for 10, 20, 30, 50 molar ratio respectively. All DNA fragments are condensed at a molar ratio of 150, corresponding to one AIF for 10 nucleotides.* (**B**) *Aspect of DNA-AIF complexes produced in the presence of Mg^{2+}. The complexes were visualised at an AIF/DNA ratio of 10 (B1), 30 (B2) and 50 (B3). Note the apparition of networks resulting from protein-protein interactions between AIF molecules ordered along DNA. Quantification was hamperered due to the impossibility to determine the number of DNA molecules involved in the networks. Increased aggregation mechanisms and network formation can be observed as a function of the AIF/DNA ratio.* (**C**) *AIF binding to negatively supercoiled DNA. AIF was incubated at a molar ratio of 30 : 1 with 2834 bp PTZ plamid. In these conditions, less than 2% of the DNA was condensed.* (**D**) *Efficient binding of AIF to single-stranded DNA. D1 illustrates the aspect of the naked FX174 single stranded DNA, D2 shows the aspect of this DNA binding to the canonical single-stranded proteins gp32. D3 exemplifies the binding of AIF to single stranded DNA, obtained at a molar ratio of 50, corresponding to one AIF for 40 nucleotides. Note that AIF covered the DNA and spread, although less efficiently than gp32. Size bars correspond to 200 nm.*

The AIF-DNA interaction was visualised by transmission electron microscopy (TEM), which confirmed the results seen in the gel retention assays and gave further insights: at first, different amounts of AIF were added to linearised dsDNA molecules of 1440 base pairs in the absence (Figure 4-20A) or presence of magnesium (Figure 4-20B). Naked dsDNA is visible as filamentous structures. In the absence of magnesium, DNA-AIF complexes were generated appearing as small “packets” of DNA. Their number and grade of condensation increased with the molar ratio of protein/DNA (Figure 4-20 A2, A3, and A4). Upon addition of magnesium, AIF did not only form “packets” of DNA, but rather caused the formation of networks that also became more compact when the AIF/DNA molar ratio was increased (Figure 4-20 B1, B2, and B3). These networks exhibited significant intermolecular contact suggesting protein-protein interactions.

When AIF was incubated with negatively supercoiled plasmid DNA, hardly any condensed molecules were detected (Figure 4-20C), only about 2% of the molecules were bound by AIF.

Naked single-stranded DNA (ssDNA) tends to form condensed structures by itself (Figure 4-20 D1). Only when bound by single-stranded DNA binding (SSB) proteins, such as gp32, an SSB protein from the phage T4, the molecules spread out (Figure 4-20 D2). AIF also caused spreading of ssDNA, indicating that it binds to ssDNA, although AIF exhibited less affinity than gp32 (Figure 4-20 D2).

4.2.2. AIF binds preferably to ssDNA over dsDNA

To test whether AIF shows any preference for binding to single-stranded or double-stranded DNA, a DNA molecule was utilized that contained both a single-stranded and a double-stranded moiety. In the absence of proteins, only the double-stranded part was clearly visible in transmission electron microscopy (Figure 4-21 1). When the SSB protein gp32 was added, the single-stranded moiety also appeared as a filamentous structure with the proteins bound to it (Figure 4-21 2). In the absence as well as in the presence of magnesium, AIF bound to the single-stranded DNA, which hence became visible (Figure 4-21 3-6). The dsDNA moiety did not change its appearance, as observed in the experiment with gp32. It thus seems that AIF had a higher affinity for ssDNA than for dsDNA. However, AIF binding did not result in a wide elongation of the ssDNA moiety as binding of gp32 did. Most importantly, in the presence of magnesium, AIF again induced the generation of intermolecular bridges, this time between the ssDNA moieties (Figure 4-21 4-6).

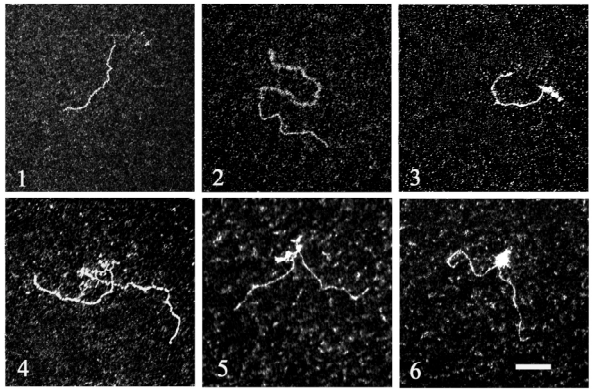

Figure 4-21. **Interaction between AIF and a hybrid DNA molecule containing single-stranded (ss) and double-stranded (ds) moieties.** *A hybrid DNA template containing 609 bp ds and 3' 831b ss DNA moieties was observed by TEM, either naked, in conditions that only reveal the double helix (**1**) or after having been covered by the ssDNA-binding gp32, which causes spreading of the ss DNA part* (**2**). *In the absence of Mg^{2+}, AIF (added at a molar ratio of 30 : 1) clearly exhibited an enhanced affinity for the single stranded DNA moiety (3). In the presence of Mg^{2+}, AIF led to the formation of intermolecular bridges* (**4**, **5**, **6**). *The bar corresponds to 200 nm.*

4.2.3. AIF ligands enhance AIF binding to DNA

AIF has been known to be able to bind to NADP, NADPH, NAD and NADH, at least *in vitro* (Miramar et al., 2001). Whether these factors can modify AIF's affinity to DNA had not yet been determined. In gel retention assays, the addition of NADP to AIF and DNA surprisingly resulted in a more efficient retention of the DNA molecules (Figure 4-22A). Moreover, at an NADP concentration of 2.5mM, the 200ng of DNA was tightly packed by 1µg of AIF, which, without NADP, was only observed at four times higher concentrations of AIF. This unique, high molecular weight band visible in horizontal gel electrophoresis suggested the ordered formation of an AIF-DNA complex. The addition of NADPH and NADH provoked a slightly higher affinity of AIF to DNA, thus showing an increased retention of the dsDNA molecules in the gel (Figure 4-22 B and C). However, they did not induce the formation of an ordered protein-nucleic acid complex as did NADP. NAD did not seem to affect the binding of AIF to DNA (Figure 4-22 D).

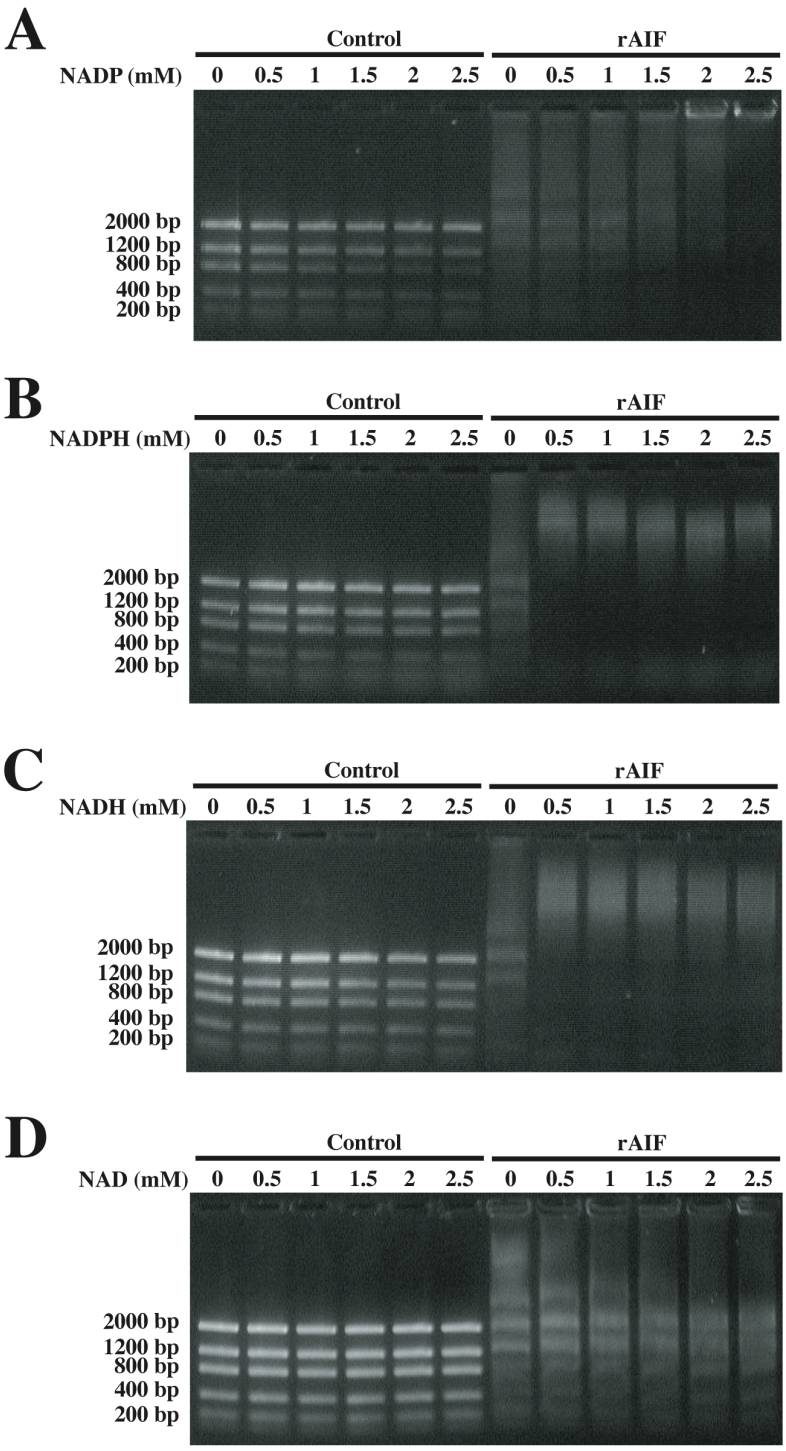

Figure 4-22. **Effects of AIF ligands on the AIF-DNA interaction.** *DNA (200ng) and AIF (1µg) were mixed in the presence of the indicated concentrations of NADP* (**A**), *NADPH* (**B**), *NADH* (**C**), or *NAD* (**D**) *followed by gel electrophoretic assessment of the AIF-DNA complexes. These experiments have been repeated three times, yielding comparable results.*

The effects of NADP on the AIF-DNA interaction were investigated and confirmed by electron microscopy. At low AIF/DNA molar ratios (10) and in the presence of NADP, intramolecular loops formed in all linearised dsDNA molecules (Figure 4-23 1-3). These loops involve juxtapositions of DNA segments of 10 to 100 base pairs indicating the formation of protein-

protein interactions. At higher AIF/DNA ratios (30 and 50), intermolecular complexes and aggregates were visible (Figure 4-23 4-8) that have never occurred in the absence of NADP. Thus, physiological concentrations of NADP can profoundly influence the assembly of AIF-DNA complexes.

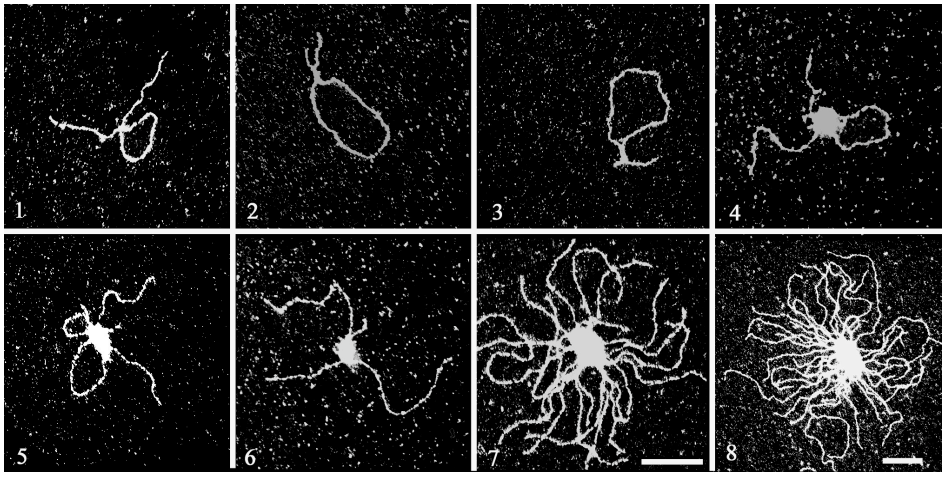

Figure 4-23. Effect of NADP on the structure of AIF-DNA complexes visualised by electron microscopy. *AIF-DNA complexes generated in the presence of NADP and Mg^{2+} revealed the formation of intramolecular loops within linear 1440 bp double stranded DNA* (**1**-**3**) *and intermolecular complexes* (**4**-**8**). *Low molar ratios between AIF and DNA (10 or 20) favour the formation of intramolecular loops mediated by protein-protein interactions. Such loops involve the juxtaposition of DNA segments of 10 to 100 bp. The formation of intermolecular complexes* (**4**, **5**, **6**) *and aggregates* (**7**, **8**) *were favored at higher AIF –DNA ratios (30 and 50). The size bar (200 nm) in 7 applies also to pictures 1-6.*

4.2.4. AIF interacts with RNA

In our research group, a series of proteins that had been retained on an AIF affinity column had recently been identified by mass spectrometry. Remarkably, a relatively high number of these proteins belonged to the heterogeneous group of RNA binding proteins including ribonucleoproteins, nucleolin, ribosomal proteins, and others. This pointed to a possible binding of AIF to RNA rather than to each one of these proteins by protein-protein interaction. When one of these RNA binding proteins, the heterogeneous nuclear ribonucleoprotein A1 (HnRNPA1), was co-immunoprecipitated with AIF from whole cell extracts, it was tested whether the interaction between the two proteins was abolished by the treatment with RNAse. Indeed, when RNAse was added to the cell extract, HnRNPA1 was no longer co-immunoprecipitated with AIF (Figure 4-24A) strongly suggesting an interaction of AIF with RNA. Accordingly, treatment with DNAse did not destroy the interaction between AIF and HnRNPA1.

RNA extracted from HeLa cells was therefore incubated with recombinant human AIF in order to check for a retention of the RNA in horizontal gel electrophoresis. Indeed, AIF

caused a retention of RNA in a concentration-dependent manner (Figure 4-24B). AIF thus binds to RNA, at least *in vitro*.

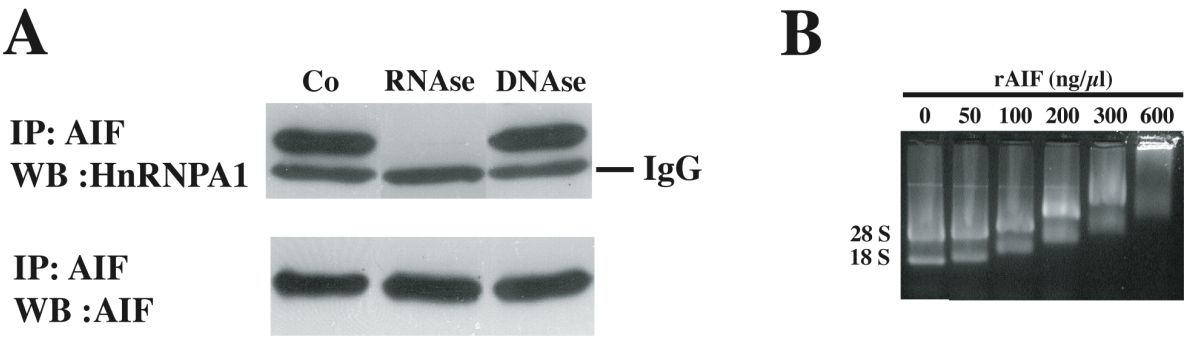

Figure 4-24. **Interaction of AIF with RNA.** (**A**) *Interaction of AIF with the RNA moiety of HnRNPA1. Sonicated HeLa cell extracts were subjected to immunoprecipitation (IP) of AIF, in the absence or presence of RNAse1 or DNAse1, followed by western blot (WB) detection of HnRNPA1 or AIF. This experiment has been done three times, yielding similar results.* (**B**) *RNA binding of recombinant human AIF. A fixed dose of total HeLa cell RNA extracts (1 µg) was incubated with the indicated doses of AIF, followed by horizontal agarose gel electrophoresis and visualisation of DNA with SybrGold®.*

This interaction was also confirmed in electron microscopy experiments. Naked poly A RNA polymers of different size (100kDa to 1.2 MDa) do not appear as clear formations (Figure 4-25 A1). When AIF is added in the absence of magnesium, small aggregates become visible (Figure 4-25 A2) indicating a physical interaction between AIF and the RNA polymers. In the presence of magnesium, AIF and poly A RNA form large ordered spheroid aggregations (Figure 4-25 A3), which proves, once again, that physiological concentrations of magnesium can enhance AIF's interaction with nucleic acids.

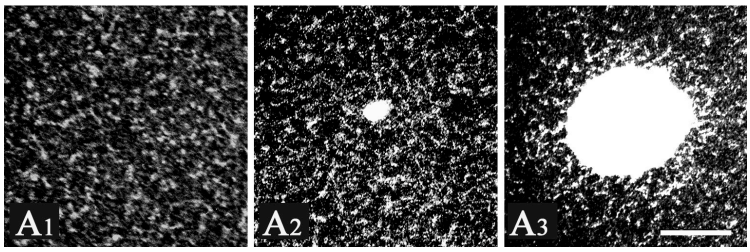

Figure 4-25. **Interaction between AIF and RNA visualised by electron microscopy.** *Interaction of AIF and the model RNA homoribopolymer poly A. RNA was visualised alone* (**A1**)*, in the presence of AIF* (**A2**)*, and in the presence of AIF plus* Mg^{2+} (**A3**)*. AIF induces small aggregates (40 to 50 nm) without* Mg^{2+}*(A2) at a protein-polyA molar ratio of 10 compared to the control without AIF (A1). The presence of* Mg^{2+} *favours the formation of ordered spherical aggregates (A3). A mean diameter of 400 nm has been obtained from measurements of 50 spherical aggregates.*

4.2.5. NADP enhances AIF binding to RNA

Based on the results obtained for the AIF-DNA interaction, it was investigated whether the AIF ligand NADP could also increase the affinity of AIF for RNA. In gel retention assays, total RNA extracts from HeLa cells were incubated with AIF in the presence of NADP or NADPH. While NADPH did not affect the binding of recombinant AIF to RNA (Figure 4-26 A), NADP

concentrations of 2 and 2.5 mM improved the retention of RNA by AIF significantly (Figure 4-26B), reflecting the observations made in gel retention assays with NADP, AIF, and DNA.

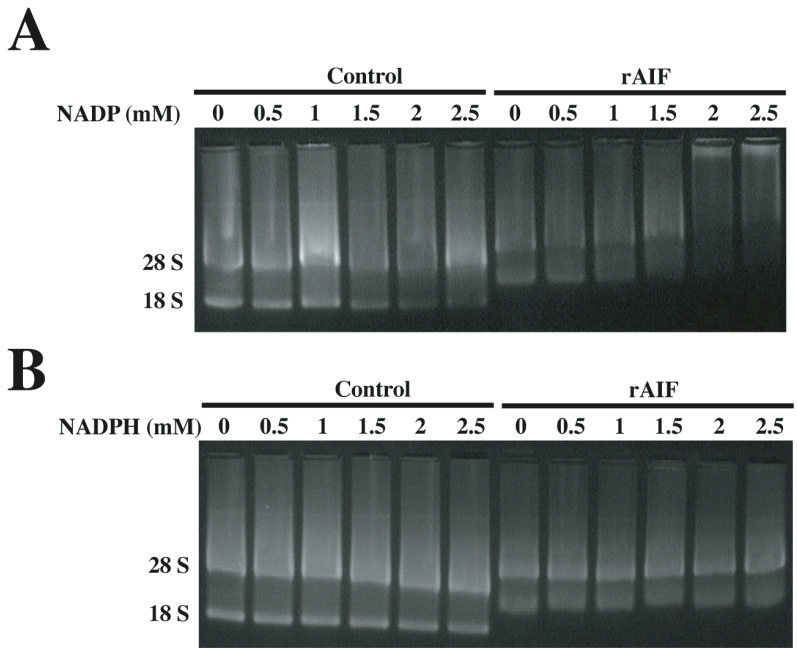

Figure 4-26. **Effects of AIF ligands on the AIF-RNA interaction.** *Total HeLa cell RNA (1μg) and AIF (3μg) were mixed in the presence of the indicated concentrations of NADP* (**A**) *or NADPH* (**B**), *followed by visualisation of the AIF-mediated retention of RNA as in A. These experiments have been repeated three times, yielding comparable results.*

4.2.6. DNA and RNA bind to AIF at similar sites

It has been shown that AIF binds to DNA via electrostatic interactions between positively charged amino acids on the protein's surface and the negatively charged DNA (Ye et al., 2002). Mutants had been generated in which some of the positively charged amino acids (lysine and arginine) that were suspected to be essential for the interaction, were replaced by neutral ones (alanine). These mutants were unable to induce cell death when expressed in cells, even though they did translocate to the nucleus (Ye et al., 2002).

Two recombinant mutants, AIF255 (K255A, R265A) and AIF510 (K510A, K518A), were utilized in *in vitro* assays to assess their capability to retain DNA and RNA in horizontal gel electrophoresis. As expected, both mutants exhibited lower affinity to DNA that resulted in a decreased retention of the DNA molecules when compared to the wild-type AIF (Figure 4-27A). Interestingly, the same mutations also attenuated the interaction between AIF and RNA. Mutants AIF255 and AIF510 were not able to cause a retention of total RNA extracts to the same extent as wild-type recombinant AIF did (Figure 4-27B). This strongly suggested that the two nucleic acids bind to AIF by a similar mechanism and/or that their binding sites overlap.

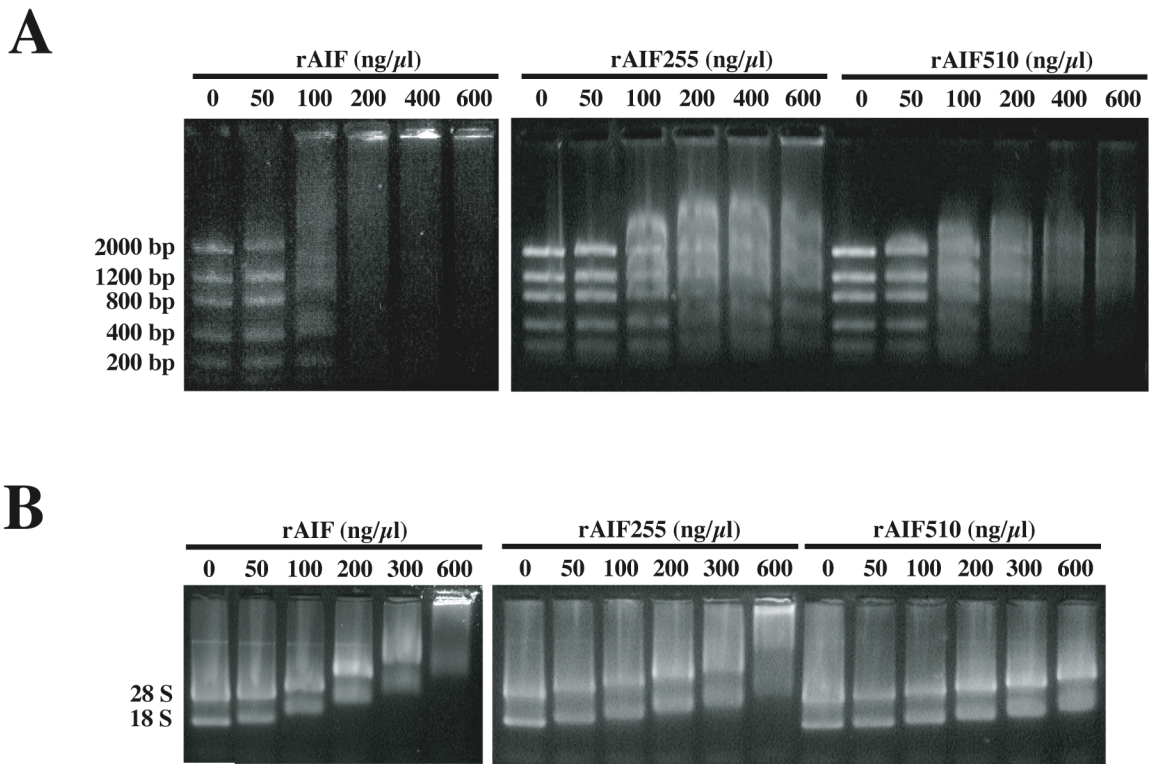

Figure 4-27. **DNA and RNA binding of recombinant AIF mutants.** (**A**) *DNA binding of recombinant human AIF and AIF mutants. A fixed dose of DNA ladder (200ng) was incubated with the indicated doses of AIF, followed by horizontal agarose gel electrophoresis and visualisation of DNA with SybrGold®.* (**B**) *RNA binding of recombinant human AIF and AIF mutants. The experiment was done as in A, with the difference that DNA was replaced by 1μg total HeLa cell RNA. Results are representative of three independent determinations.*

RNA molecules were incubated with AIF and DNA to verify the hypothesis that RNA and DNA bound to similar sites of the AIF protein. If that was the case, RNA should be able to attenuate the DNA retention caused by AIF in an agarose gel, since both nucleic acids would compete for the common binding site.

Indeed, single-stranded RNA's (polyA, polyG, and polyC) as well as double-stranded RNA's (polyA/U and polyG/C) inhibited the AIF-DNA interaction resulting in a re-appearance of the DNA ladder bands in gel retention assays (Figure 4-28 A-D). The efficiency of the different types of ssRNA and dsRNA were comparable among each other. This indicated that RNA binding to AIF occurred in a sequence-independent manner, as it was the case for DNA.

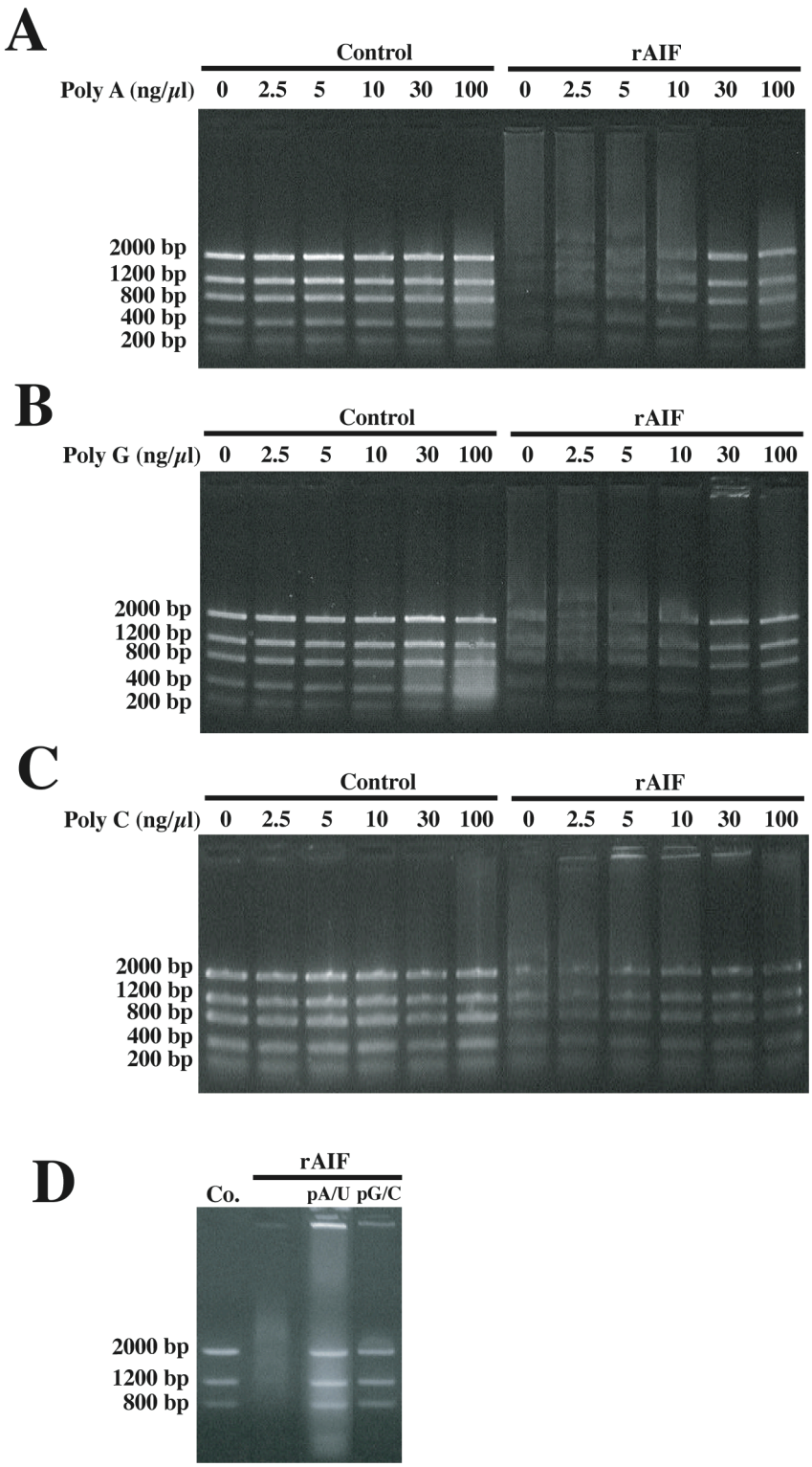

Figure 4-28. **Inhibition of the AIF-DNA interaction by RNA.** (**A**), (**B**), (**C**) *Inhibition of the AIF-DNA interaction by single-stranded RNA. 200ng DNA ladder was mixed with 1μg AIF and/or the indicated concentration of synthetic poly A (A), poly G (B) or poly C (C) RNA, and DNA was visualised with SybrGold® after electrophoresis.* (**D**) *Inhibition of the AIF-DNA interaction by double-stranded RNA. DNA fragments (200ng) were incubated with recombinant AIF (1μg), in the presence of the indicated double-stranded RNA species (300ng) and analyzed as above.*

4.2.7. AIF is devoid of RNAse activity

Finally, it was investigated, *in vitro* and *in vivo*, whether AIF exhibited an RNAse activity. When recombinant human AIF was incubated with total RNA extract from HeLa cells at 37°C, the RNA was not degraded as determined by gel electrophoresis using an EDTA-containing agarose gel (Figure 4-29A). EDTA abolishes the AIF-RNA interaction and thus RNA retention, which allows an easier comparison of the amount of RNA in the non-treated sample and in the AIF-treated one. As a control, RNAse A was incubated with RNA extracts, which readily degraded the RNA (Figure 4-29A).

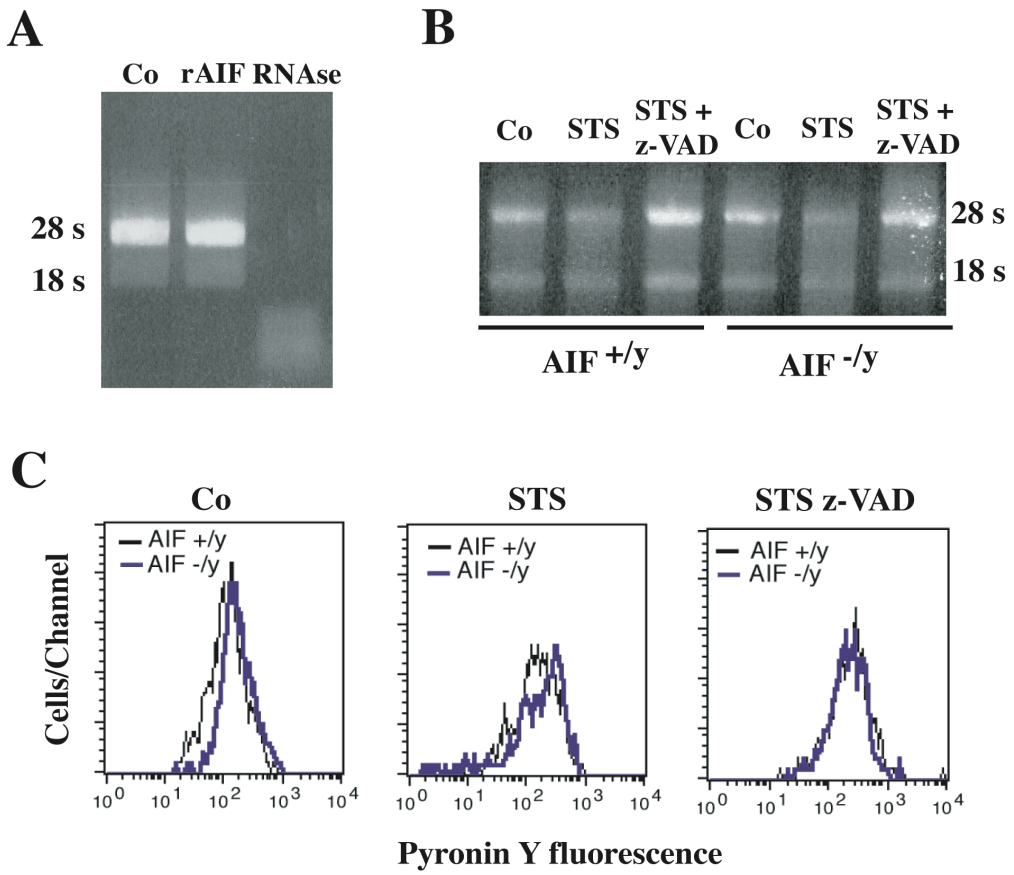

Figure 4-29. **AIF is devoid of RNAse activity.** (**A**) *Effect of recombinant AIF on purified RNA in vitro. Total RNA (1µg) from untreated HeLa cells was exposed during 2 hours at 37°C to recombinant AIF (1µg/ml) or RNAse A (1 µg/ml) and loaded on an agarose gel for horizontal electrophoresis and visualisation with ethidium bromide.* (**B**) *Effect of the AIF knock-out on apoptotic RNA degradation. Total RNA was extracted from normal ($AIF^{+/y}$) or AIF-deficient ($AIF^{-/y}$) ES cells that had been incubated during 24 hours in the presence of staurosporine (STS, 2µM) and/or Z-VAD.fmk (100µM). Note the degradation of 28 S RNA occurring in the presence of STS and in the absence of Z-VAD-fmk, both in $AIF^{+/y}$ and in $AIF^{-/y}$ cells.* (**C**) *Effect of AIF on the RNA content of dying cells. ES cells with the indicated genotype were exposed to STS and/or Z-VAD.fmk (as in B), followed by staining with pyronin and analysis in a cytofluorometer, while gating on the viable cell population. Note that STS reduces the RNA content in a fraction of cells.*

To find out if AIF played a role in RNA degradation during apoptosis, maybe not as an active RNAse, but as a co-factor or a recruitment-factor, RNA degradation was compared in apoptotic AIF-deficient murine embryonic stem cells and their wild-type counterparts.

Apoptosis was induced by treatment with the serine-threonine kinase inhibitor staurosporine (STS), RNA was extracted and subsequently analysed by horizontal gel electrophoresis. The RNA degradation seen after apoptosis induction was comparable in both cell lines (Figure 4-29B), indicating that $AIF^{-/y}$ cells did not lack RNAse activity. When the cells were treated with STS and the pan-caspase inhibitor Z-VAD-fmk., apoptotic RNA degradation was inhibited (Figure 4-29C). This also applied to both cell lines.

Similar results were obtained when the total cellular RNA content was evaluated by staining with the RNA probe pyronin Y followed by cytometric analysis. The intensity of pyronin Y was nearly the same in $AIF^{-/y}$ and $AIF^{+/y}$ cells before and after apoptosis induction, with or without Z-VAD-fmk (Figure 4-29C). Thus, AIF did not seem to have an effect on RNA degradation *in vitro* and *in vivo*.

4.2.8. AIF does not always translocate to the nucleus during apoptosis

In a cooperation with the research group of Dr.Klaus-Michael Debatin at the university children's hospital of Ulm, the mitochondrial release and nuclear translocation of several apoptotic factors were monitored in HLA-A1 specific cytotoxic T lymphocytes (CTL's) after apoptosis induction by the DNA-damaging drug cyclophosphamide (CY). After stimulation with the chemotherapeutic agent, the dying cells exhibited apoptotic DNA high molecular weight fragments of 50 kb independent of the presence or absence of the caspase inhibitor Z-VAD-fmk (not shown; (Strauss et al., 2005)). Immunofluorescent studies revealed highly condensed nuclei in about 90% of the cells confirming an apoptotic phenotype (Figure 4-30 A-C). However, translocation of AIF to the nucleus was only detected in 10-15% of the apoptotic cells (Figure 4-30A). Mitochondrial release of AIF was seen in about 40% of the cells after CY-stimulation. Nuclear translocation of EndoG took place in about 40% of the cells, although the percentage was reduced (25%) by the caspase inhibitor Z-VAD.fmk (Figure 4-30B). EndoG was released in nearly all apoptotic cells. The nuclear translocation of Cyt *c* was difficult to quantify since this protein is known to be degraded once released from the mitochondria. Nevertheless, like EndoG, it was found to be released from mitochondria in nearly all apoptotic cells and nuclear staining was clearly visible in a large number of cells (Figure 4-30C).

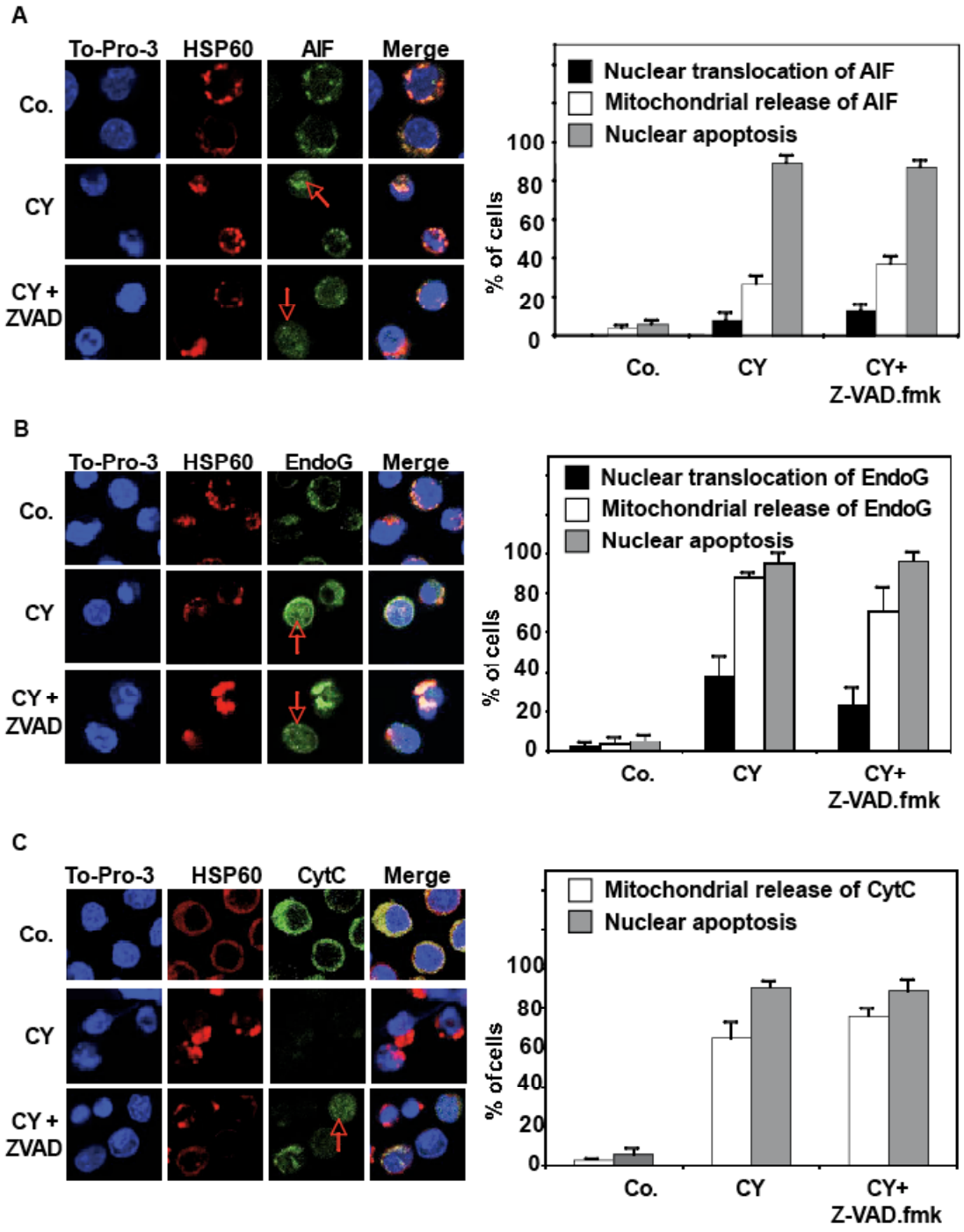

Figure 4-30. **CY induced nuclear translocation of AIF, EndoG and cytochrome c.** *HLA-A1-specific CTLs were treated with CY (3µg/ml) for 48 hours in the absence or presence of Z-VAD.fmk (100µM). AIF* (**A**), *EndoG* (**B**) *or cytochrome C* (**C**) *and the mitochondrial resident protein HSP60 (A,B,C) were detected by immunofluorescent staining. Nuclei were stained with To-Pro-3 and cells were analysed by confocal microscopy. Red arrows point to cells in which nuclear translocation has occured. To determine the percentage of cells in which proteins had been released from mitochondria or translocated to the nucleus, at least 200 cells were counted. Results are representative for a minimum of 2 different experiments.*

4.2.9. Short summary of "AIF and the nucleic acids"

AIF was shown to interact with both, DNA and RNA utilizing gel retention assays as well as electron microscopy images. AIF's affinity to nucleic acids and its capability to compact them were increased by magnesium as well as by NADP. AIF was shown to preferably bind to ssDNA over dsDNA. DNA and RNA seem to bind to a similar site of the protein since RNA can inhibit the binding of DNA to AIF. Further, AIF mutants that have lower affinity to DNA also bound to RNA less effectively. AIF does not exhibit an RNAse activity. In CTL's treated with CY, AIF is released from mitochondria but was not found in the nucleus of the large majority of apoptotic cells.

5. Discussion

5.1. AIF compromises oxidative phosphorylation

Several proteins involved in apoptosis have been shown to fulfill a completely different, vital function as long as programmed cell death is not induced (Garrido and Kroemer, 2004). Grim19, for example, is a subunit of the complex I of the respiratory chain (Huang et al., 2004) and HtrA2/Omi is a mitochondrial protease that is involved in the maintenance of mitochondrial homeostasis (Jones et al., 2003).

AIF has been known for its translocation to the nucleus during apoptosis (Cao et al., 2003; Susin et al., 1999; Zhang et al., 2002). Here, we reveal a completely new function of AIF showing that AIF deficiency results in an oxidative phosphorylation (OXPHOS) defect mostly involving complex I. *In vitro*, this defect was detected by polarographic measurements in murine embryonic stem cells lacking AIF due to homologous recombination ($AIF^{-/y}$; Figure 4-5), as well as in the human HeLa cell line in which AIF expression had been downregulated by RNA interference (Figure 4-8). These findings explained the initial observations of high dependency on glycolysis and thus glucose in $AIF^{-/y}$ cells (Figure 4-3), which also show an increased production of lactate in the presence of glucose (Figure 4-1).

A respiratory chain defect was equally found in the brain and in the retina of harlequin mice, which only exhibit 20% of AIF expression due to a retroviral insertion in the AIF gene (Klein et al., 2002), confirming the observations of a respiratory chain defect due to AIF deficiency *in vivo* (Figure 4-17). A second mouse model lacking AIF in heart and muscle tissue (Joza et al., 2005) showed a reduced OXPHOS activity in these organs (Figure 4-18). These results indicated an important role of AIF in the functioning of the respiratory chain in different tissues and species. Indeed, stimulated by these results, OXPHOS defects were also found in AIF-deficient yeast and flies. A Saccharomyces cerevisiae strain lacking the yeast AIF homologue (aifp1) exhibited a significantly lower doubling time than wild-type cells on media in which glucose was replaced by glycerol or lactate, whereas the doubling time on rich glucose media was equal for both strains (Vahsen et al., 2004). It thus seems that AIF-knockout yeast cells also highly rely on glycolysis and cannot use glucose substitutes as an energy source, as it was observed in $AIF^{-/y}$ ES cells (Figure 4-4). Loss-of-function mutations in the *Drosophila* Aif orthologue resulted in a complete growth arrest during early larval development and defects in mitochondrial OXPHOS (Joza and Penninger, unpublished data). Altogether, these data pointed to an evolutionary conserved role for AIF in mitochondrial respiration and energy metabolism for normal growth and tissue function.

In AIF-deficient cell lines and murine tissues, complex I was affected at both activity as well as protein level. The lack of AIF resulted in downregulation of complex I activity as determined by spectrophotometric measurements of isolated respiratory chain complexes (Figure 4-6 and 4-17A). This activity defect was probably due to the reduced level of expression of all complex I subunits tested by western blot (Figure 4-10A and Figure 4-17B). Further, blue native gel analysis revealed a significantly reduced abundance of complex I as a whole in the absence of AIF (Figure 4-10D). These findings pointed to a role of AIF in the biogenesis or the maintenance of complex I.

However, in $AIF^{-/y}$ cells, not only complex I, but also complex III was reduced in activity (Figure 4-6) as well as at the protein level (Figure 4-10A). Complexes II, IV, and V of the respiratory chain did not seem affected. This phenomenon could be explained by the fact that respiratory chain complex I is not randomly distributed in the inner mitochondrial membrane but rather a constitutive of supramolecular structures, the so-called "supercomplexes" or "respirasomes" (Schägger and Pfeiffer, 2000). Increasing evidence suggests that particularly complex I, III and IV associate in higher-order assemblies that are thought to ease substrate channeling and may increase individual complex stability (Bianchi et al., 2004) (Schägger, 2002). These findings fit with observations of respiratory chain deficiencies in humans that are caused by a mutation in a subunit of a single complex, but affect the stability and functioning of several complexes. In patients harbouring a mutation in a subunit of complex III, for example, a combined deficiency of complex III and complex I was detected (Schägger, 2002). Conversely, a mutation in a subunit of complex I can also affect the stability of complex III (Ugalde et al., 2004) (Budde et al., 2000). AIF deficiency in ES cells may provoke a defect in the supercomplex assembly thus influencing the stability of complex I and III at the same time.

Interestingly, complex III was normal, at both activity and protein levels, in HeLa cells lacking AIF (Figure 4-9 and 4-10A). The downregulation of AIF in these cells is not 100% as it is the case of $AIF^{-/y}$ cells. Therefore, the defect might not be as pronounced and affecting only one respiratory chain complex. Another explanation is that the effects of AIF downregulation may vary in different tissues and cell lines. Accordingly, in the heart of the muscle-specific AIF-knockout mouse, complex I was severely affected, complex III was normal, but there was a mild downregulation in the activity of complex IV (Figure 4-18B), which is also suggested to be part of the supercomplex. Blue native gel analysis of heart mitochondria of these mice revealed a reduced expression level of all, complex I, III, and IV (Schägger, unpublished data) strongly arguing for a damage in the respirasome. Complex I and IV were also observed to be defective in AIF-deficient *Drosophila* (Joza and Penninger, unpublished data), again pointing to a combined respiratory chain defect.

Even though these data might suggest that AIF is a subunit of the NADH dehydrogenase or another complex, it seems unlikely that AIF directly contributes to electron transfer within complex I since the majority of iron-sulfur redox clusters of the complex are situated in the arm that protrudes into the matrix (Hirst et al., 2003) whereas AIF is localised in the intermembrane space. AIF was not found to be associated with one of them or a supercomplex in murine brain mitochondria, within the limits of resolution of blue native-PAGE analysis (Figure 4-13). Previously, AIF had been identified in a purified fraction of complex IV from human heart mitochondria, (Devreese et al., 2002). When the experiment of Hermann Schägger was recently imitated in our laboratory with mitochondria purified from murine livers, AIF seemed to be part of a complex of a size of around 300kDa (Figure 4-13B). This complex, that is not part of one of the respiratory chain complexes, will need to be further investigated in order to find its other components as well as its function. The method of BN-PAGE is a very sensitive method and thus highly prone to different results. This might explain the controversial results found in different laboratories. The differences might also be due to a tissue-specific role of AIF. It is known that the distribution of OXPHOS proteins is strongly tissue-dependent (Devreese et al., 2002). However, in all experiments, AIF was not found to be part of complex I or III, the most affected complexes in AIF-deficient cells. This confirmed the results of other research groups that used different methods, such as two dimensional gels and reverse-phase high performance liquid chromatography followed by mass spectrometry to detect non-identified subunits of complex I and never found AIF (Carroll et al., 2002; Fearnley et al., 2001).

The transcription of nuclear encoded subunits of complex I was normal in AIF-deficient ES or HeLa cells (Figure 4-12A). This was to be expected since AIF is localised to the mitochondria and can thus only indirectly, if at all, influence transcription in the nucleus. Moreover, the OXPHOS defect does not seem to be due to a gross perturbation in mitochondria, either. The level of mRNA's of mitochondrial DNA encoded subunits of the respiratory chain complexes I, III, IV, and V was not affected by downregulation of AIF in ES cells (Figure 4-12B). The levels of the 16S RNA as well as the tRNA Leu-1, which are both known to cause mitochondriopathies in humans when mutated (DiMauro and Schon, 2003), were also analysed and found to be comparable to wild-type cells (Figure 4-12B) thus pointing to an intact mitochondrial biogenesis. Normal expression levels of other mitochondrial proteins, including matrix and membrane proteins (Figure 4-10A), as well as the normal functioning of other respiratory chain complexes (Figure 4-6 and 4-9) confirmed this assumption.

AIF has an oxidoreductase domain, which can oxidize NAD(P)H *in vitro* (Miramar et al., 2001), and has been shown to be required for the maintenance of glutathione levels in stress

conditions (Cande et al., 2004c). However, levels of oxidative stress indicators, such as ROS, GSH, and SOD activity, were normal in AIF-deficient cells (Figure 4-15). Moreover, different antioxidants could not restore the expression of complex I subunits in $AIF^{-/y}$ cells (Figure 4-14A), nor their dependence on glucose (Figure 4-14B), although the antioxidants did protect the cells from oxidative stress induced by menadione (Figure 4-14B and 4-14C). Thus, defective detoxification of ROS is unlikely to account for the complex I defect in cells lacking AIF. This conclusion was recently confirmed when the knockout of AIF in human colon carcinoma cell lines resulted in a marked reduction in both superoxide anion and ROS levels, yet the cell lines exhibited a significant downregulation of complex I activity (Urbano et al., 2005). Importantly, transient re-expression of the full-length form of AIF restored complex I expression (Figure 4-11)(Urbano et al., 2005), arguing against the notion that prolonged oxidative stress and oxygen radical-mediated protein and DNA damage are the cause of the defective OXPHOS in these cells.

Nevertheless, the increased sensitivity to hydrogen peroxide observed in AIF-deficient ES cells (Figure 4-16) and Harlequin cerebellar granule cells (Klein et al., 2002), pointed to a redox imbalance in these cells. It has been shown that intact respiration, and especially a functional complex I, is required for efficient detoxification of exogenous hydrogen peroxide (Atorino et al., 2003; Zoccarato et al., 2004). Mitochondrial respiration is also required to scavenge extramitochondrial superoxide anion (Guidot et al., 1995). Thus, the hydrogen peroxide hypersensitivity seen in AIF-deficient cells, is probably a secondary effect to the complex I defect. These secondary effects might be more pronounced *in vivo* than *in vitro* which could explain the elevated GSH levels in Harlequin cerebellar granule cells (Klein et al., 2002), which are not seen in $AIF^{-/y}$ cells (Figure4-15A).

Since AIF does not seem to be part of a respiratory chain complex and a ROS-detoxifying function does not seem to be missing in AIF-deficient cells, yet the complex I abundance is significantly reduced in these cells resulting in an OXPHOS defect, AIF is likely to be an assembly or maintenance factor of complex I, complex III, and/or the supercomplex. How AIF contributes to the biogenesis and/or the protection of these respiratory chain complexes remains a conundrum. Probably due to the complexity of the multi-protein enzymes, very little is known about the assembly of the complexes (Vogel et al., 2004). In humans, certain subunits of complex I, including ND1, ND4, and the ESSS protein, have been found to be essential for the correct assembly of the complex (Bai and Attardi, 1998; Hofhaus and Attardi, 1993; Potluri et al., 2004; Yadava et al., 2004). Assembly factors that are not a constituent of the final structure have only been found for complex IV in humans (Papadopoulou et al., 1999; Williams et al., 2004; Zhu et al., 1998). CIA30 is the human homologue of a complex I assembly factor in *Neurospora crassa*, but an OXPHOS deficiency

has not yet been associated with a functional mutation in this gene (Janssen et al., 2002). When the biogenesis of a complex is defective, non-functional subcomplexes can often be detected (Scacco et al., 2003; Williams et al., 2004). However, this was not the case in AIF-deficient cells (Figure 4-10D). The fact that AIF deficiency compromised OXPHOS in yeast is also very intriguing, since *S.cerevisiae* does not possess a complex I. AIF might therefore have a more general chaperone-like function for respiratory chain complexes or maybe for higher-order structures like the respirasome. Indeed, it was found that the assembly of supercomplexes was important for the stability of the complexes, in particular complex I (Stroh et al., 2004). When respirasome formation is prevented, complex I is the most affected in its assembly (Schägger et al., 2004). Therefore, the phenotype of AIF-deficient cells could be explained by a non-assembly of the supercomplex. It still remains to be determined how AIF exerts its effect on the respiratory chain complexes, although it seems clear that its mitochondrial localisation is required. Re-transfection of $AIF^{-/y}$ cells only resulted in an increase of the expression level of the complex I subunits in the case of full-length AIF. An AIF deletion mutant that lacks the mitochondrial localisation sequence did not have any effect on the complex I subunits (Figure 4-11). Most recently, it was shown that the oxidoreductase domain was necessary to re-induce complex I subunits expression, while domains involved in DNA binding were not required (Urbano et al., 2005). This supports the hypothesis that AIF is a multi-functional protein whose functions can be dissociated (Miramar et al., 2001). The vital function in the mitochondria seems to be independent of its apoptotic role in the cytoplasm and nucleus. The redox activity of AIF might play a role in controlling the redox status of one or more key components of complex I or the supercomplex constituents, necessary for the correct assembly or maintenance of the complex or supercomplex.

The fact that AIF deficiency leads to an OXPHOS dysfunction could explain the phenotype of harlequin mice. Pathological features like progressive neurodegeneration with ataxia and retinal degeneration resemble symptoms of mitochondriopathies in patients (Orth and Schapira, 2001; Triepels et al., 2001). Indeed, OXPHOS deficiencies can lead to cell death, in particular in tissues that heavily rely on energy, and thus mitochondrial ATP generation, like the brain. Klein *et al.* proposed that AIF functions as a radical scavenger. Previous and recent findings do not support this theory. There is little doubt that AIF can exert a redox activity, but it has been shown, that the protein produces rather than scavenges oxygen radicals (Miramar et al., 2001). Moreover, typical radical scavengers normally possess a significant amount of metals, which AIF does not (Lipton and Bossy-Wetzel, 2002). Genetically altered mice carrying mutations in antioxidant defense genes, such as the SOD2 or frataxin knockout mice (Melov et al., 1999; Puccio et al., 2001), present a characteristic

loss of several complexes, including complex II, which was unaffected in harlequin mice (Figure 4-17). Considering the data presented here demonstrating an essential role for AIF in complex I expression and function and, more generally, in OXPHOS, an alternative interpretation of the harlequin phenotype can be suggested, namely that the primary defect in this mutant strain is impaired OXPHOS. This hypothesis is consistent with observations that primary defects in the respiratory chain result in oxidative stress *in vivo* (Larsson and Rustin, 2001). Accordingly, brain cells from harlequin mice exhibited increased DNA oxidation (Stringer et al., 2004), which can also be due to their reduced ability to fight exogenous oxidants as a secondary effect of the complex I defect, as explained above. Even though the respiratory chain defect seems to be present to the same extent in neonatal and three months-old mice (Figure 4-17C), pathological symptoms in mice worsen over time (Klein et al., 2002). Moreover, the amount of damage induced by ischemia/reperfusion in hearts of harlequin mice increased with the age of the animal, which was not the case in their wild-type littermates (van Empel et al., 2005). The progressiveness of diseases involving an increasing number of organs is characteristic for mitochondrial disorders (Munnich and Rustin, 2001). One possible explanation for these phenomena in the case of harlequin mice is the genomic instability which results from the oxidative damage to DNA (Stringer et al., 2004).

Interestingly, the OXPHOS defect was only detected in the brain and in the retina of harlequin mice, while liver and heart exhibited normal respiration (Figure 4-17). Moreover, AIF downregulation in murine embryonic stem cells and HeLa cells generated different kinds of respiratory chain defects, one involving complex III and the other not involving complex III, respectively. This points to a hitherto unexplained organ-specific role of AIF with regard to OXPHOS function. The responses to AIF deficiency varied even in different types of neurons (Klein and Ackerman, 2003), indicating the complexity of this tissue-specificity. Indeed, it has been shown for several other assembly factors that loss-of-function mutations resulted in tissue-specific diseases (Jaksch et al., 2000; Papadopoulou et al., 1999; Valnot et al., 2000). The molecular mechanisms that determine these effects in different tissues remain elusive. The association or non-association of AIF with diverse complexes (Figure 4-13A and B) is probably related to this phenomenon.

It further seems, that threshold effects can explain the impact of AIF deficiency in different organs. While the downregulation of AIF by 80% in hearts of harlequin mice do not lead to a detectable OXPHOS deficiency (Figure 4-17), the complete elimination of AIF expression in muscle-specific knockout mice results in a significant respiratory chain defect in heart tissue (Figure 4-18). Thus, low levels of AIF expression can be sufficient for proper functioning of OXPHOS in certain organs but not in others. However, a total loss of AIF provokes in most if not all tissues a respiratory chain defect.

The pathological manifestations observed in the muscle-specific AIF mutant mice, such as cardiac hypertrophy, progressive muscle atrophy, and lactic acidosis (Joza et al., 2005), resemble mitochondrial myopathies and cardiomyopathies in patients with primary defects in OXPHOS (Wallace, 1999). In accordance with the findings in harlequin mice, it can be assumed once more, that the respiratory chain defect caused by AIF deficiency is responsible for this pathology. The heart-specific AIF knockout mice as well as the harlequin mice can therefore serve as animal models for complex I diseases. This can prove to be very important in the development of therapies in order to treat patients suffering from respiratory chain defects.

However, human mitochondriopathies have never been associated with mutations in the AIF gene. But there is a very high number of patients, whose causative mutation for the respiratory chain disease was not identified. Thus, in the future, downregulation of AIF expression or function may be discovered in human pathologies. Mitochondrial dysfunction has been associated with neurodegenerative disorders like Alzheimer's disease, Chorea Huntington, and Parkinson (Schon and Manfredi, 2003). It has been suggested, in particular for Parkinson's disease, that complex I downregulation can be one of the central causes (Dawson and Dawson, 2003). Further investigations therefore need to take into account that AIF might play a role in the pathological scenario.

Failure to detect AIF loss-of-function mutations in diseases might be due to embryonic lethality caused by AIF deficiency, as seen in mice (Joza et al., 2001). That AIF-KO embryos did not develop was explained by impaired apoptosis in these cells. Respiration and particularly complex I is essential for development (Gorman et al., 2000; Huang et al., 2004; Ndegwa and Lemire, 2004). Thus, the respiratory chain defect in AIF-deficient cells could allow a re-interpretation of the $AIF^{-/y}$ cell lethality.

AIF obviously has two completely different functions, a fact that underscores the notion that the apparatus involved in the suicide of a cell is intimately linked to basic cellular life-sustaining processes. Due to its dual function, downregulation of AIF can result in both increased or decreased cell death depending on cell type and death inducing conditions. Moreover, *in vivo*, the importance of the vital or the deadly function may vary during different stages of development (Zhu et al., 2005). In order to use modulation of AIF activity in the treatment of diseases, associated with respiratory chain dysfunction or apoptosis dysregulation, both functions have to be further investigated and the impact of each function in different pathologies needs to be analysed.

5.2. Physical interaction of AIF with DNA and RNA

Using two different approaches, namely gel retention assays and electron microscopy, the interactions of AIF with DNA and RNA were analysed. While the binding of AIF to DNA had

been investigated before, the association of AIF with RNA was a new discovery. This *in vitro* study provided new insights into the molecular mechanisms of the AIF-nucleic acid interactions that may be involved in AIF-induced apoptosis. DNA and RNA were found to bind to a similar domain of AIF. Both interactions relied on the presence of magnesium and were enhanced by the co-factor NADP.

It has been described for many cell death scenarios in different cell types that AIF translocates to the nucleus, where it is supposed to participate in chromatin condensation and large-scale DNA fragmentation by binding directly to DNA (Cande et al., 2004b; Susin et al., 1999; Ye et al., 2002; Zhang et al., 2002). Accordingly, recombinant AIF has been shown to induce pyknosis when added to isolated nuclei or when injected into living cells (Loeffler et al., 2001; Susin et al., 2000). Here, AIF binding to DNA was detected in gel retention assays utilizing a standard DNA ladder as DNA molecules. Since the fragments of different size and sequence were equally retained by increasing amounts of recombinant AIF, the interaction seems to be sequence-independent (Figure 4-19A), which confirms previous data (Ye et al., 2002). The yeast orthologue of AIF, which displays 22% identity and 41% similarity with human AIF, bound to DNA in a similar fashion (Figure 4-19B), thus emphasizing the evolutionary conserved function of AIF. In disaccord with the literature (Wissing et al., 2004), there was no DNAse activity detected for recombinant yeast AIF.

Similar investigations were made for the interaction of AIF with RNA. To perform experiments using RNA instead of DNA was stimulated by the fact that the AIF interactome, as determined by mass spectrometry, contained a large panel of RNA binding proteins. The hypothesis, that AIF binds to these proteins through their RNA moiety rather than through protein-protein interactions was supported when the interaction between AIF and the RNA-binding protein HnRNPA1 was abolished by treatment with RNAse, as shown by co-immunoprecipitation experiments (Figure 4-24A). This hypothesis was further confirmed when recombinant AIF was shown to retain total RNA extracts from HeLa cells in horizontal gel electrophoresis (Figure 4-24B) and was found to form aggregates of poly-A RNA when analysed by electron microscopy (Figure 4-25). Moreover, AIF binding to RNA was attenuated by the same mutations that affected the AIF-DNA interaction (Figure 4-27), indicating that both kinds of nucleic acids could bind to the same domain of the protein. Ye *et al.* had proposed that, based on the crystal structure of human AIF, the interaction with DNA is mediated by the presence of a strong positive electrostatic potential at the surface of the protein (Ye et al., 2002). Indeed, replacement of positively charged amino acids by neutral ones abolished the interaction with DNA, thus explaining how AIF can bind to DNA even though no known DNA binding motif was found in human or murine AIF (Mate et al., 2002; Ye et al., 2002). Two of these recombinant AIF mutants were found to have a decreased affinity to both DNA and RNA in gel retention assays (Figure 4-27). It therefore seems likely

that the interaction with RNA is mediated via the same molecular mechanism as it is for DNA. An RNA binding motif has been found in human AIF (Lorenzo and Susin, 2004), which may also be responsible for the association of AIF and RNA. However, a molecular model predicted that the RNA oligonucleotides mainly interact with AIF through their phosphate backbone (Vahsen et al., 2005). Based on this model, R265, K446, and R450 are the basic residues on the AIF surface which are most frequently targeted for electrostatic interactions. Since these residues were also shown to play a key role in the AIF-DNA binding (Ye et al., 2002), these data strongly suggest that RNA binds to AIF at the same binding site as DNA. In accord with this theory, DNA binding of AIF was inhibited by the presence of RNA molecules, as determined by gel retention assays (Figure 4-28). As polyA, polyC, and polyG as well as the double-stranded RNA's polyA/U and polyG/C inhibited the association of AIF with DNA to a comparable degree, the binding of AIF to RNA seems to be sequence-independent.

Electron microscopy studies provided biophysical confirmation of the direct binding of AIF to DNA as well as to RNA. Both of these interactions are highly dependent on the presence of magnesium (Figure 4-19C and 4-25), which had also been shown for interactions of other proteins with DNA, like DNAse I (Simon et al., 1971) or the caspase-activated DNAse (CAD) (Widlak and Garrard, 2001). The fact that the optimal magnesium concentration resembles physiological conditions (Figure 4-19C) underlines the notion that these effects can take place in a cellular environment and are most likely not only *in vitro* artefacts. In the absence of magnesium, AIF was already found to bind to both DNA and RNA and induce aggregate formation. However, upon addition of magnesium, the aggregates were highly condensed and, most importantly, networks occurred pointing to the presence of protein-protein interactions (Figure 4-20 and 4-25). The hypothesis that these higher-order structures are formed in a cooperative fashion is supported by the observation that a few DNA molecules are compacted by AIF, while other DNA strands remain in their natural state. If there was no cooperativity, each DNA molecule would probably bind a similar number of AIF molecules.

Even though DNA and RNA seem to bind to AIF through a similar mechanism using overlapping, if not the same, binding sites, it is not very likely that this competition plays an important regulatory role *in vivo*. The strongest argument against an intracellular competition is the subcellular distribution of the two nucleic acids: while RNA is the predominant nucleic acids in the cytoplasm, DNA is much more abundant than RNA in the nucleus. Thus, once AIF has translocated to the nucleus during apoptosis, the protein will be more likely to bind to DNA than to RNA molecules. Whether AIF is passed on via transient interactions with RNA or RNA moieties of ribonucleoproteins in the cytoplasm or in the nucleus remains a conundrum. However, observations in CTL's (Figure 4-30) as well as in sensory neurons (Yamashita et al., 2004) suggest that, in certain cell death scenarios, AIF is released from

mitochondria but stays in the cytosol rather than translocates to the nucleus. It can be speculated that if the AIF-RNA interaction was not only an effect seen *in vitro* but AIF truly had an RNA-related role *in vivo* it would be most likely to take place in the cytosol. Therefore, it is worthy to investigate different hypothetical roles of AIF related to RNA. Since AIF takes part in the degradation of DNA during apoptosis, it was tested whether AIF also played a role in RNA degradation during programmed cell death. The results obtained clearly indicated that the presence or absence of AIF did not have an influence on the amount of RNA found in apoptotic cells (Figure 4-29). STS-induced apoptosis reduced the RNA content of ES cells significantly. In accordance with the literature, that was not the case when caspases were inhibited (Asselbergs and Widmer, 2003; King et al., 2000; Rutjes et al., 1999). Thus, although little is known about the RNA degradation process during programmed cell death, different kinds of RNA species seem to be fragmented by caspase-dependent and AIF-independent mechanisms. Another possibility would be that AIF has an influence on translation processes in the cytosol; it could act as a recruitment factor causing the formation of a complex to stop translation. Due to the lack of evidence, this role of AIF remains pure speculation. AIF has been shown to have a negative impact on cytoplasmic stress granule formation (Cande et al., 2004c), which is a cellular defense mechanism against redox stress that brings translation to a halt, probably in order to avoid the generation of misfolded proteins. However, AIF was not found to be associated with these cytoplasmic foci, but suppresses their formation while localised in the mitochondria (Cande et al., 2004c). Therefore, this particular function of AIF does most likely not play an important role in apoptosis.

The cytosolic factor HSP70 is known to bind to AIF and can therefore block its translocation to the nucleus as well as its pro-apoptotic activity (Ravagnan et al., 2001). If HSP70 also has an effect on a possible AIF-RNA interaction in the cytosol needs to be investigated. Since the heat shock protein and RNA bind to different domains of AIF (Schmitt et al., 2003), HSP70 would have to induce a conformational change of the protein in order to inhibit RNA binding.

While the biological significance of AIF binding to RNA remains enigmatic, the interaction between AIF and DNA has been analysed much further. It appears clear that AIF can mediate chromatin condensation *in vivo* (Cregan et al., 2002; Loeffler et al., 2001; Yuste et al., 2005b; Zhu et al., 2003) and strong evidence suggests that AIF is involved in large-scale DNA fragmentation (Cheung et al., 2005; Susin et al., 1999; Zhang et al., 2002). The electron microscopy pictures shown here point out that AIF alone can induce DNA compaction, which is probably mediated by protein-protein interactions (Figure 4-20). However, there was no DNAse activity detected when the protein was added to naked DNA suggesting that other factors need to be present to induce DNA degradation. CypA in mammalian cells and EndoG in *C.elegans* had already been identified as AIF-cooperating enzymes (Cande et al., 2004b;

Wang et al., 2002). The nuclear events during programmed cell death are very complex and most likely there is an interplay of numerous proteins that is responsible for the apoptotic phenotype. There is an ongoing scientific discussion on which factors can induce chromatinolysis and, in particular, high-molecular weight DNA degradation. CAD has been described to induce both, high- and low-molecular weight DNA cleavage (Enari et al., 1998; Widlak, 2000), although some argue that CAD is dispensable for large-scale DNA fragmentation (Samejima et al., 2001). Similarly contradictory observations have been made for AIF. Even though AIF has been shown to induce large-scale DNA fragmentation in several cell death scenarios (Cheung et al., 2005; Susin et al., 1999; Zhang et al., 2002), AIF does not seem to be the responsible enzyme for caspase-independent DNA degradation in cyclophosphamide-treated CTL's (Figure 4-30). The latter exhibit apoptotic nuclei as well as large-scale DNA fragmentation, but AIF was only found to have translocated to the nucleus in a small fraction of the cells. Moreover, Yuste et al. recently showed that silencing of endogenous AIF did not abolish DNA fragmentation in staurosporine-induced apoptosis (Yuste et al., 2005b). There must hence be other factors involved in high-molecular weight DNA fragmentation, at least in certain cell types. Even though, EndoG and Cyt *c* readily translocate to the nucleus in a large number of CTL's after cyclophosphamide treatment (Figure 4-30), there has been no evidence, yet, to prove that these enzymes are capable of inducing large-scale DNA fragmentation.

It seems that AIF's role in DNA degradation is, just like its vital function in the respiratory chain, cell type specific. Moreover, high-molecular weight DNA fragmentation can be caspase-dependent or independent and AIF-dependent or independent in the same cell type according to the apoptotic stimulus, as it has been described for cerebellar granule neurons (Slagsvold et al., 2003).

However, it seems clear that AIF binds to DNA and induces chromatin condensation in a large number of cell types. Since AIF preferentially binds to single-stranded DNA (Figure 4-21) and hardly interacts with supercoiled DNA (Figure 4-20), AIF is likely to invade the chromatin at the site of pre-existing lesions. It could then, by means of cooperative interactions, propagate through the adjacent double-stranded DNA, causing its condensation. This hypothesis is consistent with observations made in chronological aging of yeast where AIF has been found to interact with discrete foci of nuclear chromatin before it redistributes throughout the nucleus (Vahsen et al., 2005). Chronological aging is a physiological inducer of apoptosis in yeast (Herker et al., 2004) and serves as a very good model to study programmed cell death, because the different stages of the process are much longer and therefore more precisely definable.

Once AIF is bound to DNA, it could also play a role in recruiting other factors to DNA including CypA or EndoG. Due to its capability to form compact DNA packages, AIF might

further facilitate the DNA degrading actions of other enzymes by bringing the DNA molecules close together. AIF can therefore act as a co-factor in DNA and nuclear degradation. These hypotheses are in accordance with a model of a "degradosome" proposed by Parrish and Xue. The finding that several nucleases of *C.elegans* including the orthologues of EndoG and AIF can interact *in vitro*, led to the conclusion that they might form a multinuclease complex *in vivo* to execute chromosome degradation (Parrish and Xue, 2003). Further investigations will hopefully allow more insights into the complex processes inside the nucleus during apoptosis.

Taken together these data, AIF is one of the factors involved in chromatin condensation and DNA fragmentation, but it is most likely that the latter requires additional proteins. In certain cell types, AIF seems to be dispensable for nuclear apoptosis, as it was shown for CTL's. Similar observations have been made for CAD, which is not even expressed in all human tissues (Mukae et al., 1998). Thus, the roles of various pro-apoptotic factors acting on DNA are cell-type and cell-stimulus dependent.

Interestingly, the co-factor NADP could enhance AIF's affinity for DNA (Figure 4-22A) as well as for RNA (Figure 4-26B). This effect might be due to a conformational change of the protein that is induced once NADP is bound. A conformational change has also been observed when NADH binds to the bacterial ferredoxin reductase BphA4, which is evolutionary and structurally closely related to AIF (Senda et al., 2000). Electron microscopy pictures pointed out the difference between AIF's effect on DNA with and without NADP (Figure 4-23), the latter inducing extremely large networks of DNA molecules. However, whether NADP plays an important role in the AIF-DNA interaction *in vivo* remains uncertain. NADP/NADPH is known for its important function as an electron donor and acceptor in redox systems like thioredoxin or glutathione, but has not been associated with apoptosis. Intriguingly, recent studies revealed that the AIF-homologue AMID can bind to DNA and that this interaction is inhibited by both NADP and NADPH (Marshall et al., 2005). It was suggested that the binding sites for DNA and NADP(H) overlap. However, this does not seem to be the case for AIF. It therefore remains to be determined by which mechanism NADP increases AIF's affinity for DNA and RNA. Since NADP is involved in redox reactions, it needs to be reconsidered if the redox domain of AIF is involved in the apoptotic process of chromatin condensation and possibly degradation. However, previous data showing that the oxidoreductase domain of AIF is not important for its DNA degrading activities, does not support this hypothesis (Ye et al., 2002) (Miramar et al., 2001).

Thus, AIF's interaction with nucleic acids requires further investigation, although it seems clear that AIF can condense chromatin while some of AIF's functions in the nucleus require additional proteins and can be modified by co-factors.

The apoptotic and the mitochondrial role of AIF are most likely to be independent from each other since they take place in completely different compartments of the cell.

In conclusion, AIF's roles in the life and death of a cell have been further characterised. In vital cells, AIF plays a crucial role in the proper functioning of the respiratory chain as an assembly and/or a maintenance factor for complex I and/or the respirasome. AIF-deficiency can thus lead to phenotypes resembling severe mitochondriopathies. Upon apoptosis induction, AIF is released from mitochondria to translocate to the cytosol and, in a variety of different cell types, to the nucleus. Its role in the cytosol is hitherto unknown but it might be associated with its ability to interact with RNA. Once in the nucleus, AIF binds to DNA to induce chromatin condensation and to cooperate with other factors to induce DNA degradation. Its vital as well as its apoptotic function seem to depend on the cell type and, in the case of the apoptotic function, the cell death stimulus.

The different functions of AIF need to be investigated further in order to understand how they can be manipulated to fight disease. Hopefully, experiments with Harlequin mice as a newly discovered animal model for respiratory chain diseases will contribute to the development of effective therapies for patients suffering from mitochondriopathies.

6. Summary

The apoptosis-inducing factor (AIF) is a phylogenetically old flavoprotein that is localised in mitochondria of healthy cells. It has been known to play an important role in the process of apoptosis, a genetically programmed cell suicide that removes supernumerous or potentially dangerous cells from a multicellular organism. Upon apoptosis induction, AIF translocates from the mitochondria via the cytosol to the nucleus, where it is involved in apoptosis-associated chromatinolysis.

Here, I describe a hitherto unknown role of AIF in the functioning of the respiratory chain, the cell's major source of energy. AIF-deficient murine embryonic stem cells were found to be highly dependent on glycolysis. This abnormal dependency was due to defective oxidative phosphorylation affecting in particular complex I and III of the respiratory chain. Similar observations were made in HeLa cells, in which the AIF expression had been downregulated by RNA interference. However, in the human cell line, reduced activity was found in complex I, but not in complex III. The respiratory chain defect was detectable not only at the functional but also at the protein level. All tested complex I subunits as well as the whole complex I were found to be less abundant in AIF-deficient cells than in their wild-type counterparts. This seemed to be a post-transcriptional phenomenon since the absence of AIF did not modify the levels of mRNA's. Moreover, AIF does not seem to be a part of complex I or any other known respiratory chain complex, but retransfection with mitochondrially targeted AIF did cause re-expression of complex I and III subunits in AIF-KO cells. Since AIF has an oxidoreductase domain, it was speculated that AIF protected the respiratory chain complexes against ROS-induced damage, but treatment with several antioxidants could not restore the expression of complex I subunits in AIF-deficient cells. Therefore, AIF seems to play a role in the assembly or the maintenance of complex I and maybe other complexes. The existence of so-called supercomplexes, which comprise several respiratory chain complexes, could explain why the stability of more than one complex is affected. Harlequin mice, which exhibit only 20% of AIF expression due to a retroviral insertion in the Aif gene, were also found to have a complex I defect in different tissues including brain and retina but not heart and liver. That allowed for a re-interpretation of the harlequin phenotype, which is characterised by progressive neuronal and retinal degradation resembling symptoms of mitochondriopathies in humans. Harlequin mice can therefore serve as a mouse model to study complex I diseases. Moreover, it was shown that conditional knock-out mice (developed in Dr.Penninger's laboratory) that did not express AIF in heart and muscle tissues and suffered from cardiomyopathy and muscle atrophy, had a respiratory chain defect in the affected tissues. In this animal model a complex I defect was also detected in the heart. It thus seems that AIF's role in respiration is tissue-specific and also threshold-dependent.

In a second part of this work, AIF's role in apoptosis was further characterised by defining the interaction of AIF with nucleic acids. While the interaction of AIF with DNA had been described before, the binding of AIF to RNA was a new discovery. Recombinant AIF retained DNA fragments as well as RNA extracted from HeLa cells in a gel retention assay in a size and sequence independent manner. The direct interaction was also observed in electron microscopy experiments, where the presence of AIF induced the compaction of DNA and the formation of large aggregates of both DNA and RNA. Moreover, AIF showed a preferential binding to single-stranded over double-stranded DNA. Since different RNA molecules inhibited the retention of DNA by AIF, it was hypothesized that the nucleic acids bind to a similar or the same site of the protein. This hypothesis was further supported by the finding that two AIF mutants lacking positively charged amino acids, which had been described to mediate the AIF-DNA interaction, were less efficient in retaining both DNA and RNA in a horizontal agarose gel electrophoresis. Interestingly, the affinity for nucleic acids was enhanced by the co-factor NADP. While the role of the AIF-RNA interaction *in vivo* remains a conundrum, the AIF-DNA interaction plays an important role in chromatin condensation and, in certain cell death scenarios, large-scale DNA fragmentation.

7. References

Alano, C.C., Ying, W. and Swanson, R.A. (2004) Poly(ADP-ribose) polymerase-1-mediated cell death in astrocytes requires NAD+ depletion and mitochondrial permeability transition. *J Biol Chem*, **279**, 18895-18902.

Antonicka, H., Ogilvie, I., Taivassalo, T., Anitori, R.P., Haller, R.G., Vissing, J., Kennaway, N.G. and Shoubridge, E.A. (2003) Identification and characterization of a common set of complex I assembly intermediates in mitochondria from patients with complex I deficiency. *J Biol Chem*, **278**, 43081-43088.

Arnoult, D., Gaume, B., Karbowski, M., Sharpe, J.C., Cecconi, F. and Youle, R.J. (2003) Mitochondrial release of AIF and EndoG requires caspase activation downstream of Bax/Bak-mediated permeabilization. *Embo J*, **22**, 4385-4399.

Arnoult, D., Parone, P., Martinou, J.C., Antonsson, B., Estaquier, J. and Ameisen, J.C. (2002) Mitochondrial release of apoptosis-inducing factor occurs downstream of cytochrome c release in response to several proapoptotic stimuli. *J Cell Biol*, **159**, 923-929.

Arnoult, D., Tatischeff, I., Estaquier, J., Girard, M., Sureau, F., Tissier, J.P., Grodet, A., Dellinger, M., Traincard, F., Kahn, A., Ameisen, J.C. and Petit, P.X. (2001) On the evolutionary conservation of the cell death pathway: mitochondrial release of an apoptosis-inducing factor during Dictyostelium discoideum cell death. *Mol Biol Cell*, **12**, 3016-3030.

Asselbergs, F.A. and Widmer, R. (2003) Rapid detection of apoptosis through real-time reverse transcriptase polymerase chain reaction measurement of the small cytoplasmic RNA Y1. *Anal Biochem*, **318**, 221-229.

Atorino, L., Silvestri, L., Koppen, M., Cassina, L., Ballabio, A., Marconi, R., Langer, T. and Casari, G. (2003) Loss of m-AAA protease in mitochondria causes complex I deficiency and increased sensitivity to oxidative stress in hereditary spastic paraplegia. *J Cell Biol*, **163**, 777-787.

Bai, Y. and Attardi, G. (1998) The mtDNA-encoded ND6 subunit of mitochondrial NADH dehydrogenase is essential for the assembly of the membrane arm and the respiratory function of the enzyme. *Embo J*, **17**, 4848-4858.

Beloin, C., Jeusset, J., Révet, B., G., M., F., L.H. and E., L.C. (2003) Contribution of DNA conformation and topology in right-handed DNA-wrapping by the Bacillus subtilis LrpC protein. *J Biol Chem.*, **278**, 5333-5342.

Bianchi, C., Genova, M.L., Parenti Castelli, G. and Lenaz, G. (2004) The mitochondrial respiratory chain is partially organized in a supercomplex assembly: kinetic evidence using flux control analysis. *J Biol Chem*, **279**, 36562-36569.

Bidere, N., Lorenzo, H.K., Carmona, S., Laforge, M., Harper, F., Dumont, C. and Senik, A. (2003) Cathepsin D triggers Bax activation, resulting in selective apoptosis-inducing factor (AIF) relocation in T lymphocytes entering the early commitment phase to apoptosis. *J Biol Chem*, **278**, 31401-31411.

Braun, J.S., Sublett, J.E., Freyer, D., Mitchell, T.J., Cleveland, J.L., Tuomanen, E.I. and Weber, J.R. (2002) Pneumococcal pneumolysin and H(2)O(2) mediate brain cell apoptosis during meningitis. *J Clin Invest*, **109**, 19-27.

Brenner, C., Cadiou, H., Vieira, H.L., Zamzami, N., Marzo, I., Xie, Z., Leber, B., Andrews, D., Duclohier, H., Reed, J.C. and Kroemer, G. (2000) Bcl-2 and Bax regulate the channel activity of the mitochondrial adenine nucleotide translocator. *Oncogene*, **19**, 329-336.

Brown, G.C. and Brand, M.D. (1988) Proton/electron stoichiometry of mitochondrial complex I estimated from the equilibrium thermodynamic force ratio. *Biochem J*, **252**, 473-479.

Budde, S.M., van den Heuvel, L.P., Janssen, A.J., Smeets, R.J., Buskens, C.A., DeMeirleir, L., Van Coster, R., Baethmann, M., Voit, T., Trijbels, J.M. and Smeitink, J.A. (2000) Combined enzymatic complex I and III deficiency associated with mutations in the nuclear encoded NDUFS4 gene. *Biochem Biophys Res Commun*, **275**, 63-68.

Cande, C., Cecconi, F., Dessen, P. and Kroemer, G. (2002) Apoptosis-inducing factor (AIF): key to the conserved caspase-independent pathways of cell death? *J Cell Sci*, **115**, 4727-4734.

Cande, C., Vahsen, N., Garrido, C. and Kroemer, G. (2004a) Apoptosis-inducing factor (AIF): caspase-independent after all. *Cell Death Differ*, **11**, 591-595.

Cande, C., Vahsen, N., Kouranti, I., Schmitt, E., Daugas, E., Spahr, C., Luban, J., Kroemer, R.T., Giordanetto, F., Garrido, C., Penninger, J.M. and Kroemer, G. (2004b) AIF and cyclophilin A cooperate in apoptosis-associated chromatinolysis. *Oncogene*, **23**, 1514-1521.

Cande, C., Vahsen, N., Metivier, D., Tourriere, H., Chebli, K., Garrido, C., Tazi, J. and Kroemer, G. (2004c) Regulation of cytoplasmic stress granules by apoptosis-inducing factor. *J Cell Sci*, **117**, 4461-4468.

Cao, G., Clark, R.S., Pei, W., Yin, W., Zhang, F., Sun, F.Y., Graham, S.H. and Chen, J. (2003) Translocation of apoptosis-inducing factor in vulnerable neurons after transient cerebral ischemia and in neuronal cultures after oxygen-glucose deprivation. *J Cereb Blood Flow Metab*, **23**, 1137-1150.

Carroll, J., Shannon, R.J., Fearnley, I.M., Walker, J.E. and Hirst, J. (2002) Definition of the nuclear encoded protein composition of bovine heart mitochondrial complex I. Identification of two new subunits. *J Biol Chem*, **277**, 50311-50317.

Castedo, M., Perfettini, J.L., Andreau, K., Roumier, T., Piacentini, M. and Kroemer, G. (2003) Mitochondrial apoptosis induced by the HIV-1 envelope. *Ann N Y Acad Sci*, **1010**, 19-28.

Cerisano, V., Aalto, Y., Perdichizzi, S., Bernard, G., Manara, M.C., Benini, S., Cenacchi, G., Preda, P., Lattanzi, G., Nagy, B., Knuutila, S., Colombo, M.P., Bernard, A., Picci, P. and Scotlandi, K. (2004) Molecular mechanisms of CD99-induced caspase-independent cell death and cell-cell adhesion in Ewing's sarcoma cells: actin and zyxin as key intracellular mediators. *Oncogene*, **23**, 5664-5674.

Cheung, E.C., Melanson-Drapeau, L., Cregan, S.P., Vanderluit, J.L., Ferguson, K.L., McIntosh, W.C., Park, D.S., Bennett, S.A. and Slack, R.S. (2005) Apoptosis-inducing factor is a key factor in neuronal cell death propagated by BAX-dependent and BAX-independent mechanisms. *J Neurosci*, **25**, 1324-1334.

Chipuk, J.E., Kuwana, T., Bouchier-Hayes, L., Droin, N.M., Newmeyer, D.D., Schuler, M. and Green, D.R. (2004) Direct activation of Bax by p53 mediates mitochondrial membrane permeabilization and apoptosis. *Science*, **303**, 1010-1014.

Chretien, D., Benit, P., Chol, M., Lebon, S., Rotig, A., Munnich, A. and Rustin, P. (2003) Assay of mitochondrial respiratory chain complex I in human lymphocytes and cultured skin fibroblasts. *Biochem Biophys Res Commun.*, **301**, 222-224.

Cregan, S.P., Dawson, V.L. and Slack, R.S. (2004) Role of AIF in caspase-dependent and caspase-independent cell death. *Oncogene*, **23**, 2785-2796.

Cregan, S.P., Fortin, A., MacLaurin, J.G., Callaghan, S.M., Cecconi, F., Yu, S.W., Dawson, T.M., Dawson, V.L., Park, D.S., Kroemer, G. and Slack, R.S. (2002) Apoptosis-inducing factor is involved in the regulation of caspase-independent neuronal cell death. *J Cell Biol*, **158**, 507-517.

Dahl, H.H. and Thorburn, D.R. (2001) Mitochondrial diseases: beyond the magic circle. *Am J Med Genet*, **106**, 1-3.

Daugas, E., Nochy, D., Ravagnan, L., Loeffler, M., Susin, S.A., Zamzami, N. and Kroemer, G. (2000a) Apoptosis-inducing factor (AIF): a ubiquitous mitochondrial oxidoreductase involved in apoptosis. *FEBS Lett*, **476**, 118-123.

Daugas, E., Susin, S.A., Zamzami, N., Ferri, K.F., Irinopoulou, T., Larochette, N., Prevost, M.C., Leber, B., Andrews, D., Penninger, J. and Kroemer, G. (2000b) Mitochondrio-nuclear translocation of AIF in apoptosis and necrosis. *Faseb J*, **14**, 729-739.

Dawson, T.M. and Dawson, V.L. (2003) Molecular pathways of neurodegeneration in Parkinson's disease. *Science*, **302**, 819-822.

Deas, O., Dumont, C., MacFarlane, M., Rouleau, M., Hebib, C., Harper, F., Hirsch, F., Charpentier, B., Cohen, G.M. and Senik, A. (1998) Caspase-independent cell death induced by anti-CD2 or staurosporine in activated human peripheral T lymphocytes. *J. Immunol.*, **161**, 3375-3383.

Delain, E. and LeCam, E. (1995) Visualisation of nucleic acids. G. Morel, CRC Press: 35-56.

Devreese, B., Vanrobaeys, F., Smet, J., Van Beeumen, J. and Van Coster, R. (2002) Mass spectrometric identification of mitochondrial oxidative phosphorylation subunits separated by two-dimensional blue-native polyacrylamide gel electrophoresis. *Electrophoresis*, **23**, 2525-2533.

DiMauro, S. and Schon, E.A. (2003) Mitochondrial respiratory-chain diseases. *N Engl J Med*, **348**, 2656-2668.

Du, C., Fang, M., Li, Y., Li, L. and Wang, X. (2000) Smac, a mitochondrial protein that promotes cytochrome c-dependent caspase activation by eliminating IAP inhibition. *Cell*, **102**, 33-42.

Du, L., Zhang, X., Han, Y.Y., Burke, N.A., Kochanek, P.M., Watkins, S.C., Graham, S.H., Carcillo, J.A., Szabo, C. and Clark, R.S. (2003) Intra-mitochondrial poly(ADP-ribosylation) contributes to NAD+ depletion and cell death induced by oxidative stress. *J Biol Chem*, **278**, 18426-18433.

Dubochet, J., Ducommun, M., Zollinger, M. and Kellenberger, E. (1971) A new preparation method for dark-field electron microscopy of biomacromolecules. *J. Ultrastruct. Res.*, **35**, 147-167.

Dumont, C., Durrbach, A., Bidere, N., Rouleau, M., Kroemer, G., Bernard, G., Hirsch, F., Charpentier, B., Susin, S.A. and Senik, A. (2000) Caspase-independent commitment phase to apoptosis in activated blood T lymphocytes: reversibility at low apoptotic insult. *Blood*, **96**, 1030-1038.

Dyall, S.D., Brown, M.T. and Johnson, P.J. (2004) Ancient invasions: from endosymbionts to organelles. *Science*, **304**, 253-257.

Elston, T., Wang, H. and Oster, G. (1998) Energy transduction in ATP synthase. *Nature*, **391**, 510-513.

Enari, M., Sakahira, H., Yokoyama, H., Okawa, K., Iwamatsu, A. and Nagata, S. (1998) A caspase-activated DNase that degrades DNA during apoptosis, and its inhibitor ICAD. *Nature*, **391**, 43-50.

Fadok, V.A., Bratton, D.L., Rose, D.M., Pearson, A., Ezekewitz, R.A. and Henson, P.M. (2000) A receptor for phosphatidylserine-specific clearance of apoptotic cells. *Nature*, **405**, 85-90.

Fearnley, I.M., Carroll, J., Shannon, R.J., Runswick, M.J., Walker, J.E. and Hirst, J. (2001) GRIM-19, a cell death regulatory gene product, is a subunit of bovine mitochondrial NADH:ubiquinone oxidoreductase (complex I). *J Biol Chem*, **276**, 38345-38348.

Ferri, K.F., Jacotot, E., Blanco, J., Este, J.A., Zamzami, N., Susin, S.A., Xie, Z., Brothers, G., Reed, J.C., Penninger, J.M. and Kroemer, G. (2000) Apoptosis control in syncytia induced by the HIV type 1-envelope glycoprotein complex: role of mitochondria and caspases. *J Exp Med*, **192**, 1081-1092.

Foghsgaard, L., Wissing, D., Mauch, D., Lademann, U., Bastholm, L., Boes, M., Elling, F., Leist, M. and Jaattela, M. (2001) Cathepsin B acts as a dominant execution protease in tumor cell apoptosis induced by tumor necrosis factor. *J Cell Biol*, **153**, 999-1010.

Gallego, M.A., Joseph, B., Hemstrom, T.H., Tamiji, S., Mortier, L., Kroemer, G., Formstecher, P., Zhivotovsky, B. and Marchetti, P. (2004) Apoptosis-inducing factor determines the chemoresistance of non-small-cell lung carcinomas. *Oncogene*, **23**, 6282-6291.

Garrido, C., Gurbuxani, S., Ravagnan, L. and Kroemer, G. (2001) Heat shock proteins: endogenous modulators of apoptotic cell death. *Biochem Biophys Res Commun*, **286**, 433-442.

Garrido, C. and Kroemer, G. (2004) Life's smile, death's grin: vital functions of apoptosis-executing proteins. *Curr Opin Cell Biol*, **16**, 639-646.

Geromel, V., Darin, N., Chretien, D., Benit, P., DeLonlay, P., Rotig, A., Munnich, A. and Rustin, P. (2002) Coenzyme Q(10) and idebenone in the therapy of respiratory chain diseases: rationale and comparative benefits. *Mol Genet Metab*, **77**, 21-30.

Gorman, A.M., Ceccatelli, S. and Orrenius, S. (2000) Role of mitochondria in neuronal apoptosis. *Dev Neurosci*, **22**, 348-358.

Gougeon, M.L. (2003) Apoptosis as an HIV strategy to escape immune attack. *Nat Rev Immunol*, **3**, 392-404.

Gray, M.W., Burger, G. and Lang, B.F. (1999) Mitochondrial evolution. *Science*, **283**, 1476-1481.

Green, D.R. (2005) Apoptotic pathways: ten minutes to dead. *Cell*, **121**, 671-674.

Green, D.R. and Kroemer, G. (2004) The pathophysiology of mitochondrial cell death. *Science*, **305**, 626-629.

Guenebaut, V., Vincentelli, R., Mills, D., Weiss, H. and Leonard, K.R. (1997) Three-dimensional structure of NADH-dehydrogenase from Neurospora crassa by electron microscopy and conical tilt reconstruction. *J Mol Biol*, **265**, 409-418.

Guidot, D.M., Repine, J.E., Kitlowski, A.D., Flores, S.C., Nelson, S.K., Wright, R.M. and McCord, J.M. (1995) Mitochondrial respiration scavenges extramitochondrial superoxide anion via a nonenzymatic mechanism. *J Clin Invest*, **96**, 1131-1136.

Gurbuxani, S., Schmitt, E., Cande, C., Parcellier, A., Hammann, A., Daugas, E., Kouranti, I., Spahr, C., Pance, A., Kroemer, G. and Garrido, C. (2003) Heat shock protein 70 binding inhibits the nuclear import of apoptosis-inducing factor. *Oncogene*, **22**, 6669-6678.

Hanahan, D. and Weinberg, R.A. (2000) The hallmarks of cancer. *Cell*, **100**, 57-70.

Harborth, J., Elbashir, S.M., Bechert, K., Tuschl, T. and Weber, K. (2001) Identification of essential genes in cultured mammalian cells using small interfering RNAs. *J Cell Sci*, **114**, 4557-4565.

Hegde, R., Srinivasula, S.M., Zhang, Z., Wassell, R., Mukattash, R., Cilenti, L., DuBois, G., Lazebnik, Y., Zervos, A.S., Fernandes-Alnemri, T. and Alnemri, E.S. (2002) Identification of Omi/HtrA2 as a mitochondrial apoptotic serine protease that disrupts inhibitor of apoptosis protein-caspase interaction. *J Biol Chem*, **277**, 432-438.

Hengartner, M.O. (2000) The biochemistry of apoptosis. *Nature*, **407**, 770-776.

Herker, E., Jungwirth, H., Lehmann, K.A., Maldener, C., Froehlich, K.U., Wissing, S., Buttner, S., Fehr, M., Sigrist, S. and Madeo, F. (2004) Chronological aging leads to apoptosis in yeast. *J Cell Biol*, **164**, 501-507.

Hirst, J., Carroll, J., Fearnley, I.M., Shannon, R.J. and Walker, J.E. (2003) The nuclear encoded subunits of complex I from bovine heart mitochondria. *Biochim Biophys Acta*, **1604**, 135-150.

Hofhaus, G. and Attardi, G. (1993) Lack of assembly of mitochondrial DNA-encoded subunits of respiratory NADH dehydrogenase and loss of enzyme activity in a human cell mutant lacking the mitochondrial ND4 gene product. *Embo J*, **12**, 3043-3048.

Hong, S.J., Dawson, T.M. and Dawson, V.L. (2004) Nuclear and mitochondrial conversations in cell death: PARP-1 and AIF signaling. *Trends Pharmacol Sci*, **25**, 259-264.

Huang, G., Lu, H., Hao, A., Ng, D.C., Ponniah, S., Guo, K., Lufei, C., Zeng, Q. and Cao, X. (2004) GRIM-19, a cell death regulatory protein, is essential for assembly and function of mitochondrial complex I. *Mol Cell Biol*, **24**, 8447-8456.

Irvine, R.A., Adachi, N., Shibata, D.K., Cassell, G.D., Yu, K., Karanjawala, Z.E., Hsieh, C.L. and Lieber, M.R. (2005) Generation and characterization of endonuclease G null mice. *Mol Cell Biol*, **25**, 294-302.

Jaattela, M., Cande, C. and Kroemer, G. (2004) Lysosomes and mitochondria in the commitment to apoptosis: a potential role for cathepsin D and AIF. *Cell Death Differ*, **11**, 135-136.

Jaksch, M., Ogilvie, I., Yao, J., Kortenhaus, G., Bresser, H.G., Gerbitz, K.D. and Shoubridge, E.A. (2000) Mutations in SCO2 are associated with a distinct form of hypertrophic cardiomyopathy and cytochrome c oxidase deficiency. *Hum Mol Genet*, **9**, 795-801.

Janssen, R., Smeitink, J., Smeets, R. and van Den Heuvel, L. (2002) CIA30 complex I assembly factor: a candidate for human complex I deficiency? *Hum Genet*, **110**, 264-270.

Johnson, D.E. (2000) Noncaspase proteases in apoptosis. *Leukemia*, **14**, 1695-1703.

Jones, J.M., Datta, P., Srinivasula, S.M., Ji, W., Gupta, S., Zhang, Z., Davies, E., Hajnoczky, G., Saunders, T.L., Van Keuren, M.L., Fernandes-Alnemri, T., Meisler, M.H. and Alnemri, E.S. (2003) Loss of Omi mitochondrial protease activity causes the neuromuscular disorder of mnd2 mutant mice. *Nature*, **425**, 721-727.

Joza, N., Oudit, G.Y., Brown, D., Benit, P.,Kassiri, Z., Vahsen, N., Benoit, L., Patel, M.M., Nowikovsky, K., Vassault, Backx, P., Wada, T., Kroemer, G., Rustin, P., and Penninger, J. (2005) Muscle-specific loss of apoptosis-inducing factor leads to mitochondrial dysfunction, skeletal muscle atrophy, and dilated cardiomyopathy. *Mol Cell Biol* **in press**.

Joza, N., Susin, S.A., Daugas, E., Stanford, W.L., Cho, S.K., Li, C.Y., Sasaki, T., Elia, A.J., Cheng, H.Y., Ravagnan, L., Ferri, K.F., Zamzami, N., Wakeham, A., Hakem, R., Yoshida, H., Kong, Y.Y., Mak, T.W., Zuniga-Pflucker, J.C., Kroemer, G. and Penninger, J.M. (2001) Essential role of the mitochondrial apoptosis-inducing factor in programmed cell death. *Nature*, **410**, 549-554.

Kang, Y.H., Yi, M.J., Kim, M.J., Park, M.T., Bae, S., Kang, C.M., Cho, C.K., Park, I.C., Park, M.J., Rhee, C.H., Hong, S.I., Chung, H.Y., Lee, Y.S. and Lee, S.J. (2004) Caspase-independent cell death by arsenic trioxide in human cervical cancer cells: reactive oxygen species-mediated poly(ADP-ribose) polymerase-1 activation signals apoptosis-inducing factor release from mitochondria. *Cancer Res*, **64**, 8960-8967.

Kerr, J.F., Wyllie, A.H. and Currie, A.R. (1972) Apoptosis: a basic biological phenomenon with wide-ranging implications in tissue kinetics. *Br J Cancer*, **26**, 239-257.

Khaled, A.R., Kim, K., Hofmeister, R., Muegge, K. and Durum, S.K. (1999) Withdrawal of IL-7 induces Bax translocation from cytosol to mitochondria through a rise in intracellular pH. *Proc Natl Acad Sci U S A*, **96**, 14476-14481.

Kim, G.T., Chun, Y.S., Park, J.W. and Kim, M.S. (2003) Role of apoptosis-inducing factor in myocardial cell death by ischemia-reperfusion. *Biochem Biophys Res Commun*, **309**, 619-624.

King, K.L., Jewell, C.M., Bortner, C.D. and Cidlowski, J.A. (2000) 28S ribosome degradation in lymphoid cell apoptosis: evidence for caspase and Bcl-2-dependent and -independent pathways. *Cell Death Differ*, **7**, 994-1001.

Kischkel, F.C., Hellbardt, S., Behrmann, I., Germer, M., Pawlita, M., Krammer, P.H. and Peter, M.E. (1995) Cytotoxicity-dependent APO-1 (Fas/CD95)-associated proteins form a death-inducing signaling complex (DISC) with the receptor. *Embo J*, **14**, 5579-5588.

Klein, J.A. and Ackerman, S.L. (2003) Oxidative stress, cell cycle, and neurodegeneration. *J Clin Invest*, **111**, 785-793.

Klein, J.A., Longo-Guess, C.M., Rossmann, M.P., Seburn, K.L., Hurd, R.E., Frankel, W.N., Bronson, R.T. and Ackerman, S.L. (2002) The harlequin mouse mutation downregulates apoptosis-inducing factor. *Nature*, **419**, 367-374.

Krammer, P.H. (2000) CD95's deadly mission in the immune system. *Nature*, **407**, 789-795.

Kroemer, G. and Martin, S.J. (2005) Caspase-independent cell death. *Nat Med*, **11**, 725-730.

Kroemer, G. and Reed, J.C. (2000) Mitochondrial control of cell death. *Nat Med*, **6**, 513-519.

Kudin, A.P., Bimpong-Buta, N.Y., Vielhaber, S., Elger, C.E. and Kunz, W.S. (2004) Characterization of superoxide-producing sites in isolated brain mitochondria. *J Biol Chem*, **279**, 4127-4135.

Kuffner, R., Rohr, A., Schmiede, A., Krull, C. and Schulte, U. (1998) Involvement of two novel chaperones in the assembly of mitochondrial NADH:Ubiquinone oxidoreductase (complex I). *J Mol Biol*, **283**, 409-417.

Larsson, N.G. and Rustin, P. (2001) Animal models for respiratory chain disease. *Trends Mol Med*, **7**, 578-581.

Lecoeur, H. (2002) Nuclear apoptosis detection by flow cytometry: infuence of endogenous endonucleases. *Exp Cell Res*, **277**, 1-14.

Li, H., Zhu, H., Xu, C.J. and Yuan, J. (1998) Cleavage of BID by caspase 8 mediates the mitochondrial damage in the Fas pathway of apoptosis. *Cell*, **94**, 491-501.

Li, L.Y., Luo, X. and Wang, X. (2001) Endonuclease G is an apoptotic DNase when released from mitochondria. *Nature*, **412**, 95-99.

Li, P., Nijhawan, D., Budihardjo, I., Srinivasula, S.M., Ahmad, M., Alnemri, E.S. and Wang, X. (1997) Cytochrome c and dATP-dependent formation of Apaf-1/caspase-9 complex initiates an apoptotic protease cascade. *Cell*, **91**, 479-489.

Lipton, S.A. and Bossy-Wetzel, E. (2002) Dueling activities of AIF in cell death versus survival: DNA binding and redox activity. *Cell*, **111**, 147-150.

Liu, T., Brouha, B. and Grossman, D. (2004) Rapid induction of mitochondrial events and caspase-independent apoptosis in Survivin-targeted melanoma cells. *Oncogene*, **23**, 39-48.

Liu, X., Zou, H., Slaughter, C. and Wang, X. (1997) DFF, a heterodimeric protein that functions downstream of caspase-3 to trigger DNA fragmentation during apoptosis. *Cell*, **89**, 175-184.

Loeffler, M., Daugas, E., Susin, S.A., Zamzami, N., Metivier, D., Nieminen, A.L., Brothers, G., Penninger, J.M. and Kroemer, G. (2001) Dominant cell death induction by extramitochondrially targeted apoptosis-inducing factor. *Faseb J*, **15**, 758-767.

Lorenzo, H.K. and Susin, S.A. (2004) Mitochondrial effectors in caspase-independent cell death. *FEBS Lett*, **557**, 14-20.

Lorenzo, H.K., Susin, S.A., Penninger, J. and Kroemer, G. (1999) Apoptosis inducing factor (AIF): a phylogenetically old, caspase-independent effector of cell death. *Cell Death Differ*, **6**, 516-524.

Majno, G. and Joris, I. (1995) Apoptosis, oncosis, and necrosis. An overview of cell death. *Am J Pathol.*, **146**, 3-15.

Mannella, C.A., Pfeiffer, D.R., Bradshaw, P.C., Moraru, II, Slepchenko, B., Loew, L.M., Hsieh, C.E., Buttle, K. and Marko, M. (2001) Topology of the mitochondrial inner membrane: dynamics and bioenergetic implications. *IUBMB Life*, **52**, 93-100.

Marshall, K.R., Gong, M., Wodke, L., Lamb, J.H., Jones, D.J., Farmer, P.B., Scrutton, N.S. and Munro, A.W. (2005) The human apoptosis inducing protein AMID is an oxidoreductase with a modified flavin cofactor and DNA binding activity. *J Biol Chem*.

Martin-Villalba, A., Hahne, M., Kleber, S., Vogel, J., Falk, W., Schenkel, J. and Krammer, P.H. (2001) Therapeutic neutralization of CD95-ligand and TNF attenuates brain damage in stroke. *Cell Death Differ*, **8**, 679-686.

Martinez, J., Patkaniowska, A., Urlaub, H., Luhrmann, R. and Tuschl, T. (2002) Single-stranded antisense siRNAs guide target RNA cleavage in RNAi. *Cell*, **110**, 563-574.

Marzo, I., Brenner, C., Zamzami, N., Jurgensmeier, J.M., Susin, S.A., Vieira, H.L., Prevost, M.C., Xie, Z., Matsuyama, S., Reed, J.C. and Kroemer, G. (1998) Bax and adenine nucleotide translocator cooperate in the mitochondrial control of apoptosis. *Science*, **281**, 2027-2031.

Mate, M.J., Ortiz-Lombardia, M., Boitel, B., Haouz, A., Tello, D., Susin, S.A., Penninger, J., Kroemer, G. and Alzari, P.M. (2002) The crystal structure of the mouse apoptosis-inducing factor AIF. *Nat Struct Biol*, **9**, 442-446.

Matsumori, Y., Hong, S.M., Aoyama, K., Fan, Y., Kayama, T., Sheldon, R.A., Vexler, Z.S., Ferriero, D.M., Weinstein, P.R. and Liu, J. (2005) Hsp70 overexpression sequesters AIF and reduces neonatal hypoxic/ischemic brain injury. *J Cereb Blood Flow Metab*.

Mattson, M.P., Zhu, H., Yu, J. and Kindy, M.S. (2000) Presenilin-1 mutation increases neuronal vulnerability to focal ischemia in vivo and to hypoxia and glucose deprivation in cell culture: involvement of perturbed calcium homeostasis. *J Neurosci*, **20**, 1358-1364.

Mazzio, E. and Soliman, K.F. (2003) The role of glycolysis and gluconeogenesis in the cytoprotection of neuroblastoma cells against 1-methyl 4-phenylpyridinium ion toxicity. *Neurotoxicology*, **24**, 137-147.

McIlroy, D., Tanaka, M., Sakahira, H., Fukuyama, H., Suzuki, M., Yamamura, K., Ohsawa, Y., Uchiyama, Y. and Nagata, S. (2000) An auxiliary mode of apoptotic DNA fragmentation provided by phagocytes. *Genes Dev*, **14**, 549-558.

Melov, S., Coskun, P., Patel, M., Tuinstra, R., Cottrell, B., Jun, A.S., Zastawny, T.H., Dizdaroglu, M., Goodman, S.I., Huang, T.T., Miziorko, H., Epstein, C.J. and Wallace, D.C. (1999) Mitochondrial disease in superoxide dismutase 2 mutant mice. *Proc Natl Acad Sci U S A*, **96**, 846-851.

Mikhailov, V., Mikhailova, M., Pulkrabek, D.J., Dong, Z., Venkatachalam, M.A. and Saikumar, P. (2001) Bcl-2 prevents Bax oligomerization in the mitochondrial outer membrane. *J Biol Chem*, **276**, 18361-18374.

Miramar, M.D., Costantini, P., Ravagnan, L., Saraiva, L.M., Haouzi, D., Brothers, G., Penninger, J.M., Peleato, M.L., Kroemer, G. and Susin, S.A. (2001) NADH oxidase activity of mitochondrial apoptosis-inducing factor. *J Biol Chem*, **276**, 16391-16398.

Montague, J.W., Gaido, M.L., Frye, C. and Cidlowski, J.A. (1994) A calcium-dependent nuclease from apoptotic rat thymocytes is homologous with cyclophilin. Recombinant cyclophilins A, B, and C have nuclease activity. *J Biol Chem*, **269**, 18877-18880.

Mukae, N., Enari, M., Sakahira, H., Fukuda, Y., Inazawa, J., Toh, H. and Nagata, S. (1998) Molecular cloning and characterization of human caspase-activated DNase. *Proc Natl Acad Sci U S A*, **95**, 9123-9128.

Munnich, A. and Rustin, P. (2001) Clinical spectrum and diagnosis of mitochondrial disorders. *Am J Med Genet*, **106**, 4-17.

Murahashi, H., Azuma, H., Zamzami, N., Furuya, K.J., Ikebuchi, K., Yamaguchi, M., Yamada, Y., Sato, N., Fujihara, M., Kroemer, G. and Ikeda, H. (2003) Possible contribution of apoptosis-inducing factor (AIF) and reactive oxygen species (ROS) to UVB-induced caspase-independent cell death in the T cell line Jurkat. *J Leukoc Biol*, **73**, 399-406.

Muzio, M., Stockwell, B.R., Stennicke, H.R., Salvesen, G.S. and Dixit, V.M. (1998) An induced proximity model for caspase-8 activation. *J Biol Chem*, **273**, 2926-2930.

Ndegwa, S. and Lemire, B.D. (2004) Caenorhabditis elegans development requires mitochondrial function in the nervous system. *Biochem Biophys Res Commun*, **319**, 1307-1313.

Nicholson, D.W. (1999) Caspase structure, proteolytic substrates, and function during apoptotic cell death. *Cell Death Differ*, **6**, 1028-1042.

Nur, E.K.A., Gross, S.R., Pan, Z., Balklava, Z., Ma, J. and Liu, L.F. (2004) Nuclear translocation of cytochrome c during apoptosis. *J Biol Chem*, **279**, 24911-24914.

Ohiro, Y., Garkavtsev, I., Kobayashi, S., Sreekumar, K.R., Nantz, R., Higashikubo, B.T., Duffy, S.L., Higashikubo, R., Usheva, A., Gius, D., Kley, N. and Horikoshi, N. (2002) A novel p53-inducible apoptogenic gene, PRG3, encodes a homologue of the apoptosis-inducing factor (AIF). *FEBS Lett*, **524**, 163-171.

Opferman, J.T. and Korsmeyer, S.J. (2003) Apoptosis in the development and maintenance of the immune system. *Nat Immunol*, **4**, 410-415.

Orth, M. and Schapira, A.H. (2001) Mitochondria and degenerative disorders. *Am J Med Genet*, **106**, 27-36.

Otera, H., Ohsakaya, S., Nagaura, Z., Ishihara, N. and Mihara, K. (2005) Export of mitochondrial AIF in response to proapoptotic stimuli depends on processing at the intermembrane space. *Embo J*, **24**, 1375-1386.

Ott, M., Robertson, J.D., Gogvadze, V., Zhivotovsky, B. and Orrenius, S. (2002) Cytochrome c release from mitochondria proceeds by a two-step process. *Proc Natl Acad Sci U S A*, **99**, 1259-1263.

Papadopoulou, L.C., Sue, C.M., Davidson, M.M., Tanji, K., Nishino, I., Sadlock, J.E., Krishna, S., Walker, W., Selby, J., Glerum, D.M., Coster, R.V., Lyon, G., Scalais, E., Lebel, R., Kaplan, P., Shanske, S., De Vivo, D.C., Bonilla, E., Hirano, M., DiMauro, S. and Schon, E.A. (1999) Fatal infantile cardioencephalomyopathy with COX deficiency and mutations in SCO2, a COX assembly gene. *Nat Genet*, **23**, 333-337.

Pardo, J., Perez-Galan, P., Gamen, S., Marzo, I., Monleon, I., Kaspar, A.A., Susin, S.A., Kroemer, G., Krensky, A.M., Naval, J. and Anel, A. (2001) A role of the mitochondrial apoptosis-inducing factor in granulysin-induced apoptosis. *J Immunol*, **167**, 1222-1229.

Parrish, J., Li, L., Klotz, K., Ledwich, D., Wang, X. and Xue, D. (2001) Mitochondrial endonuclease G is important for apoptosis in C. elegans. *Nature*, **412**, 90-94.

Parrish, J.Z. and Xue, D. (2003) Functional genomic analysis of apoptotic DNA degradation in C. elegans. *Mol Cell*, **11**, 987-996.

Parrish, J.Z., Yang, C., Shen, B. and Xue, D. (2003) CRN-1, a Caenorhabditis elegans FEN-1 homologue, cooperates with CPS-6/EndoG to promote apoptotic DNA degradation. *Embo J*, **22**, 3451-3460.

Perfettini, J.L. and Kroemer, G. (2003) Caspase activation is not death. *Nat Immunol*, **4**, 308-310.

Polster, B.M., Basanez, G., Etxebarria, A., Hardwick, J.M. and Nicholls, D.G. (2005) Calpain I induces cleavage and release of apoptosis-inducing factor from isolated mitochondria. *J Biol Chem*, **280**, 6447-6454.

Potluri, P., Yadava, N. and Scheffler, I.E. (2004) The role of the ESSS protein in the assembly of a functional and stable mammalian mitochondrial complex I (NADH-ubiquinone oxidoreductase). *Eur J Biochem*, **271**, 3265-3273.

Puccio, H., Simon, D., Cossee, M., Criqui-Filipe, P., Tiziano, F., Melki, J., Hindelang, C., Matyas, R., Rustin, P. and Koenig, M. (2001) Mouse models for Friedreich ataxia exhibit cardiomyopathy, sensory nerve defect and Fe-S enzyme deficiency followed by intramitochondrial iron deposits. *Nat Genet*, **27**, 181-186.

Punj, V. and Chakrabarty, A.M. (2003) Redox proteins in mammalian cell death: an evolutionarily conserved function in mitochondria and prokaryotes. *Cell Microbiol*, **5**, 225-231.

Radi, R., Turrens, J.F., Chang, L.Y., Bush, K.M., Crapo, J.D. and Freeman, B.A. (1991) Detection of catalase in rat heart mitochondria. *J Biol Chem*, **266**, 22028-22034.

Rao, R.V., Poksay, K.S., Castro-Obregon, S., Schilling, B., Row, R.H., del Rio, G., Gibson, B.W., Ellerby, H.M. and Bredesen, D.E. (2004) Molecular components of a cell death pathway activated by endoplasmic reticulum stress. *J Biol Chem*, **279**, 177-187.

Rashmi, R., Kumar, S. and Karunagaran, D. (2004) Ectopic expression of Hsp70 confers resistance and silencing its expression sensitizes human colon cancer cells to curcumin-induced apoptosis. *Carcinogenesis*, **25**, 179-187.

Ravagnan, L., Gurbuxani, S., Susin, S.A., Maisse, C., Daugas, E., Zamzami, N., Mak, T., Jaattela, M., Penninger, J.M., Garrido, C. and Kroemer, G. (2001) Heat-shock protein 70 antagonizes apoptosis-inducing factor. *Nat Cell Biol*, **3**, 839-843.

Reichmann, H. and Janetzky, B. (2000) Mitochondrial dysfunction--a pathogenetic factor in Parkinson's disease. *J Neurol*, **247 Suppl 2**, II63-68.

Riedl, S.J. and Shi, Y. (2004) Molecular mechanisms of caspase regulation during apoptosis. *Nat Rev Mol Cell Biol*, **5**, 897-907.

Roue, G., Bitton, N., Yuste, V.J., Montange, T., Rubio, M., Dessauge, F., Delettre, C., Merle-Beral, H., Sarfati, M. and Susin, S.A. (2003) Mitochondrial dysfunction in CD47-mediated caspase-independent cell death: ROS production in the absence of cytochrome c and AIF release. *Biochimie*, **85**, 741-746.

Rustin, P., Chretien, D., Bourgeron, T., Gerard, B., Rotig, A., Saudubray, J.M. and Munnich, A. (1994) Biochemical and molecular investigations in respiratory chain deficiencies. *Clin. Chem. Acta*, **228**, 35-51.

Rustin, P., Chretien, D., Bourgeron, T., Wucher, A., Saudubray, J.M., Rotig, A. and Munnich, A. (1991) Assessment of the mitochondrial respiratory chain. *Lancet*, **338**, 60.

Rutjes, S.A., van der Heijden, A., Utz, P.J., van Venrooij, W.J. and Pruijn, G.J. (1999) Rapid nucleolytic degradation of the small cytoplasmic Y RNAs during apoptosis. *J Biol Chem*, **274**, 24799-24807.

Saelens, X., Festjens, N., Vande Walle, L., van Gurp, M., van Loo, G. and Vandenabeele, P. (2004) Toxic proteins released from mitochondria in cell death. *Oncogene*, **23**, 2861-2874.

Sakahira, H., Enari, M. and Nagata, S. (1998) Cleavage of CAD inhibitor in CAD activation and DNA degradation during apoptosis. *Nature*, **391**, 96-99.

Saleh, A., Srinivasula, S.M., Balkir, L., Robbins, P.D. and Alnemri, E.S. (2000) Negative regulation of the Apaf-1 apoptosome by Hsp70. *Nat Cell Biol*, **2**, 476-483.

Salvesen, G.S. and Duckett, C.S. (2002) IAP proteins: blocking the road to death's door. *Nat Rev Mol Cell Biol*, **3**, 401-410.

Samejima, K., Tone, S. and Earnshaw, W.C. (2001) CAD/DFF40 nuclease is dispensable for high molecular weight DNA cleavage and stage I chromatin condensation in apoptosis. *J Biol Chem*, **276**, 45427-45432.

Scacco, S., Petruzzella, V., Budde, S., Vergari, R., Tamborra, R., Panelli, D., van den Heuvel, L.P., Smeitink, J.A. and Papa, S. (2003) Pathological mutations of the human NDUFS4 gene of the 18-kDa (AQDQ) subunit of complex I affect the expression of the protein and the assembly and function of the complex. *J Biol Chem*, **278**, 44161-44167.

Schapira, A.H. (2002) Primary and secondary defects of the mitochondrial respiratory chain. *J Inherit Metab Dis*, **25**, 207-214.

Schmitt, E., Parcellier, A., Gurbuxani, S., Cande, C., Hammann, A., Morales, M.C., Hunt, C.R., Dix, D.J., Kroemer, R.T., Giordanetto, F., Jaattela, M., Penninger, J.M., Pance, A., Kroemer, G. and Garrido, C. (2003) Chemosensitization by a non-apoptogenic heat shock protein 70-binding apoptosis-inducing factor mutant. *Cancer Res*, **63**, 8233-8240.

Schon, E.A. and Manfredi, G. (2003) Neuronal degeneration and mitochondrial dysfunction. *J Clin Invest*, **111**, 303-312.

Schägger, H. (2002) Respiratory chain supercomplexes of mitochondria and bacteria. *Biochim Biophys Acta*, **1555**, 154-159.

Schägger, H. (2003) Blue native electrophoresis. In Hunte, C., von Jagow, G. & Schägger, H. (eds), Membrane Protein Purification and Crystallization. Academic Press, San Diego, USA, pp. 105-129.

Schägger, H., de Coo, R., Bauer, M.F., Hofmann, S., Godinot, C. and Brandt, U. (2004) Significance of respirasomes for the assembly/stability of human respiratory chain complex I. *J Biol Chem*, **279**, 36349-36353.

Schägger, H. and Pfeiffer, K. (2000) Supercomplexes in the respiratory chains of yeast and mammalian mitochondria. *Embo J*, **19**, 1777-1783.

Schägger, H. and von Jagow, G. (1991) Blue native electrophoresis for isolation of membrane protein complexes in enzymatically active form. *Anal Biochem*, **199**, 223-231.

Scott, J. (2004) Pathophysiology and biochemistry of cardiovascular disease. *Curr Opin Genet Dev*, **14**, 271-279.

Senda, T., Yamada, T., Sakurai, N., Kubota, M., Nishizaki, T., Masai, E., Fukuda, M. and Mitsuidagger, Y. (2000) Crystal structure of NADH-dependent ferredoxin reductase component in biphenyl dioxygenase. *J Mol Biol*, **304**, 397-410.

Shankar, S.L., Mani, S., O'Guin, K.N., Kandimalla, E.R., Agrawal, S. and Shafit-Zagardo, B. (2001) Survivin inhibition induces human neural tumor cell death through caspase-independent and -dependent pathways. *J Neurochem*, **79**, 426-436.

Sharpe, J.C., Arnoult, D. and Youle, R.J. (2004) Control of mitochondrial permeability by Bcl-2 family members. *Biochim Biophys Acta*, **1644**, 107-113.

Shertzer, H.G. and Racker, E. (1976) Reconstitution and characterization of the adenine nucleotide transporter derived from bovine heart mitochondria. *J Biol Chem*, **251**, 2446-2452.

Shimizu, S., Narita, M. and Tsujimoto, Y. (1999) Bcl-2 family proteins regulate the release of apoptogenic cytochrome c by the mitochondrial channel VDAC. *Nature*, **399**, 483-487.

Simon, M., Chang, H.C. and Laskowski, M., Sr. (1971) Action of pancreatic deoxyribonuclease I on crab d(A-T) polymer. *Biochim Biophys Acta*, **232**, 462-471.

Slagsvold, H.H., Rosseland, C.M., Jacobs, C., Khuong, E., Kristoffersen, N., Gaarder, M., Fallgren, A.B., Huitfeldt, H.S. and Paulsen, R.E. (2003) High molecular weight DNA fragments are processed by caspase sensitive or caspase independent pathways in cultures of cerebellar granule neurons. *Brain Res*, **984**, 111-121.

Strauss, G., Vahsen, N., Schanbacher, M., Kroemer, G. and Debatin, K.-M. (2005) Caspase-independent T-cell apoptosis in vitro and in vivo induced by cyclophosphamide. *submitted*.

Stringer, J.R., Larson, J.S., Fischer, J.M. and Stringer, S.L. (2004) Increased mutation in mice genetically predisposed to oxidative damage in the brain. *Mutat Res*, **556**, 127-134.

Stroh, A., Anderka, O., Pfeiffer, K., Yagi, T., Finel, M., Ludwig, B. and Schagger, H. (2004) Assembly of respiratory complexes I, III, and IV into NADH oxidase supercomplex stabilizes complex I in Paracoccus denitrificans. *J Biol Chem*, **279**, 5000-5007.

Susin, S.A., Daugas, E., Ravagnan, L., Samejima, K., Zamzami, N., Loeffler, M., Costantini, P., Ferri, K.F., Irinopoulou, T., Prevost, M.C., Brothers, G., Mak, T.W., Penninger, J., Earnshaw, W.C. and Kroemer, G. (2000) Two distinct pathways leading to nuclear apoptosis. *J Exp Med*, **192**, 571-580.

Susin, S.A., Lorenzo, H.K., Zamzami, N., Marzo, I., Snow, B.E., Brothers, G.M., Mangion, J., Jacotot, E., Costantini, P., Loeffler, M., Larochette, N., Goodlett, D.R., Aebersold, R., Siderovski, D.P., Penninger, J.M. and Kroemer, G. (1999) Molecular characterization of mitochondrial apoptosis-inducing factor. *Nature*, **397**, 441-446.

Torriglia, A., Chaudun, E., Chany-Fournier, F., Courtois, Y. and Counis, M.F. (2001) Involvement of L-DNase II in nuclear degeneration during chick retina development. *Exp Eye Res*, **72**, 443-453.

Triepels, R.H., Van Den Heuvel, L.P., Trijbels, J.M. and Smeitink, J.A. (2001) Respiratory chain complex I deficiency. *Am J Med Genet*, **106**, 37-45.

Tuschen, G., Sackmann, U., Nehls, U., Haiker, H., Buse, G. and Weiss, H. (1990) Assembly of NADH: ubiquinone reductase (complex I) in Neurospora mitochondria. Independent pathways of nuclear-encoded and mitochondrially encoded subunits. *J Mol Biol*, **213**, 845-857.

Ugalde, C., Janssen, R.J., van den Heuvel, L.P., Smeitink, J.A. and Nijtmans, L.G. (2004) Differences in assembly or stability of complex I and other mitochondrial OXPHOS complexes in inherited complex I deficiency. *Hum Mol Genet*, **13**, 659-667.

Urbano, A., Lakshmanan, U., Choo, P.H., Kwan, J.C., Ng, P.Y., Guo, K., Dhakshinamoorthy, S. and Porter, A. (2005) AIF suppresses chemical stress-induced apoptosis and maintains the transformed state of tumor cells. *Embo J*, **24**, 2815-2826.

Uren, R.T., Dewson, G., Bonzon, C., Lithgow, T., Newmeyer, D.D. and Kluck, R.M. (2005) Mitochondrial release of pro-apoptotic proteins: electrostatic interactions can hold cytochrome c but not Smac/DIABLO to mitochondrial membranes. *J Biol Chem*, **280**, 2266-2274.

Vahsen, N., Cande, C., Briere, J.J., Benit, P., Joza, N., Larochette, N., Mastroberardino, P.G., Pequignot, M.O., Casares, N., Lazar, V., Feraud, O., Debili, N., Wissing, S., Engelhardt, S., Madeo, F., Piacentini, M., Penninger, J.M., Schagger, H., Rustin, P. and Kroemer, G. (2004) AIF deficiency compromises oxidative phosphorylation. *Embo J*, **23**, 4679-4689.

Vahsen, N., Cande, C., Dupaigne, P., Giordanetto, F., Kroemer, R.T., Herker, E., Scholz, S., Modjtahedi, N., Madeo, F., Le Cam, E. and Kroemer, G. (2005) Physical interaction of apoptosis-inducing factor (AIF) with DNA and RNA. *Oncogene*, **in press**.

Valnot, I., Osmond, S., Gigarel, N., Mehaye, B., Amiel, J., Cormier-Daire, V., Munnich, A., Bonnefont, J.P., Rustin, P. and Rotig, A. (2000) Mutations of the SCO1 gene in mitochondrial cytochrome c oxidase deficiency with neonatal-onset hepatic failure and encephalopathy. *Am J Hum Genet*, **67**, 1104-1109.

van Empel, V.P., Bertrand, A.T., van der Nagel, R., Kostin, S., Doevendans, P.A., Crijns, H.J., de Wit, E., Sluiter, W., Ackerman, S.L. and De Windt, L.J. (2005) Downregulation of apoptosis-inducing factor in harlequin mutant mice sensitizes the myocardium to oxidative stress-related cell death and pressure overload-induced decompensation. *Circ Res*, **96**, e92-e101.

Vancompernolle, K., Van Herreweghe, F., Pynaert, G., Van de Craen, M., De Vos, K., Totty, N., Sterling, A., Fiers, W., Vandenabeele, P. and Grooten, J. (1998) Atractyloside-induced release of cathepsin B, a protease with caspase-processing activity. *FEBS Lett*, **438**, 150-158.

Vaux, D.L. and Korsmeyer, S.J. (1999) Cell death in development. *Cell*, **96**, 245-254.

Verhagen, A.M., Ekert, P.G., Pakusch, M., Silke, J., Connolly, L.M., Reid, G.E., Moritz, R.L., Simpson, R.J. and Vaux, D.L. (2000) Identification of DIABLO, a mammalian protein that promotes apoptosis by binding to and antagonizing IAP proteins. *Cell*, **102**, 43-53.

Vila, M. and Przedborski, S. (2003) Targeting programmed cell death in neurodegenerative diseases. *Nat Rev Neurosci*, **4**, 365-375.

Vogel, R., Nijtmans, L., Ugalde, C., van den Heuvel, L. and Smeitink, J. (2004) Complex I assembly: a puzzling problem. *Curr Opin Neurol*, **17**, 179-186.

Vousden, K.H. and Lu, X. (2002) Live or let die: the cell's response to p53. *Nat Rev Cancer*, **2**, 594-604.

Walker, J.E. (1992) The NADH:ubiquinone oxidoreductase (complex I) of respiratory chains. *Q Rev Biophys*, **25**, 253-324.

Wallace, D.C. (1999) Mitochondrial diseases in man and mouse. *Science*, **283**, 1482-1488.

Wang, H.G., Pathan, N., Ethell, I.M., Krajewski, S., Yamaguchi, Y., Shibasaki, F., McKeon, F., Bobo, T., Franke, T.F. and Reed, J.C. (1999) Ca2+-induced apoptosis through calcineurin dephosphorylation of BAD. *Science*, **284**, 339-343.

Wang, X., Yang, C., Chai, J., Shi, Y. and Xue, D. (2002) Mechanisms of AIF-mediated apoptotic DNA degradation in Caenorhabditis elegans. *Science*, **298**, 1587-1592.

Warner, B.B., Stuart, L., Gebb, S. and Wispe, J.R. (1996) Redox regulation of manganese superoxide dismutase. *Am J Physiol*, **271**, L150-158.

Widlak, P. (2000) DFF40/CAD hypersensitive sites are potentially involved in high molecular weight DNA fragmentation during apoptosis. *Cell Mol Biol Lett*, **5**, 373-379.

Widlak, P. and Garrard, W.T. (2001) Ionic and cofactor requirements for the activity of the apoptotic endonuclease DFF40/CAD. *Mol Cell Biochem*, **218**, 125-130.

Widlak, P. and Garrard, W.T. (2005) Discovery, regulation, and action of the major apoptotic nucleases DFF40/CAD and endonuclease G. *J Cell Biochem*, **94**, 1078-1087.

Widlak, P., Li, L.Y., Wang, X. and Garrard, W.T. (2001) Action of recombinant human apoptotic endonuclease G on naked DNA and chromatin substrates: cooperation with exonuclease and DNase I. *J Biol Chem*, **276**, 48404-48409.

Williams, S.L., Valnot, I., Rustin, P. and Taanman, J.W. (2004) Cytochrome c oxidase subassemblies in fibroblast cultures from patients carrying mutations in COX10, SCO1, or SURF1. *J Biol Chem*, **279**, 7462-7469.

Wissing, S., Ludovico, P., Herker, E., Buttner, S., Engelhardt, S.M., Decker, T., Link, A., Proksch, A., Rodrigues, F., Corte-Real, M., Frohlich, K.U., Manns, J., Cande, C., Sigrist, S.J., Kroemer, G. and Madeo, F. (2004) An AIF orthologue regulates apoptosis in yeast. *J Cell Biol*, **166**, 969-974.

Wolter, K.G., Hsu, Y.T., Smith, C.L., Nechushtan, A., Xi, X.G. and Youle, R.J. (1997) Movement of Bax from the cytosol to mitochondria during apoptosis. *J Cell Biol*, **139**, 1281-1292.

Wu, M., Xu, L.G., Li, X., Zhai, Z. and Shu, H.B. (2002) AMID, an apoptosis-inducing factor-homologous mitochondrion-associated protein, induces caspase-independent apoptosis. *J Biol Chem*, **277**, 25617-25623.

Xie, Q., Lin, T., Zhang, Y., Zheng, J. and Bonanno, J.A. (2005) Molecular cloning and characterization of a human AIF-like gene with ability to induce apoptosis. *J Biol Chem*.

Yadava, N., Houchens, T., Potluri, P. and Scheffler, I.E. (2004) Development and characterization of a conditional mitochondrial complex I assembly system. *J Biol Chem*, **279**, 12406-12413.

Yamashita, D., Miller, J.M., Jiang, H.Y., Minami, S.B. and Schacht, J. (2004) AIF and EndoG in noise-induced hearing loss. *Neuroreport*, **15**, 2719-2722.

Ye, H., Cande, C., Stephanou, N.C., Jiang, S., Gurbuxani, S., Larochette, N., Daugas, E., Garrido, C., Kroemer, G. and Wu, H. (2002) DNA binding is required for the apoptogenic action of apoptosis inducing factor. *Nat Struct Biol*, **9**, 680-684.

Yu, S.W., Wang, H., Poitras, M.F., Coombs, C., Bowers, W.J., Federoff, H.J., Poirier, G.G., Dawson, T.M. and Dawson, V.L. (2002) Mediation of poly(ADP-ribose) polymerase-1-dependent cell death by apoptosis-inducing factor. *Science*, **297**, 259-263.

Yuan, C.Q., Li, Y.N. and Zhang, X.F. (2004) Down-regulation of apoptosis-inducing factor protein by RNA interference inhibits UVA-induced cell death. *Biochem Biophys Res Commun*, **317**, 1108-1113.

Yuste, V.J., Moubarak, R.S., Delettre, C., Bras, M., Sancho, P., Robert, N., d'Alayer, J. and Susin, S.A. (2005a) Cysteine protease inhibition prevents mitochondrial apoptosis-inducing factor (AIF) release. *Cell Death Differ*.

Yuste, V.J., Sanchez-Lopez, I., Sole, C., Moubarak, R.S., Bayascas, J.R., Dolcet, X., Encinas, M., Susin, S.A. and Comella, J.X. (2005b) The contribution of apoptosis inducing factor, caspase-activated DNase and inhibitor of caspase-activated DNase to the nuclear phenotype and DNA degradation during apoptosis. *J Biol Chem*.

Zamzami, N. and Kroemer, G. (1999) Condensed matter in cell death. *Nature*, **401**, 127-128.

Zamzami, N. and Kroemer, G. (2001) The mitochondrion in apoptosis: how Pandora's box opens. *Nat Rev Mol Cell Biol*, **2**, 67-71.

Zhang, J., Dong, M., Li, L., Fan, Y., Pathre, P., Dong, J., Lou, D., Wells, J.M., Olivares-Villagomez, D., Van Kaer, L., Wang, X. and Xu, M. (2003a) Endonuclease G is required for early embryogenesis and normal apoptosis in mice. *Proc Natl Acad Sci U S A*, **100**, 15782-15787.

Zhang, W., Shokeen, M., Li, D. and Mehta, J.L. (2003b) Identification of apoptosis-inducing factor in human coronary artery endothelial cells. *Biochem Biophys Res Commun*, **301**, 147-151.

Zhang, X., Chen, J., Graham, S.H., Du, L., Kochanek, P.M., Draviam, R., Guo, F., Nathaniel, P.D., Szabo, C., Watkins, S.C. and Clark, R.S. (2002) Intranuclear localization of apoptosis-inducing factor (AIF) and large scale DNA fragmentation after traumatic brain injury in rats and in neuronal cultures exposed to peroxynitrite. *J Neurochem*, **82**, 181-191.

Zhao, H., Yenari, M.A., Cheng, D., Barreto-Chang, O.L., Sapolsky, R.M. and Steinberg, G.K. (2004) Bcl-2 transfection via herpes simplex virus blocks apoptosis-inducing factor translocation after focal ischemia in the rat. *J Cereb Blood Flow Metab*, **24**, 681-692.

Zhu, C., Qiu, L., Wang, X., Hallin, U., Cande, C., Kroemer, G., Hagberg, H. and Blomgren, K. (2003) Involvement of apoptosis-inducing factor in neuronal death after hypoxia-ischemia in the neonatal rat brain. *J Neurochem*, **86**, 306-317.

Zhu, C., Wang, X., Xu, F., Bahr, B.A., Shibata, M., Uchiyama, Y., Hagberg, H. and Blomgren, K. (2005) The influence of age on apoptotic and other mechanisms of cell death after cerebral hypoxia-ischemia. *Cell Death Differ*, **12**, 162-176.

Zhu, Z., Yao, J., Johns, T., Fu, K., De Bie, I., Macmillan, C., Cuthbert, A.P., Newbold, R.F., Wang, J., Chevrette, M., Brown, G.K., Brown, R.M. and Shoubridge, E.A. (1998) SURF1, encoding a factor involved in the biogenesis of cytochrome c oxidase, is mutated in Leigh syndrome. *Nat Genet*, **20**, 337-343.

Zoccarato, F., Cavallini, L. and Alexandre, A. (2004) Respiration-dependent removal of exogenous H2O2 in brain mitochondria: inhibition by Ca2+. *J Biol Chem*, **279**, 4166-4174.